NASA-CR 165458
R81AEG030

Effect of a Part Span Variable Inlet Guide Vane on TF34 Fan Performance

By
José Alvarez
Paul W. Schneider

GENERAL ELECTRIC
Aircraft Engine Group
Lynn, Massachusetts

Prepared For

National Aeronautics and Space Administration

NASA Lewis Research Center
Contract NAS3-21824

1. Report No	2. Government Accession No.	3. Recipient's Catalog No.
NASA CR-165458		

4. Title and Subtitle	5. Report Date
Effect of a Part Span Variable Inlet Guide Vane on TF34 Performance	September 1981
	6. Performing Organization Code

7. Author(s)	8. Performing Organization Report No.
José Alvarez and Paul W. Schneider	R81AEG030
	10. Work Unit No.

9. Performing Organization Name and Address	11. Contract or Grant No.
General Electric Company Aircraft Engine Group Lynn, MA	NAS3-21624
	13. Type of Report and Period Covered
12. Sponsoring Agency Name and Address	Final Report
National Aeronautics and Space Administration Washington, DC	14. Sponsoring Agency Code

15. Supplementary Notes

Project Manager, George A. Bobula
U. S. Army Research and Technology Laboratory (AVRADCOM)
Propulsion Laboratory, Lewis Research Center, Cleveland, Ohio 44135

16. Abstract

Experimental aerodynamic and performance data were obtained from a NASA-LeRC Propulsion Engine Technology Program. Part span variable inlet guide vanes (VIGV) mounted in front of the fan on a TF34 engine were tested to demonstrate the feasibility of modulating air flow and thrust for VTOL aircraft systems.

The fan was mapped to stall for a range of speeds and VIGV settings. Modulated fan tip performance and unmodulated hub performance were evaluated with and without an extended fan bypass splitter. The effect of a crosswind distortion screen on performance was also evaluated.

17. Key Words (Suggested by Author(s))	18. Distribution Statement
TF34 Fan Variable Inlet Guide Vane Thrust Modulation VTOL	

19. Security Classif. (of this report)	20. Security Classif. (of this page)	21. No. of Pages	22. Price*
Unclassified	Unclassified	125	

* For sale by the National Technical Information Service, Springfield, Virginia 22161

TABLE OF CONTENTS

LIST OF TABLES

LIST OF FIGURES

LIST OF FIGURES (cont.)

FOREWORD

The test program which formed the basis for this report was conducted at the NASA Lewis Research Center under the direction of Mr. George A. Bobula of the U. S. Army Research and Technology Laboratory (AVRADCOM) Propulsion Laboratory.

SUMMARY

This report describes those efforts expended by the Contractor on NASA Contract NAS3-21624 - Task I - Support of Variable Inlet Guide Vane Program.

The objectives of the program, of which this task was a part, were to experimentally evaluate the concept of thrust modulation through control of a part span fan variable inlet guide vane (VIGV), the potential benefits of a forward extension of the fan flow splitter, and the distortion sensitivity and transfer characteristics applicable to the VIGV concept associated with a crosswind-type distortion.

The Contractor analyzed and interpreted the experimental research data furnished by the NASA from the fan VIGV program, on a modified TF34 engine, which was part of the Propulsion Engine Technology (PET) program being conducted at the NASA-Lewis Research Center. The part span VIGV and the extended fan flow splitter were designed and manufactured by GE on an earlier NASA contract. The NASA-Lewis Research Center conducted the engine tests and provided all the relevant test data to GE for analysis, interpretation and compilation of this report.

Conclusions and Recommendations

1. The concept of using a fan part span VIGV for flow and thrust modulation on a TF34 has been successfully validated.

2. A VIGV closure of 40° resulted in 30 percent flow reduction and 53 percent thrust reduction.

3. VIGV closure reduced thrust as a result of the combined mechanisms of reduction of airflow and increased losses in the fan tip region.

4. A data base for future variable IGV and VTOL applications is available from this test program.

5. The performance of the PET TF34 fan with VIGV at 0° is consistent with the basic TF34 fan without VIGV with no measurable effect on limit line, flow at speed, or efficiency.

6. Relative to the conventional splitter, the extended splitter shows improvements:

   a) In VTOL sea level takeoff performance (Minor SFC penalties for the low altitude cruise condition may occur depending on the mission).

   b) In fan efficiency above 95 percent speed and core inlet pressure at 0° IGV angle at both sea level and 15K 0.6 Mn.

   c) In fan efficiency and core inlet pressure at varying IGV angle at all flight conditions.

7. With the presence of VIGV's, fan distortion sensitivity is less than 8 percent of the sensitivity without VIGV's.

8. The distortion transfer from fan inlet to core is the same as the basic TF34 on the nominal fan operating line; but distortion transfer with the fan on a high operating line is significantly reduced with IGV closure.

INTRODUCTION

The development of a VTOL aircraft is dependent upon the mission, the propulsion system(s), the control type, and the response necessary for maintaining aircraft attitude during hover, vertical operation and transition to forward flight. The integration of the propulsion system and flight controls to achieve aircraft attitude control are critical to the successful operation of VTOL aircraft. The propulsion system is therefore of central importance in obtaining the necessary control power through the use of vectoring nozzles, variable inlet guide vanes, variable pitch fans, bleed air reaction control systems and other devices or systems.

One method of rapidly modulating thrust while maintaining full core and fan speeds is a fan variable inlet guide vane. Such a system has been shown to have short transient thrust modulation times (0.2 seconds, Reference 1) and large thrust variation needed to meet control thrust requirements. Application in a typical VTOL concept is shown in Figure 1.

In some earlier aircraft design concepts, a cross shafted propulsion system was proposed to achieve power transfer from one engine fan to the other during normal hover and vertical operation (See Figure 2). One early consideration also included the transfer of power between engines during a one-engine inoperative (OEI) emergency vertical landing condition where the operating core engine and low pressure turbine had to be capable of driving both engine fans to provide the required landing thrust plus enough excess power to develop the necessary attitude control thrust. This extreme operating condition would be the sizing point for the installed power. To achieve balanced thrust, the operating engine provides mostly gas generator nozzle thrust while its bypass fan VIGV's are closed to reduce fan thrust. This engine thrust is balanced by the fan bypass thrust of the inoperative engine which has the fan VIGV's opened. With full span VIGV's, closure of the inlet guide vanes would also decrease the fan hub supercharging into the operating core compressor resulting in a design requirement to oversize the core to provide the needed core flow and power output. This would have resulted in a larger core engine size, lower design bypass ratio, higher weight and higher SFC during cruise.

Part-span, variable inlet guide vanes are preferred over full span VIGV's as a means of modulating fan thrust because the fan bypass flow is modulated without desupercharging the core compressor flow as would occur with the full span VIGV concept. More core engine power is therefore available to provide for the transfer of shaft horsepower between engines or for other shaft horsepower applications such as torque to a rotating wing and a circulation control

compressor for the rotating wing in the case of an X-wing VTOL aircraft (See Figure 3).

A part span VIGV was designed for use on an existing GE YTF34-F5 high bypass fan engine as a test demonstrator. This GE design was tested as part of the ongoing Propulsion Engine Technology (PET) program at NASA Lewis to demonstrate the feasibility and performance of this proposed thrust modulating device on an operational engine system.

Figure 1. Typical VTOL Concept

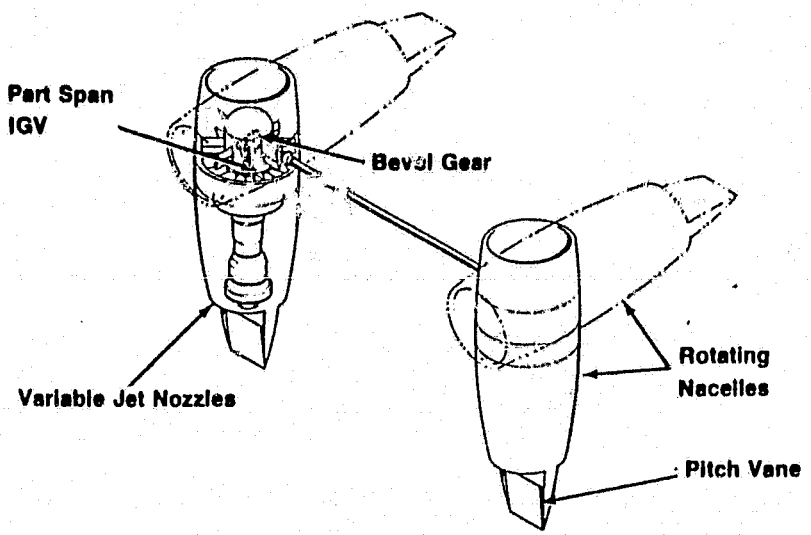

Figure 2. Rotating Nacelles Propulsion System

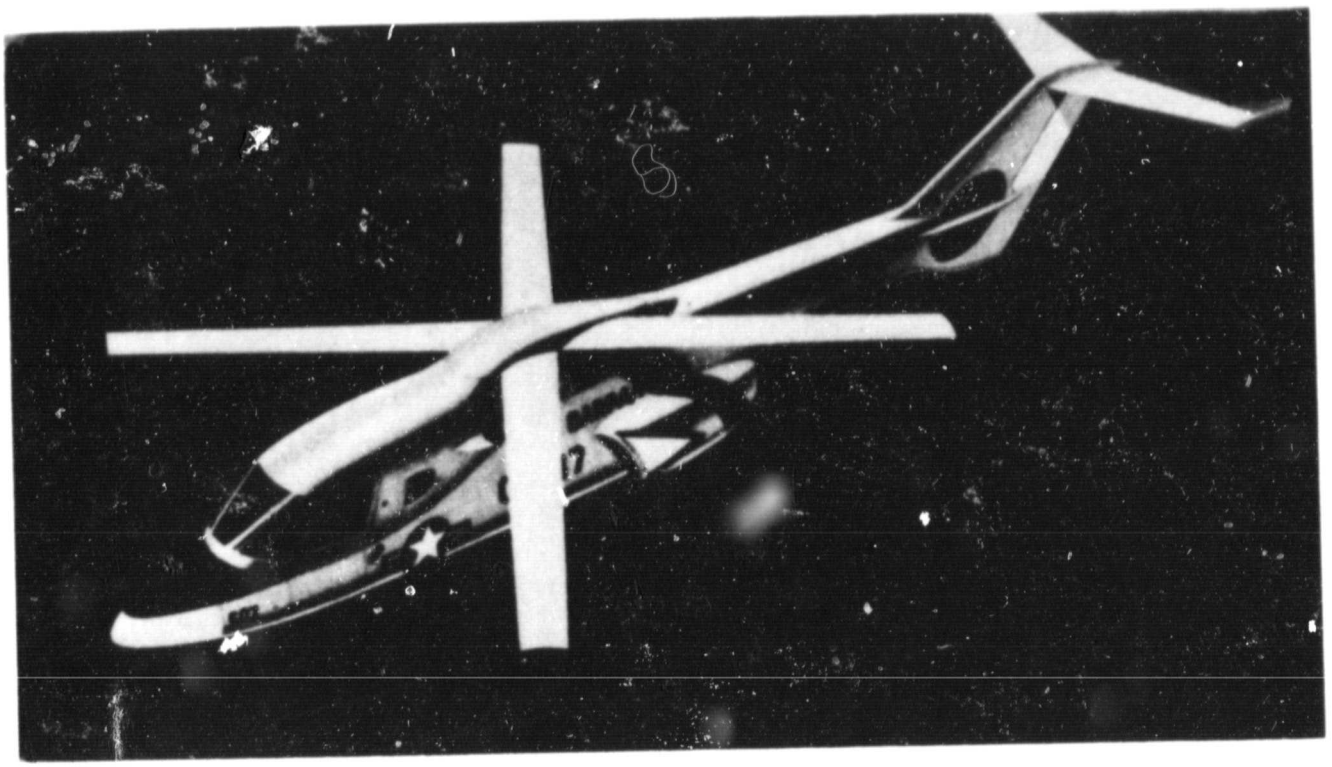

Figure 3. Typical X-Wing Vehicle

DESCRIPTION OF PART SPAN VARIABLE INLET GUIDE VANE TF34 FAN ENGINE

Design Elements

The TF34 engine used as a test demonstrator is shown with both the part span variable inlet guide vane and the extended splitter packages installed, (Figure 4). The basic TF34 fan is a 6:1 bypass ratio single stage fan of 1.5 pressure ratio which does not normally have an inlet guide vane. The selected IGV design is a zero swirl, uncambered strut-flap design. It is cantilevered from the inlet casing but supported by an annular ring at its inner extremities. Figure 5 is a photograph of the VIGV assembly mounted on the engine.

Figure 6 provides a detailed fan cross-section of the VIGV and TF34 fan with streamlines for the 0° case. It can be seen that the part span IGV feature results in modulating only the flow passing through the bypass duct. The annular shroud ring is located such that the wake from the shroud will not be ingested in the core inlet duct. A fixed strut-variable flap is used instead of a variable stagger inlet guide vane in order to preserve the leading edge incidence on the inlet guide vane at closed inlet guide vane settings. In this case, the inlet guide vane design swirl was zero to preserve the existing TF34 fan rotor and stator designs. The stator remained fixed (not variable) as in the basic TF34.

The relative importance of the part span VIGV and the extended splitter are illustrated in Table 1 where the fan hub pressure ratios of several configurations at a constant 100 percent fan speed can be compared. In the first column, test data for a nominal (zero degree) IGV is shown to have a fan hub pressure ratio of 1.425 which results in a core compressor inlet flow which we shall define as providing a base core compressor size. If, while maintaining 100 percent fan speed, a full span IGV were closed 45°, the fan hub would be decreased to a calculated pressure ratio of 1.164, as shown in Column 2. This desupercharging of the core inlet would require a 22 percent larger core compressor to achieve the base core flow. This assumes additional core flow is obtained by increased core size rather than opening core stators or increasing core speed (options of limited potential which are available to all configurations). The part-span VIGV experimental data in Column 3, however, demonstrates a much better fan hub pressure ratio to the core inlet and therefore would require only a 10 percent larger core compressor. With an extended splitter added, Column 4, an additional 2 percent hub supercharging is experimentally demonstrated, and only an 8 percent larger core size is required. Thus 12 percentage points in core size reduction can be attributed to use of a part span VIGV, while an additional 2 percentage points are attributed to the use of an extended splitter.

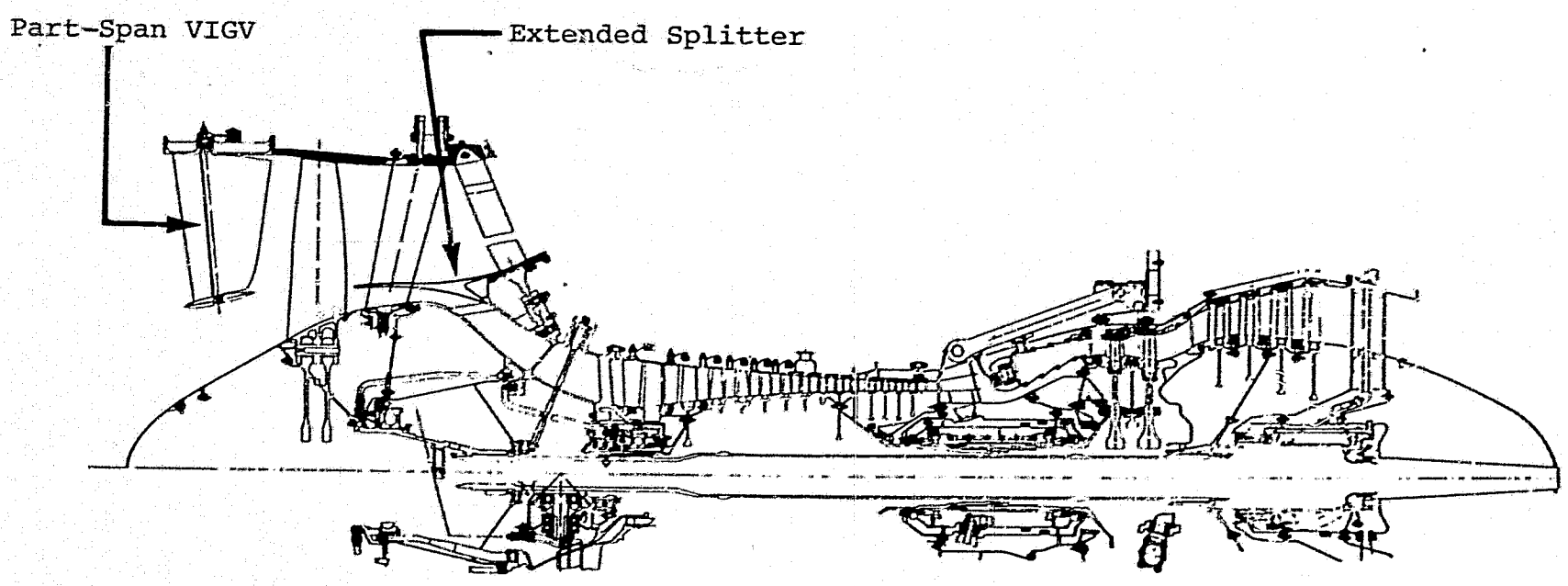

Figure 4. TF34 Turbofan Engine with Part-Span VIGV Extended Splitter Configuration

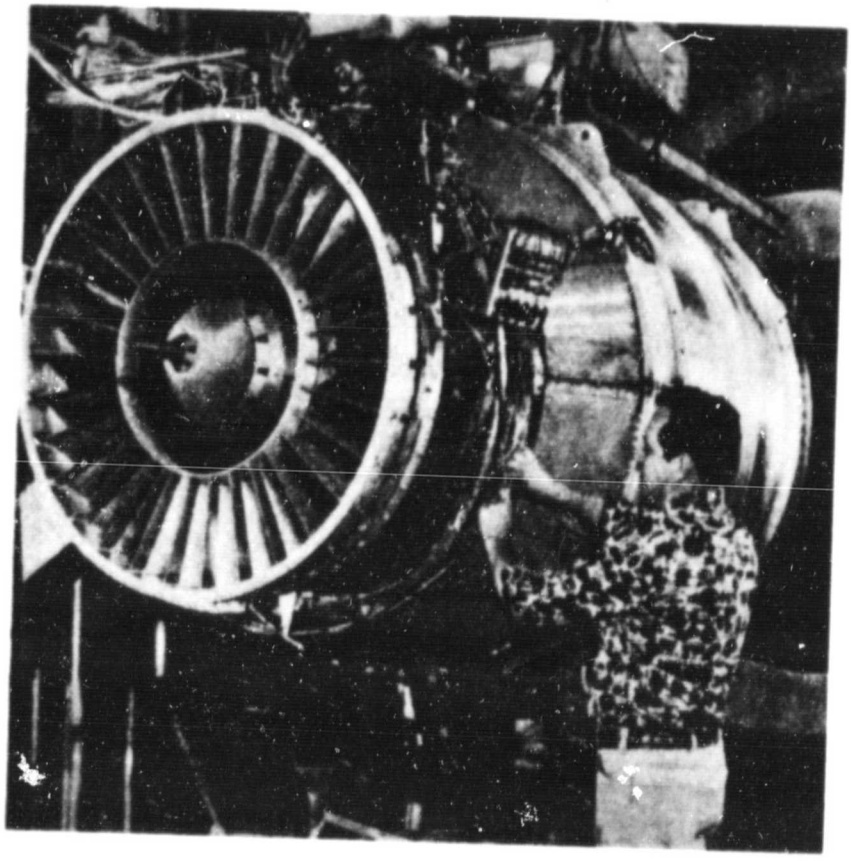

Figure 5. TF34 - PET VIGV Assembly

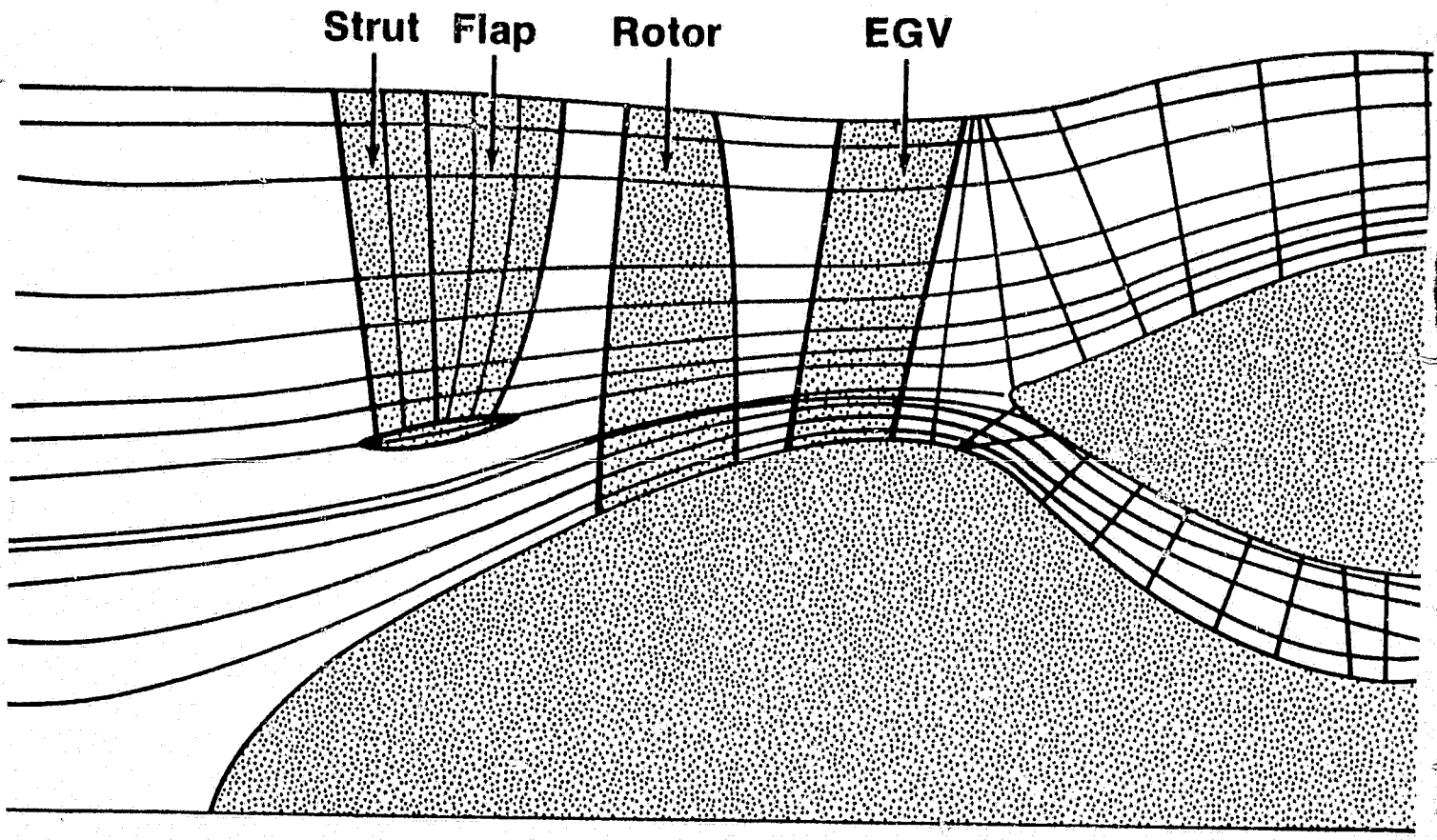

Figure 6. TF34 - Part-Span VIGV Design Streamline Flow Evaluation for the 0° Case

TABLE 1

EFFECT OF TF34 VIGV CONFIGURATION ON CORE COMPRESSOR SIZING AT CLOSED IGV SIZING POINT

Configuration	Nominal IGV	Full-Span IGV	Part-Span IGV	Part-Span IGV with Extended Splitter
IGV Angle	0° (Open)	45° Closed	45° Closed	45° Closed
Fan Corrected Speed	100%	100%	100%	100%
Fan Hub Pressure Ratio (to Core Inlet)	1.425	1.164	1.295	1.320
Approximate Relative Core Size Required	Base	+22%	+10%	+8%

TEST CONFIGURATIONS AND INSTRUMENTATION

The test configuration (Figure 7) illustrates the part-span VIGV and extended splitter design additions that are not normally a part of the basic TF34 fan.

The configurations tested at NASA consisted of a basic TF34 fan (which was tested only to the extent necessary to check out the engine, instrumentation, and facility), a TF34 fan with part-span inlet guide vane and conventional splitter, and finally the addition of the extended splitter as shown.

The extended splitter is designed such that its lower surface lies along the stagnation streamline of the conventional splitter TF34 fan at its design point. The extended splitter is mechanically fastened to the conventional splitter, and extends forward through the fixed fan stators (with airtight sealing) to within .050" of the rotor trailing edge.

Fan discharge instrumentation (Figure 8) was the same for both splitter configurations and consisted of fan tip instrumentation (station 24) having six total pressure and six total temperature radial rakes of 5 immersion elements each. A few of these rakes had 3 additional elements extending to the hub, but these elements were not used in the definition of the fan performance maps. Fan hub to core inlet performance maps were determined by the instrumentation of the core inlet (station 2C) as shown in Figures 7 and 9. Fan hub performance maps therefore include the core inlet duct loss as an integral part of the fan hub performance. This provides a better reference and comparison between splitter configurations since fan stator and stream tube diffusion wake mixing can best be sampled by the downstream (core inlet) instrumentation. Fan mapping at each data point therefore consisted of fan tip and fan hub-to-core inlet maps plotted against the fan inlet total flow.

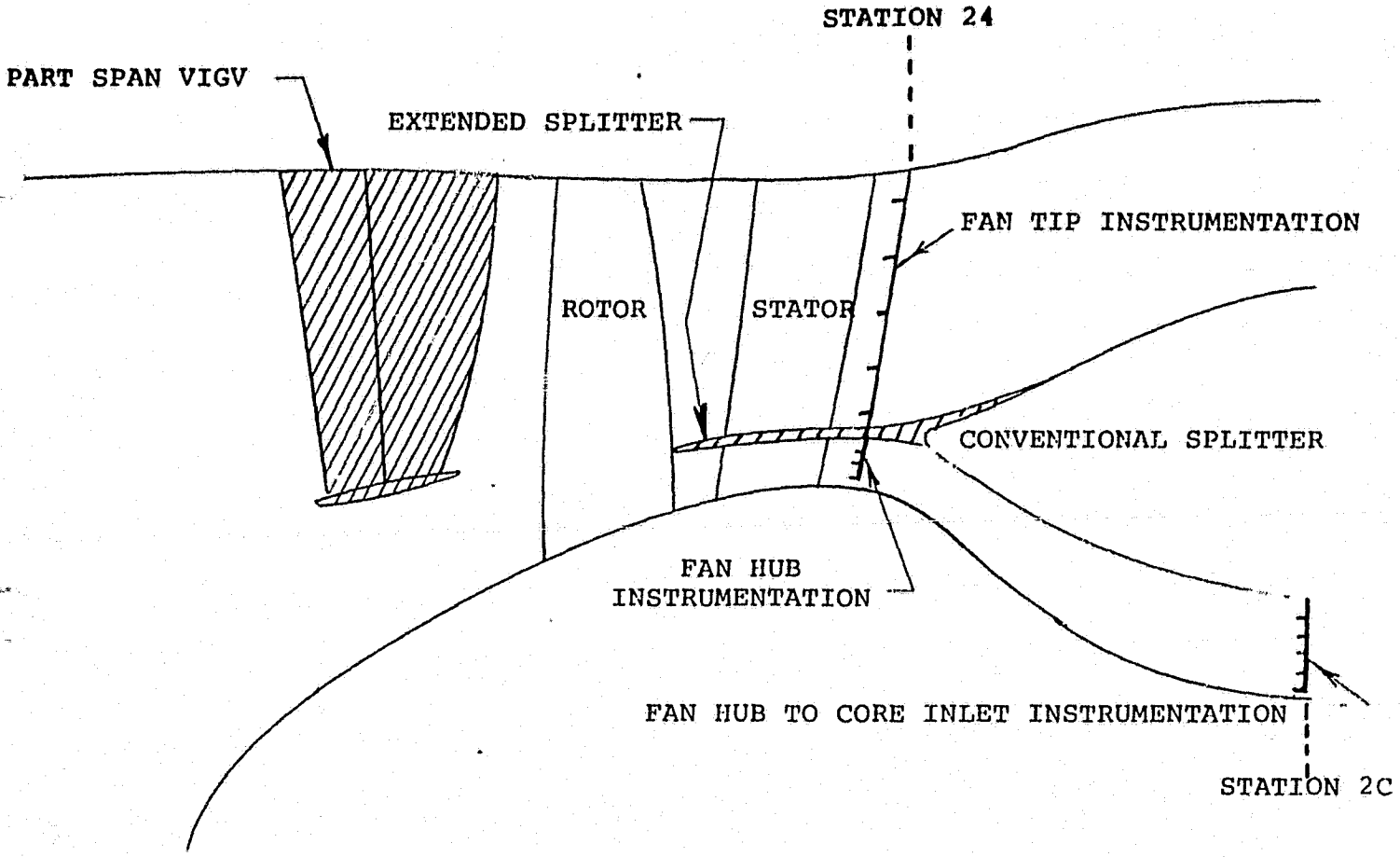

Figure 7. Test Configuration

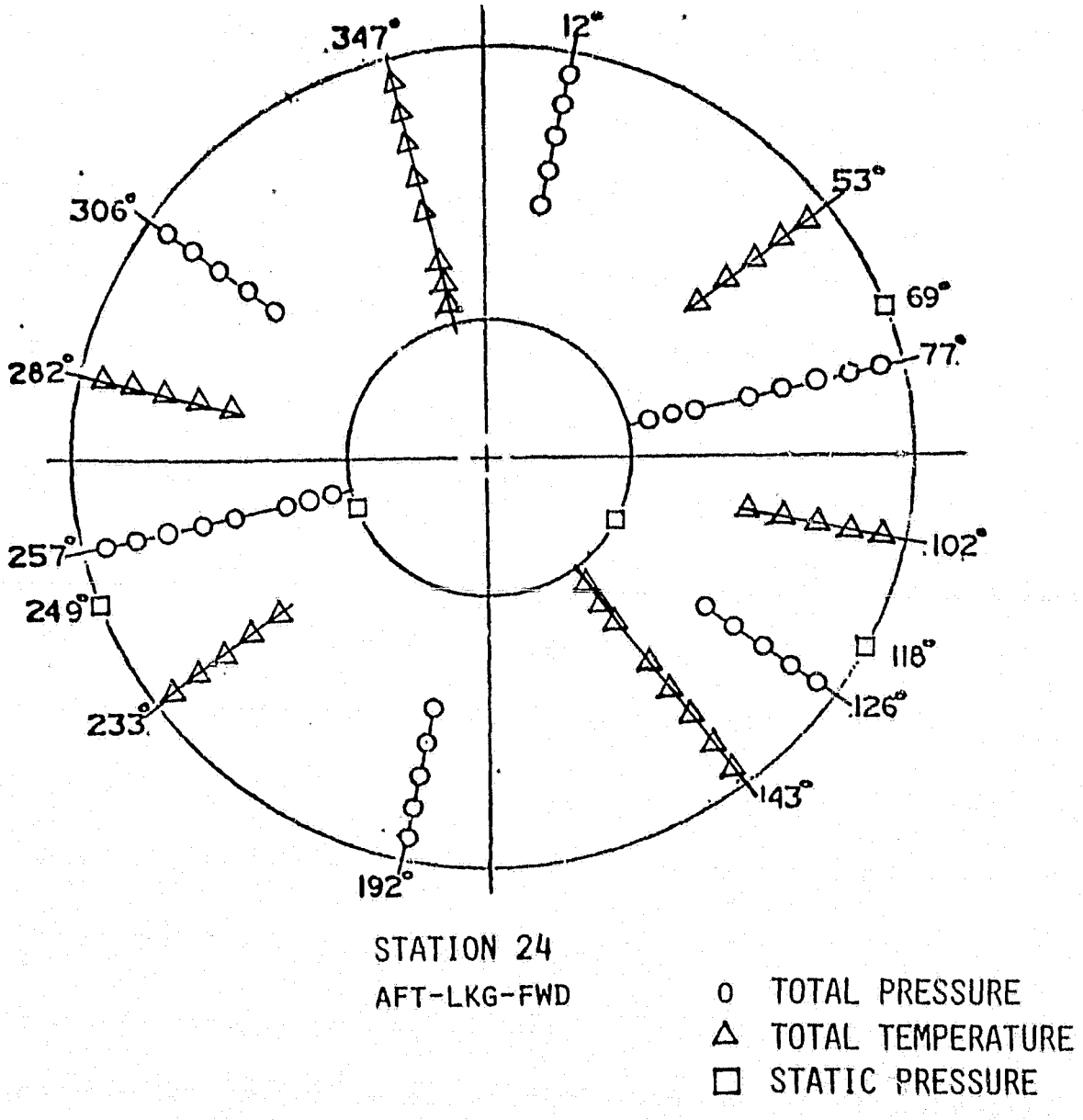

Figure 8. Fan Discharge Instrumentation

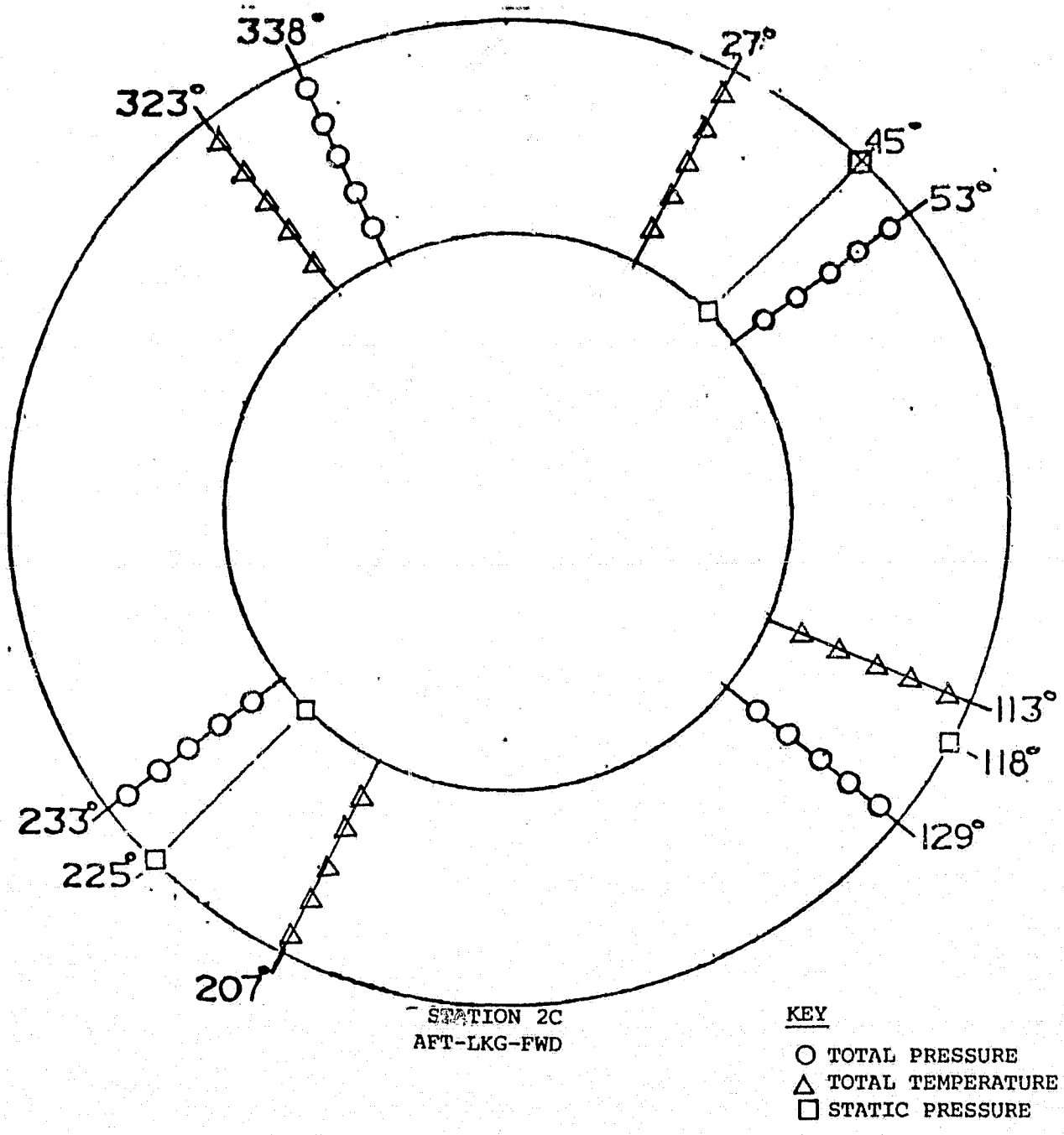

Figure 9. Compressor Core Inlet Instrumentation

TEST PROCEDURE AND TEST PROGRAM MATRIX

Undistorted Inlet - Conventional and Extended Splitter

Fan mapping on the engine was accomplished along fan operating lines for each configuration using two fan bypass duct nozzle sizes, nominal and large. Complete engine performance was taken during mapping along the fan operating lines. Mapping of the fan speed lines to stall or stress limit line was accomplished with the use of a special control to hold fan speed while the fan was throttled by simulating fan nozzle closure through the use of back pressure jet blowing (Reference 2). To insure that the engine was kept within turbine temperature limits and fan stress limits during high speeds and throttled fan conditions, all testing was conducted at simulated altitude and flight Mach number conditions of 4,572m (15,000 ft) Mach 0.6 or 9,144m (30,000 ft) Mach 0.93. These conditions were known (and demonstrated during the course of the test) not to have any Reynolds' number effect on fan or engine performance.

The test matrix for each configuration was designed to include, but not be limited to, typical operating conditions envisioned for a VTOL aircraft. Figure 10 shows six such typical points. At 100 percent constant fan corrected speed, a variation in takeoff thrust is shown as a function of the fan IGV angle where a nominal takeoff thrust is arbitrarily chosen at 15 degrees IGV angle.

Landing control thrust modulation of ±20 percent is predicted to correspond to VIGV angles of about 0 and 35 degrees. In the case of the one engine inoperative (OEI) condition, the total required thrust could be achieved at 95 percent fan speed with VIGV's closed to 35°. Thrust modulation requirements of ±20 percent could be achieved by variation of VIGV's over a range of about 30°.

These six points are represented on the matrix in Figure 11 with test points specified at fan speeds and IGV angles above and below these six conditions to provide a data bank of fan performance for this and other variable inlet guide vane applications.

The actual test matrix used for the conventional and extended splitter configurations at undistorted inlet conditions is given in Figure 12. IGV angles ranged from 10° open to 65° closed and fan speeds ranged from 105 percent to the minimum allowed by the fuel control. The conventional splitter test was conducted with IGV angles of up to 65° closed, a test condition not repeated for the extended splitter configuration since fan tip pressure ratios of less than unity occurred at these extreme IGV closures. The fan was throttled to the stall/stress limit at speeds ranging from 80 percent to 105 percent as indicated in this figure.

Inlet Distortion Testing - Conventional Splitter

Inlet distortion testing with a crosswind distortion screen was conducted on the conventional splitter configuration along the test matrix in Figure 13. Fan and compressor inlet distortion data were taken on the nominal operating line at 95 percent and 100 percent speeds and with the fan throttled to the stall/stress limit at 95 percent speed. Testing was conducted at IGV angles of both 0° and 15° closed.

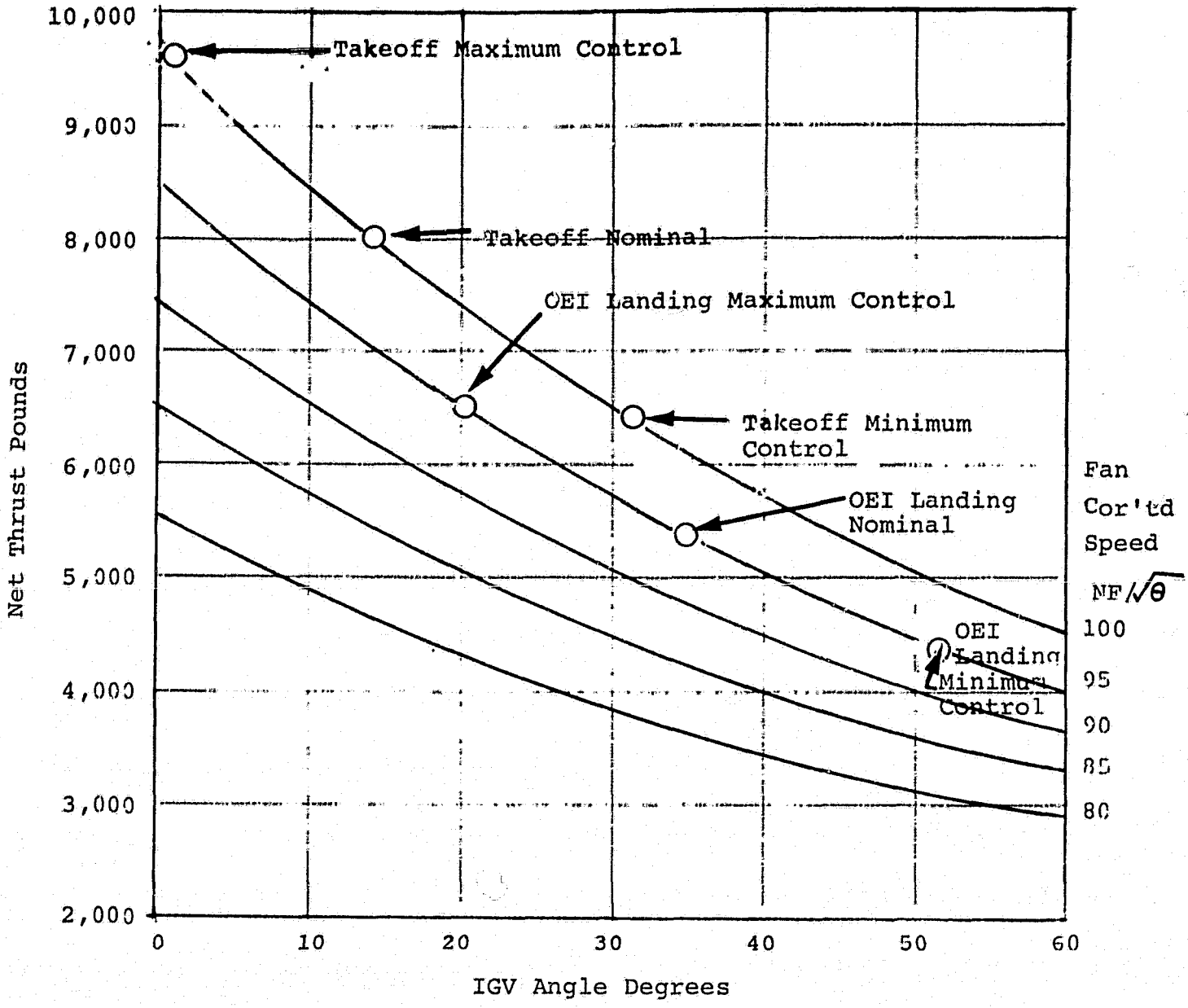

Figure 10. VTOL Estimated Performance

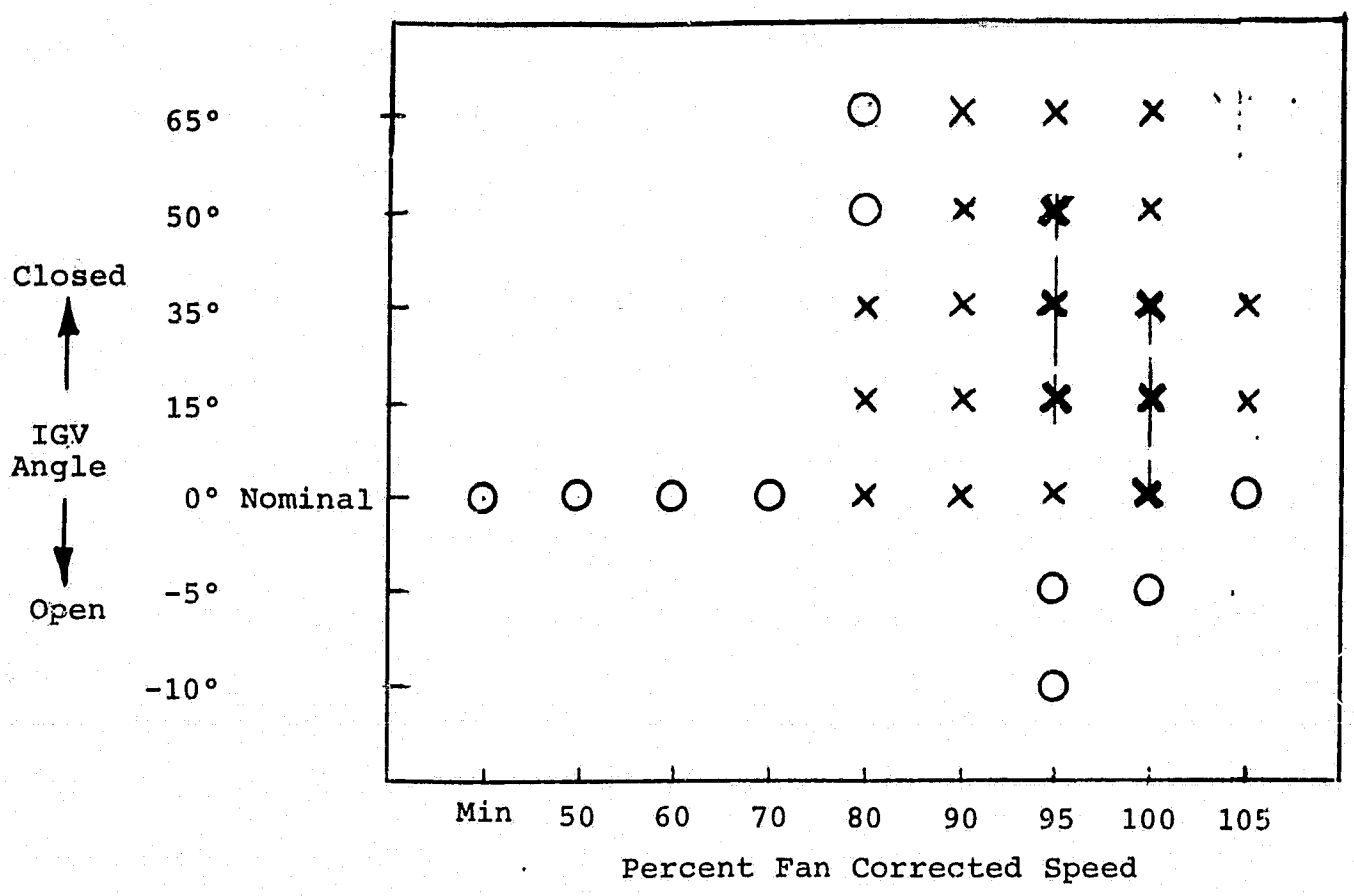

X = Fan Speed Line Throttled to Limit (Stall/Stress)

O = Operating Line, No Throttling

Figure 11. VTOL Test Matrix

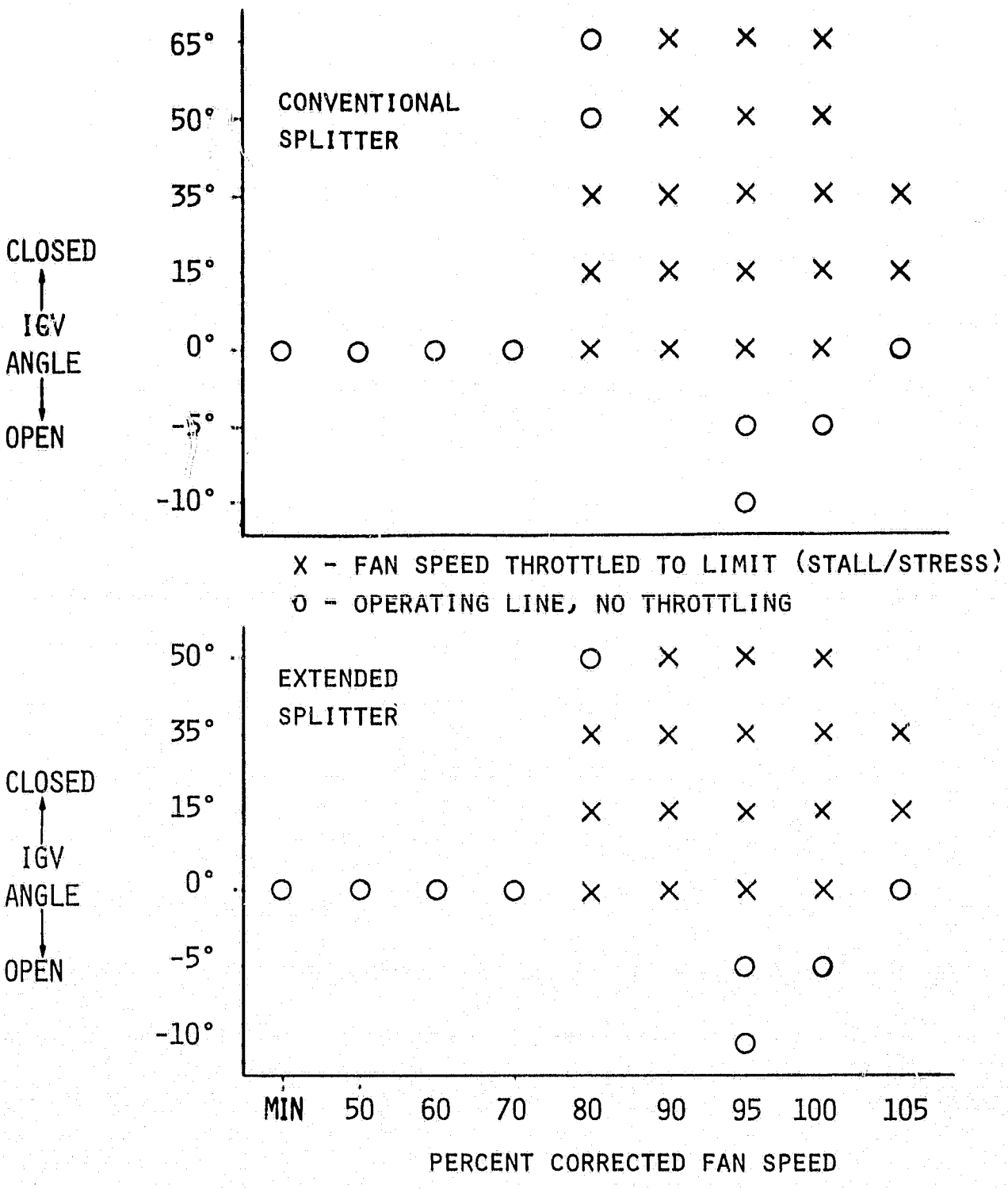

Figure 12. Test Matrix for Undistorted Inlet

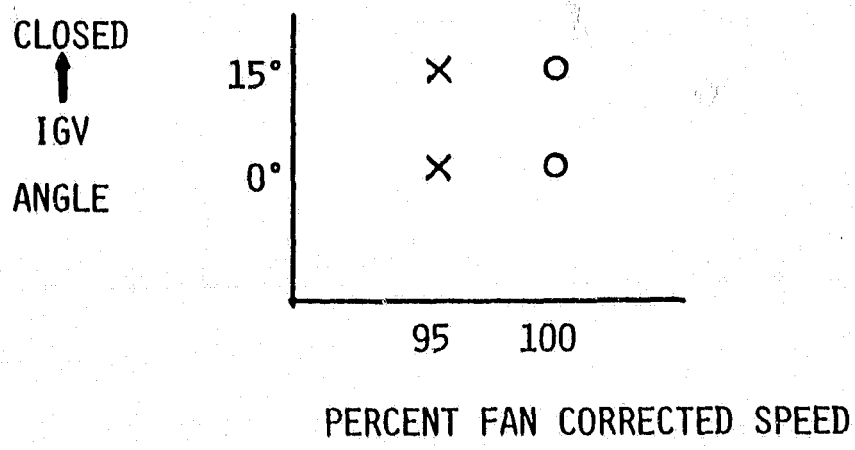

X - FAN SPEED THROTTLED TO LIMIT (STALL/STRESS)

O - OPERATING LINE, NO THROTTLING

Figure 13. Test Matrix for Distorted Inlet with Conventional Splitter

ANALYSIS AND PRESENTATION OF DATA

Undistorted Inlet Data Organization

Undistorted inlet fan data as defined by the test matrix are presented in 13 sets of fan performance maps as defined by Figure 14. These data are presented for each splitter configuration by maps of constant IGV angle and variable speed as well as by maps of constant speed and variable inlet guide vane angle. Each set with the exception of Set No. 7 consists of fan tip and fan hub performance as follows:

1) Fan tip pressure ratio versus total inlet flow.

2) Fan tip efficiency versus total inlet flow.

3) Fan hub to core inlet pressure ratio versus total flow.

4) Fan hub to core inlet efficiency versus total flow.

In Set No. 7 (65° closed VIGV and conventional splitter) efficiency data are not presented because pressure ratios of less than unity were measured.

The fifty performance maps which present the above data can be found in Appendix II. Set No. 1 is also used as an illustrative example in Figures 15 through 18.

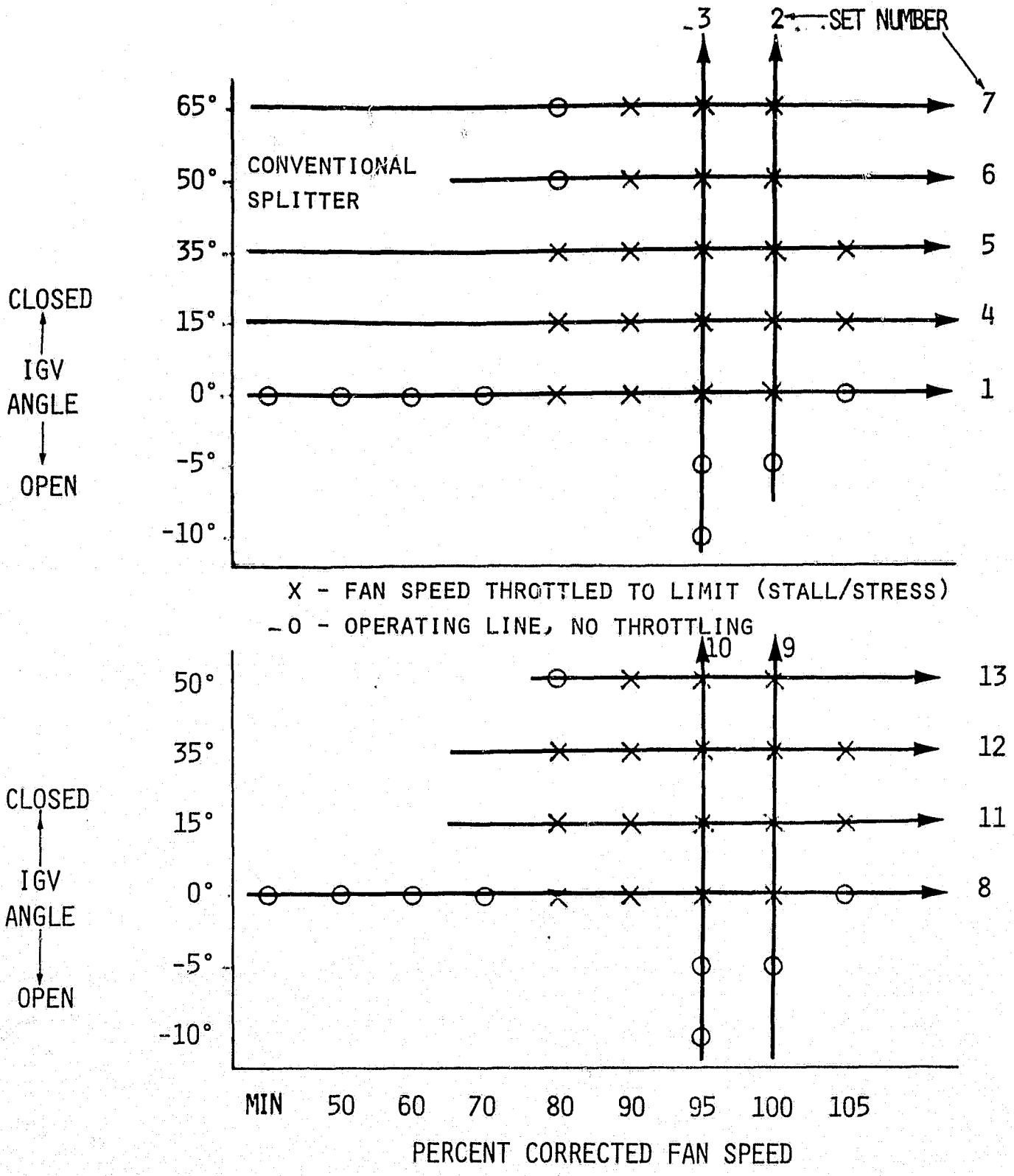

Figure 14. Fan Performance Map Matrix

ZERO DEGREE IGV FAN DATA - CONVENTIONAL SPLITTER

Comparison to Basic TF34 Fan (No IGV)

The fan configuration with a zero degree IGV and conventional splitter is similar to that of the basic TF34 fan (no IGV). The only expected performance difference therefore is in the total pressure loss of less than 1 percent due to the presence of the no swirl inlet guide vane. A comparison of this data to basic TF34 fan data taken on another engine indicated no measurable difference in stall/limit line, flow at speed, or fan efficiencies (within the ability to measure performance and considering engine to engine differences).

The zero degree inlet guide vane, conventional splitter fan performance is shown for the fan tip in Figures 15 and 16 and for the fan hub to core inlet in Figures 17 and 18. These data serve as an example of the fan data presented in the appendix and are explained as follows:

Fan tip performance (Figure 15) shows a stall/stress limit line which coincides with that of the basic TF34 fan. As in the basic TF34 fan, the limit line is defined by flexural and torsional blade stress limits, indicated by the symbol key on the maps. Other throttling limits for the fan performance data presented in the appendix are either fan stall or exit guide vane (EGV) stress limits. Sufficient fan operating margin has always been available such that these limits are not considered to present a problem. The data symbols also indicate the simulated altitude and Mach number at which the data were taken, usually 4,572m (15,000 ft), Mach 0.6 or (for high speed, throttled fan data) 9,144m (30,000 ft), Mach 0.93. The middle and lower operating line data shown are taken with the nominal and large fan nozzles respectively at 4,572m (15,000 ft), Mach 0.6. These altitude operating lines coincide with the operating lines of the basic TF34 engine. Although fan data at NASA Lewis were not taken at sea level, the sea level nominal operating line is also presented on the major fan performance maps to provide a basis of performance comparison. The fan performance data along the sea level operating line provides a basis for examining and comparing VTOL performance, while the 4,572m (15,000 ft) Mach 0.6 operating line provides data representative of cruise performance. The fan tip efficiency along these operating lines is presented in Figure 16, while Figures 17 and 18 provide the fan hub to core inlet pressure ratio and efficiency respectively.

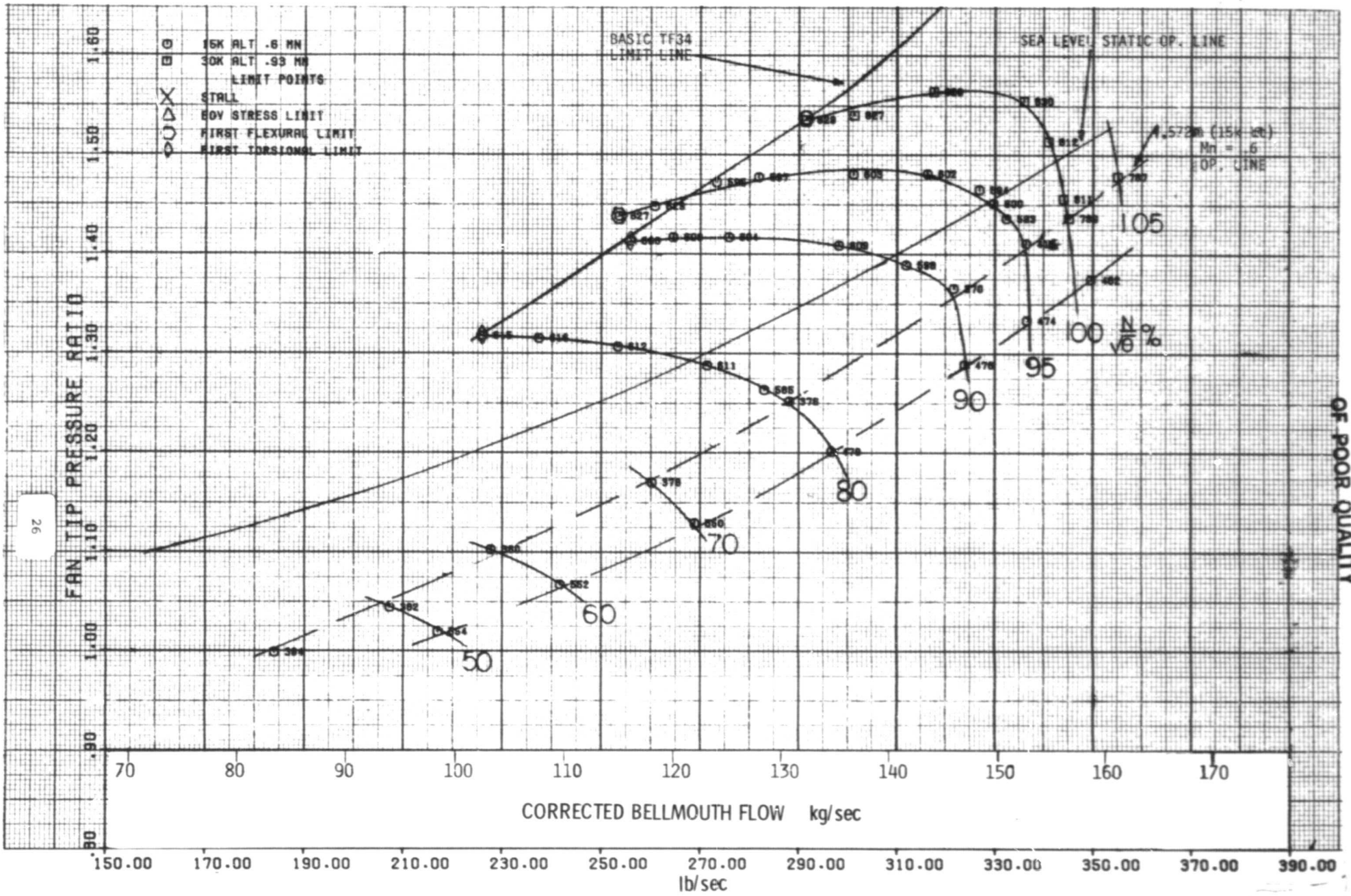

FIGURE 15 TIP PRESSURE RATIO AT IGV ANGLE OF 0° (CONVENTIONAL SPLITTER)

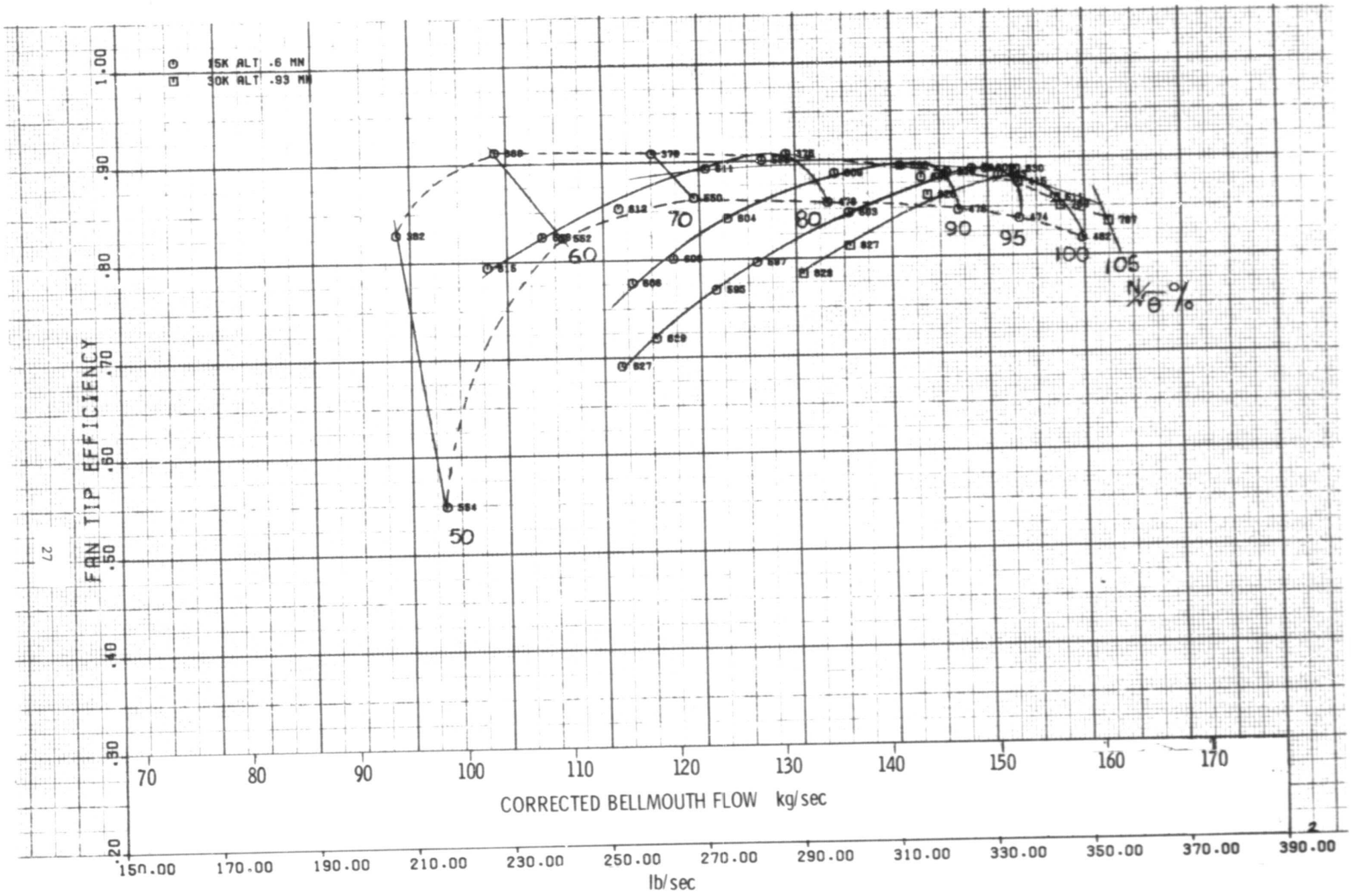

FIGURE 16 TIP EFFICIENCY AT IGV ANGLE OF 0° (CONVENTIONAL SPLITTER)

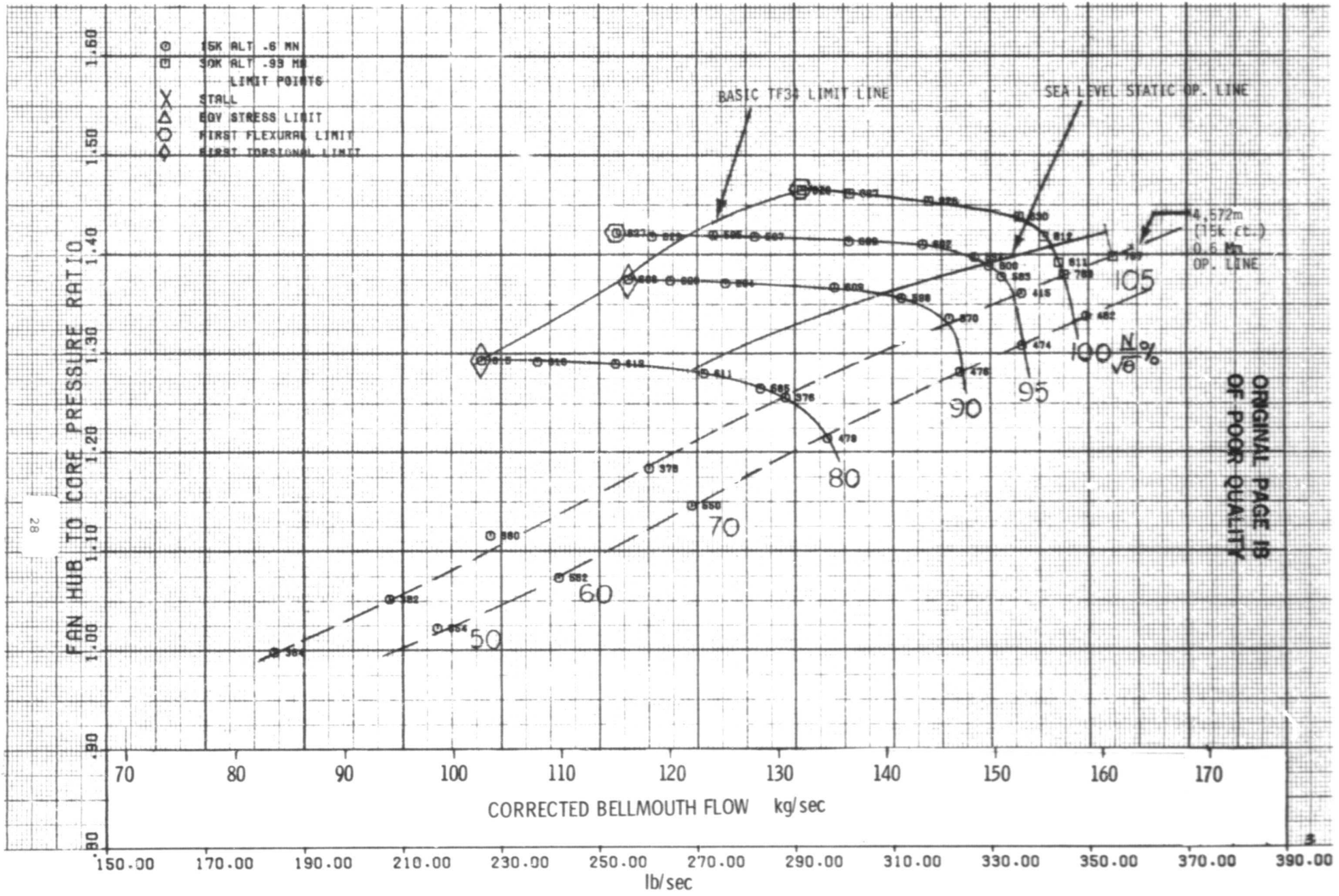

FIGURE 17 HUB PRESSURE RATIO AT IGV ANGLE OF 0° (CONVENTIONAL SPLITTER)

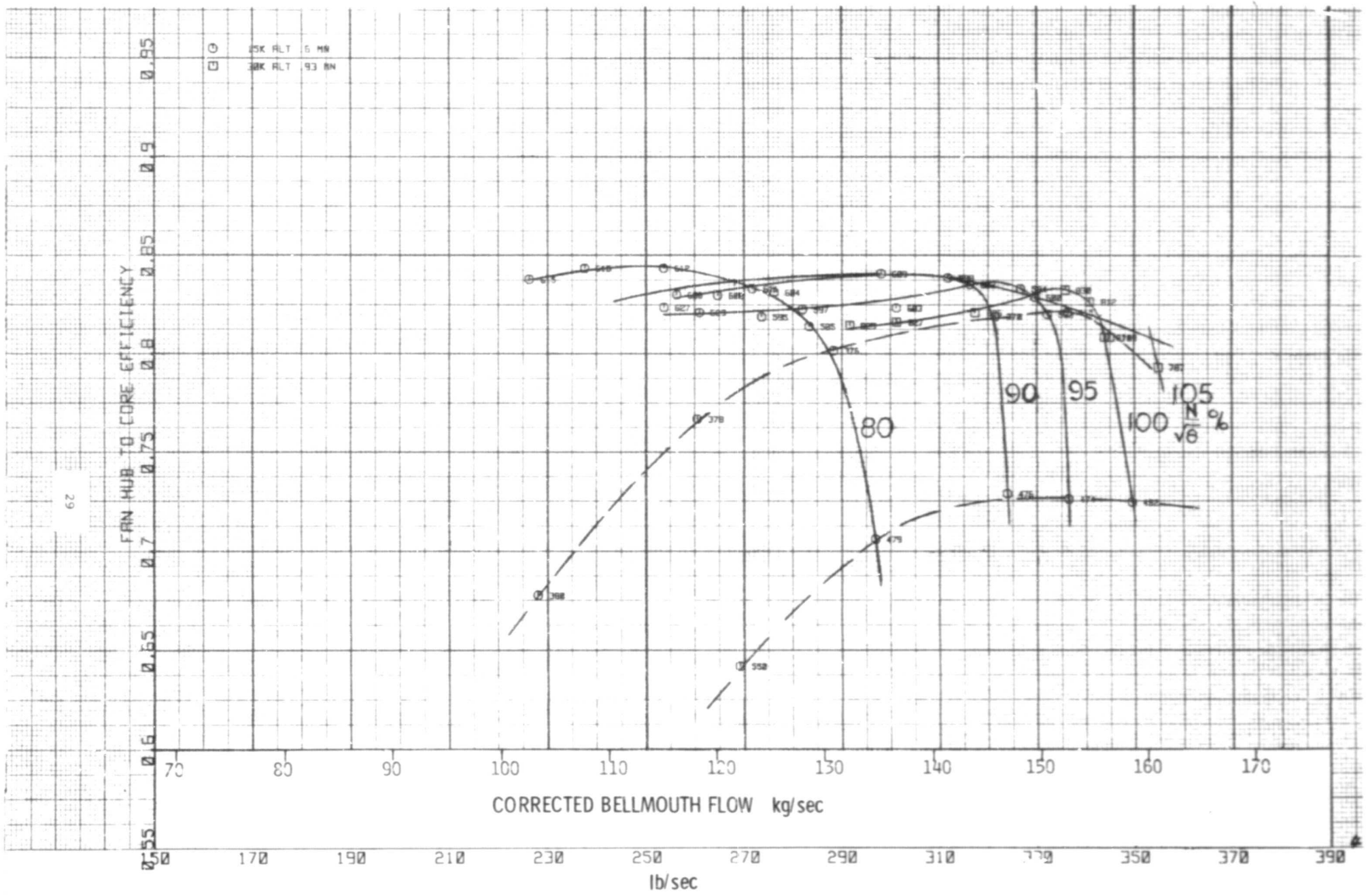

FIGURE 18 HUB EFFICIENCY AT IGV ANGLE OF 0° (CONVENTIONAL SPLITTER)

CONVENTIONAL VERSUS EXTENDED SPLITTER CONFIGURATION

Zero Degree Inlet Guide Vane, Variable Fan Speed

A superposition of the fan maps of both splitter configurations (Figure 19) indicates a somewhat more limited range of fan throttling for the extended splitter. The extended splitter configuration has a 1 percent lower limit line when throttled and a lower flow at speed on the sea level operating line which varies from 0.5 percent lower at design speed to 2.5 percent lower at 80 percent fan speed. The presence of the splitter also results in a higher fan operating line for the same fan nozzle size. Comparisons between the conventional and extended splitter data will therefore be made along the same operating line of the same fan nozzle size to provide a more objective comparison.

Sea level static operating line data (representative of VTOL operations) are compared (Figure 20) along the same fan tip operating line. The hub to core inlet operating line for the extended splitter shows a 1 percent higher hub pressure ratio at all speeds, and a higher hub and tip efficiency above 95 percent fan speed.

Along a 4,572m (15,000 ft) Mach 0.6 operating line (Figure 21) a similar comparison (representative of cruise operation) shows about a 2 percent higher hub pressure ratio for the extended splitter, higher fan hub to core efficiency at all speeds, and higher tip efficiency at speeds above 95 percent speed. The slightly lower fan tip efficiencies for the extended splitter configuration at lower fan speeds may be offset by the improved hub performance.

Varying IGV Angle, Constant Fan Speed

Performance comparisons between splitter configurations were also made at constant fan speeds with the IGV's varied to modulate flow. The flow modulation as a function of IGV angle (Figure 22) does not show significant difference between splitter configurations.

The extended splitter does offer other significant advantages when comparing constant speed fan mapping performance. The fan limit line with extended splitter is significantly better at IGV closures beyond 35 degrees (Figure 23) where EGV stress no longer defines the limit, but where an improved pressure rise capability exists and blade torsional stress finally limits. An understanding of why EGV stresses are usually limiting at high inlet guide vane closures at constant speed can be gained from the design study of EGV incidence along an operating line as a function of IGV closure angle (Figure 24). At IGV closures of 40° and beyond very large

incidences occur on the operating line (even larger near stall) and stall flow separation on the exit guide vanes occurs which induces high stresses. This large incidence is primarily a function of IGV closure angle. It can be shown analytically that the extended splitter reduces these incidences at the stalled EGV tip by concentrating the fan bypass flow over a more local area.

Sea level operating line performance is compared between the two splitter configurations at constant fan speeds of 100 percent and 95 percent in Figures 25 and 26 respectively.

At 100 percent fan speed (Figure 25) a performance comparison at a constant fan tip operating line shows that fan hub-to-core inlet pressure ratios (bottom of figure) remain relatively constant as the part span VIGV is closed up to 15 degrees. After this, fan hub pressure ratios start to diminish for both splitter configurations. Fan hub pressure ratios and efficiencies for the extended splitter configuration are higher initially than for the conventional splitter at 0° IGV and remain higher during IGV closure. The greatest advantage is shown at IGV closures beyond 35°. Fan tip efficiencies (top of figure) are 15 to 20 points higher with the extended splitter configuration than with the conventional splitter at IGV closures of 35° and beyond.

At 95 percent fan speed (Figure 26), a comparison of splitter configurations results in the same conclusions regarding the advantages of the extended splitter configuration as described above.

INLET DISTORTION DATA, CONVENTIONAL SPLITTER

Fan inlet pressure distortion testing was conducted with the same crosswind distortion screen design (Figure 27) that was tested earlier at GE on a basic TF34 fan. This screen design simulates nacelle inlet lip separation distortion due to a crosswind. A flat-plate and coarse mesh screen cover the bottom of the inlet, as shown. The rest of the inlet is open. Figure 28 is the circumferential fan inlet pressure pattern measured at the design point. The screen was rotated circumferentially to three positions at each data point to improve data sampling.

The distortion transferred through the fan to the core compressor inlet is also measured (Figure 29). The lower pressures at the hub are the result of the core inlet duct pressure profile and not due to the fan inlet distortion.

Distortion Definitions

The inlet distortion parametric definitions are presented in Figures 30 and 31. The inlet pressure measurements are divided into five equal area annular rings from which the maximum circumferential and

radial distortions (IDC and IDR respectively) are defined (Figure 30). The ratio of the loss in stall or limit line pressure ratio to the circumferential inlet distortion is called stall sensitivity (Figure 31). Distortion transfer is the ratio of maximum circumferential distortion at the core compressor inlet divided by the circumferential distortion entering the fan.

Distortion Fan Mapping

Fan mapping with inlet distortion was conducted at IGV angles of 0° and 15°. This data is superimposed over the undistorted inlet maps in Figures 32 and 33 respectively. Data points with three screen rotations were taken on the operating line at 95 percent and 100 percent fan speeds and near the limit condition at 95 percent fan speed.

The circumferential and radial components of fan inlet distortion are presented as a function of airflow (Figure 34). This distortion is at a maximum at the tip rings (Figure 35). The distortion entering the core compressor (Figure 36) is affected by the distortion attenuation properties of the fan. These distortion transfer results can be described in Figure 37 where a distortion transfer below unity indicates an attenuation rather than an amplification of distortion through the fan. From previous testing of the basic TF34 fan at General Electric, it was established that the distortion transfer was 0.7 at the design speed. The distortion transfer of the part span VIGV fan is approximately the same on the nominal operating line at both 0° and 15° IGV closure. At 0° IGV, the transfer increases significantly as the fan is throttled to stall. This increase in transfer with fan throttling is a common problem in fan engines since core stall sometimes occurs under severe circumstances. When the IGV is closed 15°, however, fan throttling resulted in an improved attenuation, thereby demonstrating additional advantages for the part span VIGV configuration.

The loss in fan limit line pressure ratio divided by the circumferential inlet distortion (Figure 38) is a measure of the fan distortion sensitivity. Previous testing of the basic TF34 fan with no IGV's indicated a fan distortion sensitivity of 0.6. With part span IGV's this sensitivity was markedly reduced to less than 0.1 due to the presence of the IGV's.

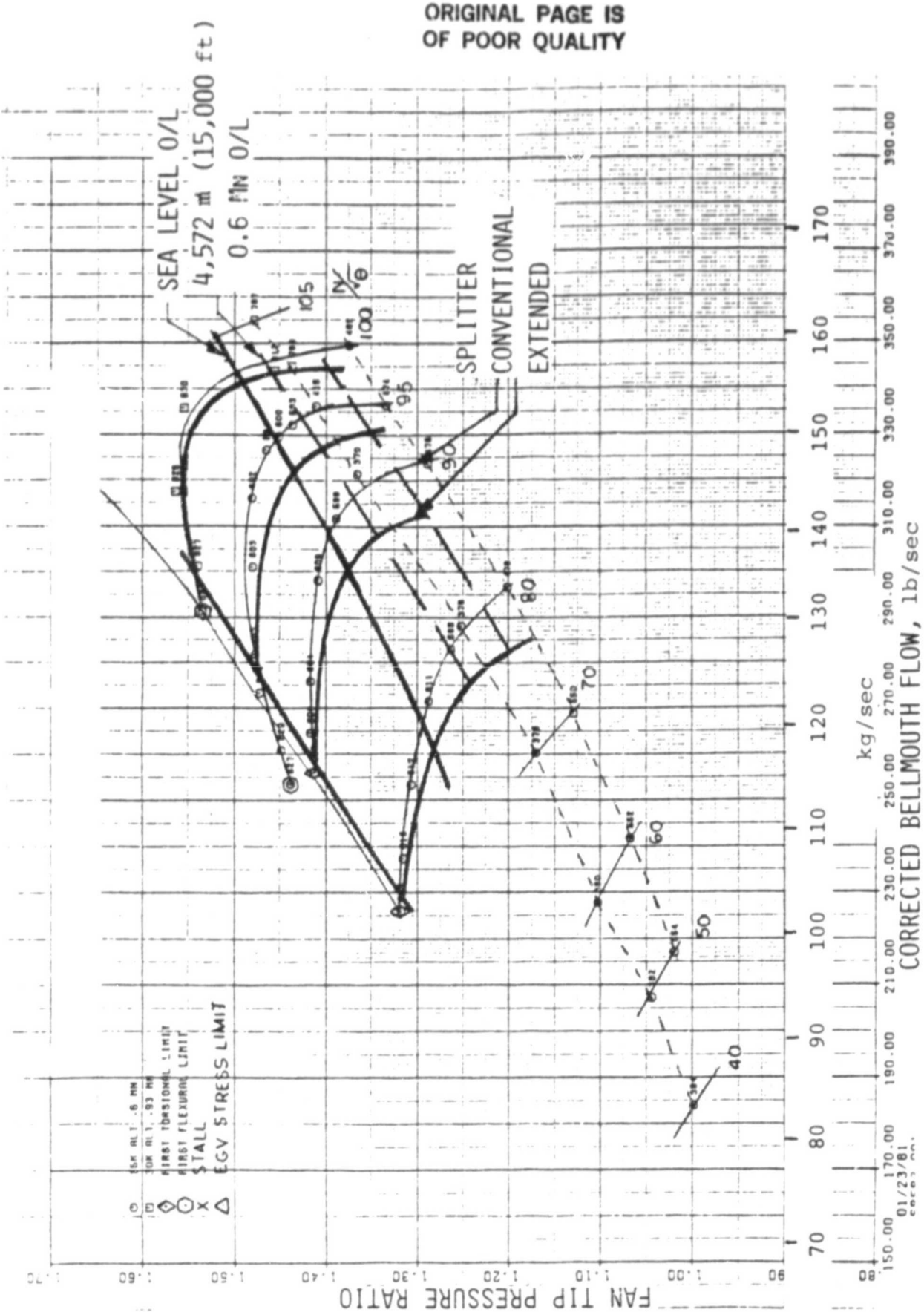

Figure 19. Fan Map Conventional Splitter, IGV Angle = 0°

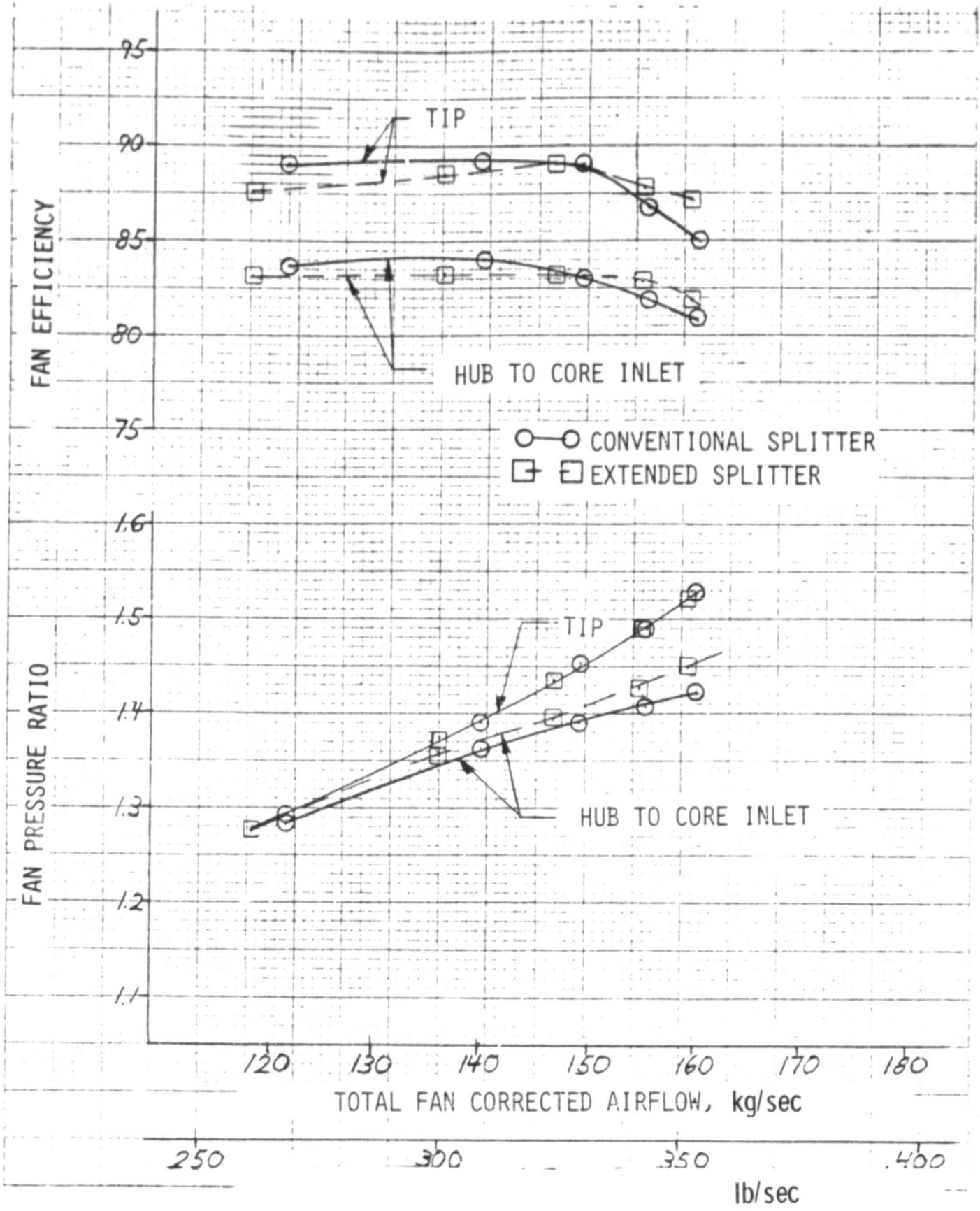

Figure 20. Conventional vs. Extended Splitter
Sea Level Operating Line 0° IGV

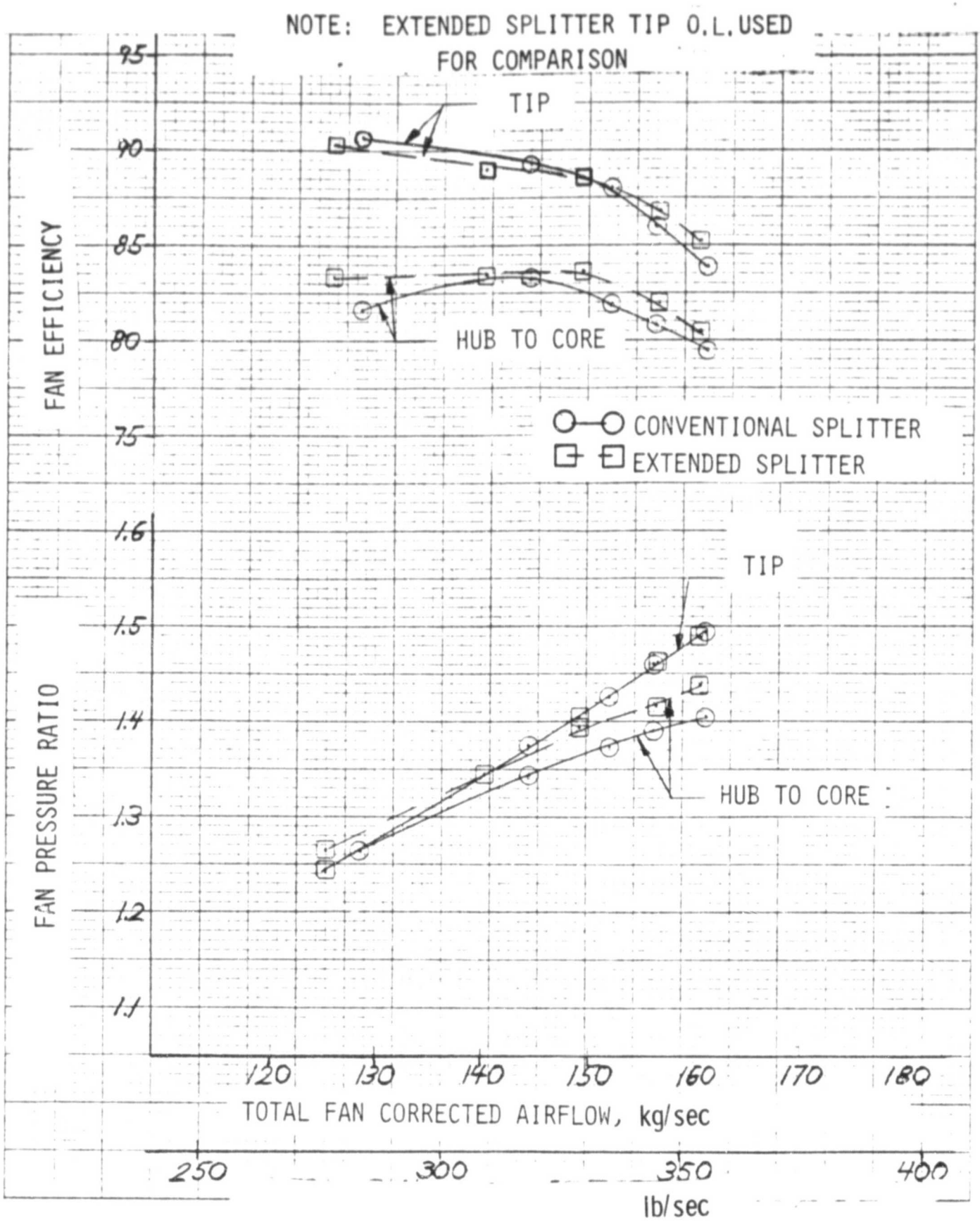

Figure 21. Conventional vs. Extended Splitter
4,572 m (15,000 ft) Mn = 0.6 Operating Line 0° IGV

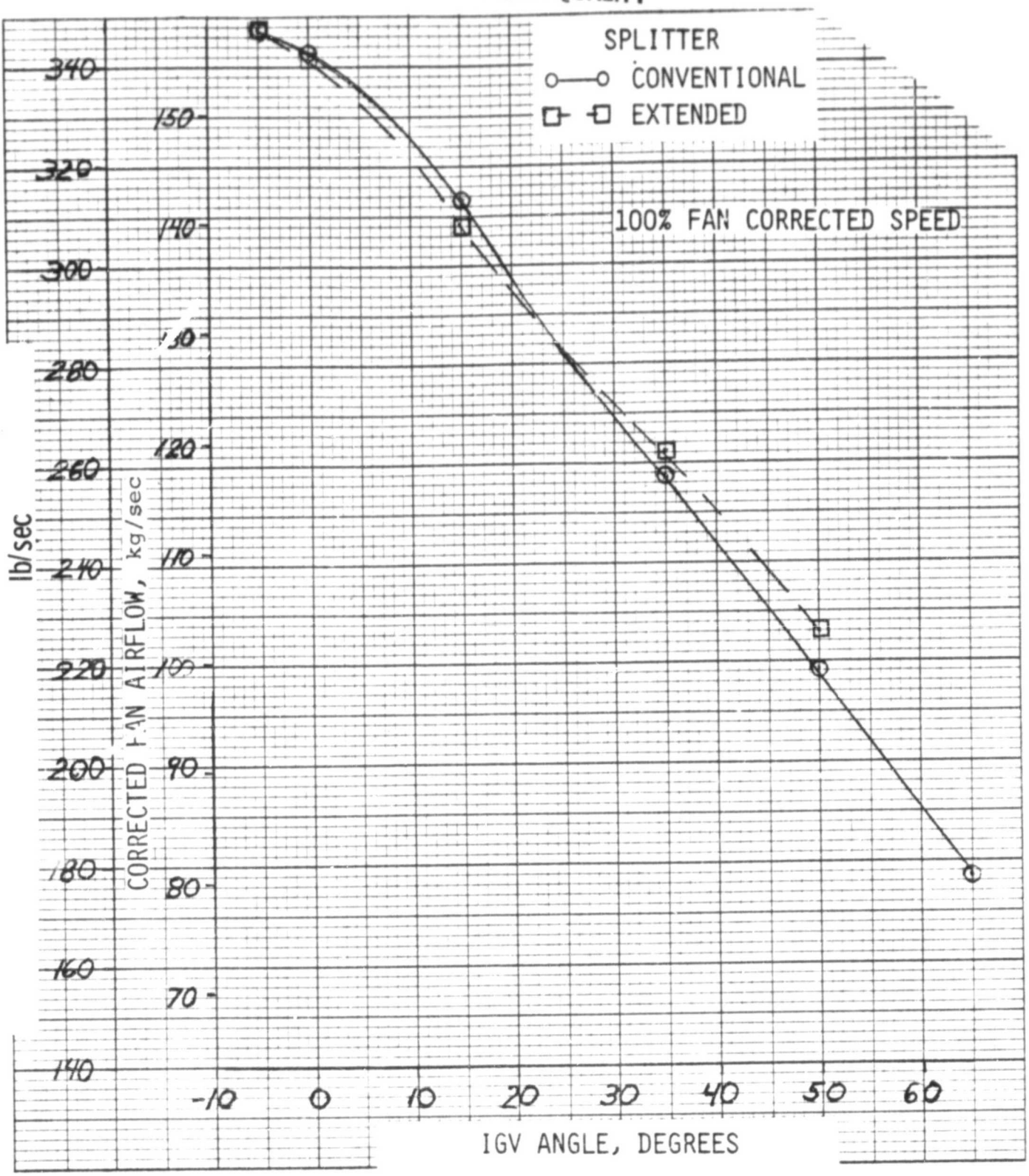

Figure 22. Conventional vs. Extended Splitter
Sea Level Operating Line
Total Flow vs. VIGV Angle

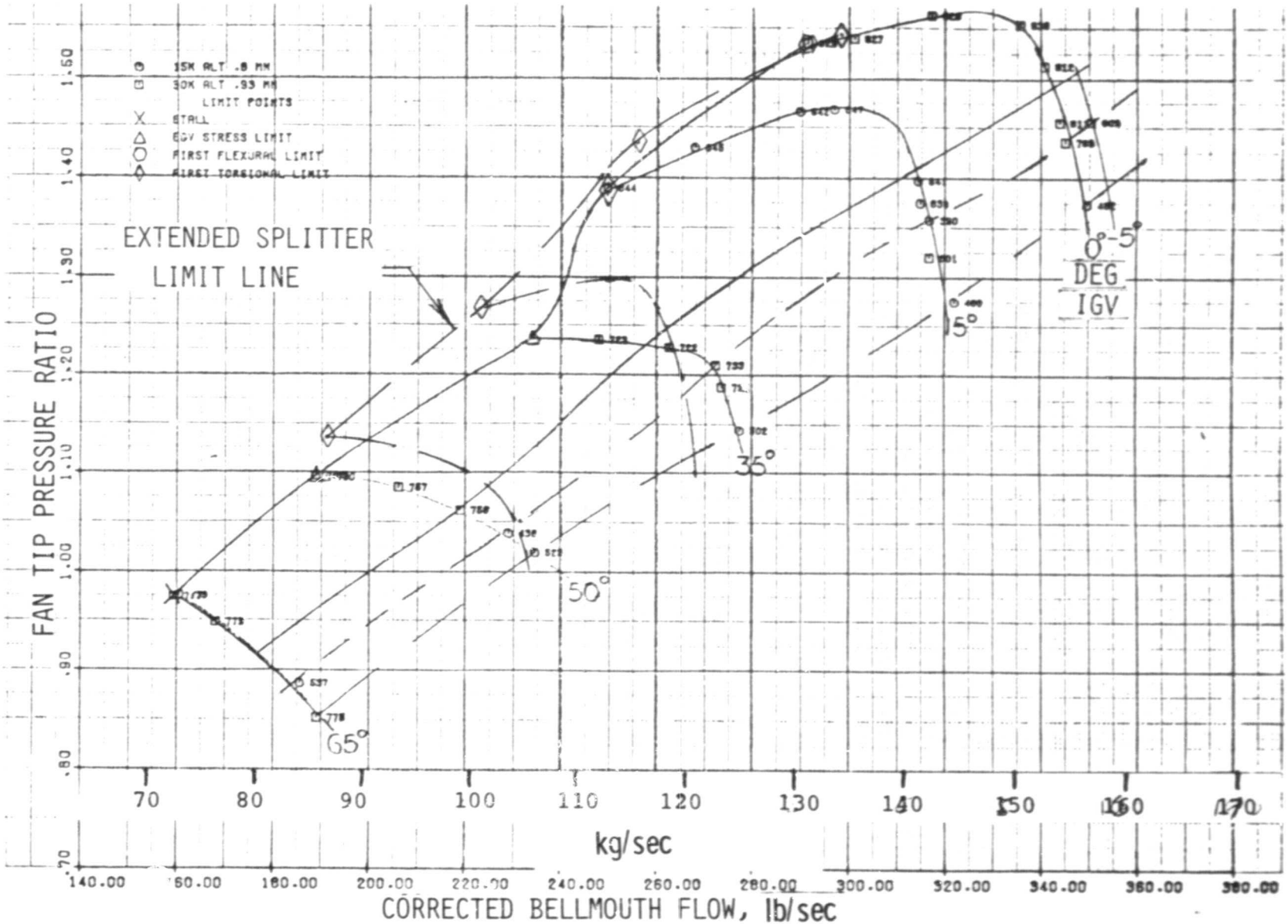

Figure 23. Limit Line Comparison, Conventional versus Extended Splitter at 100 Percent Speed

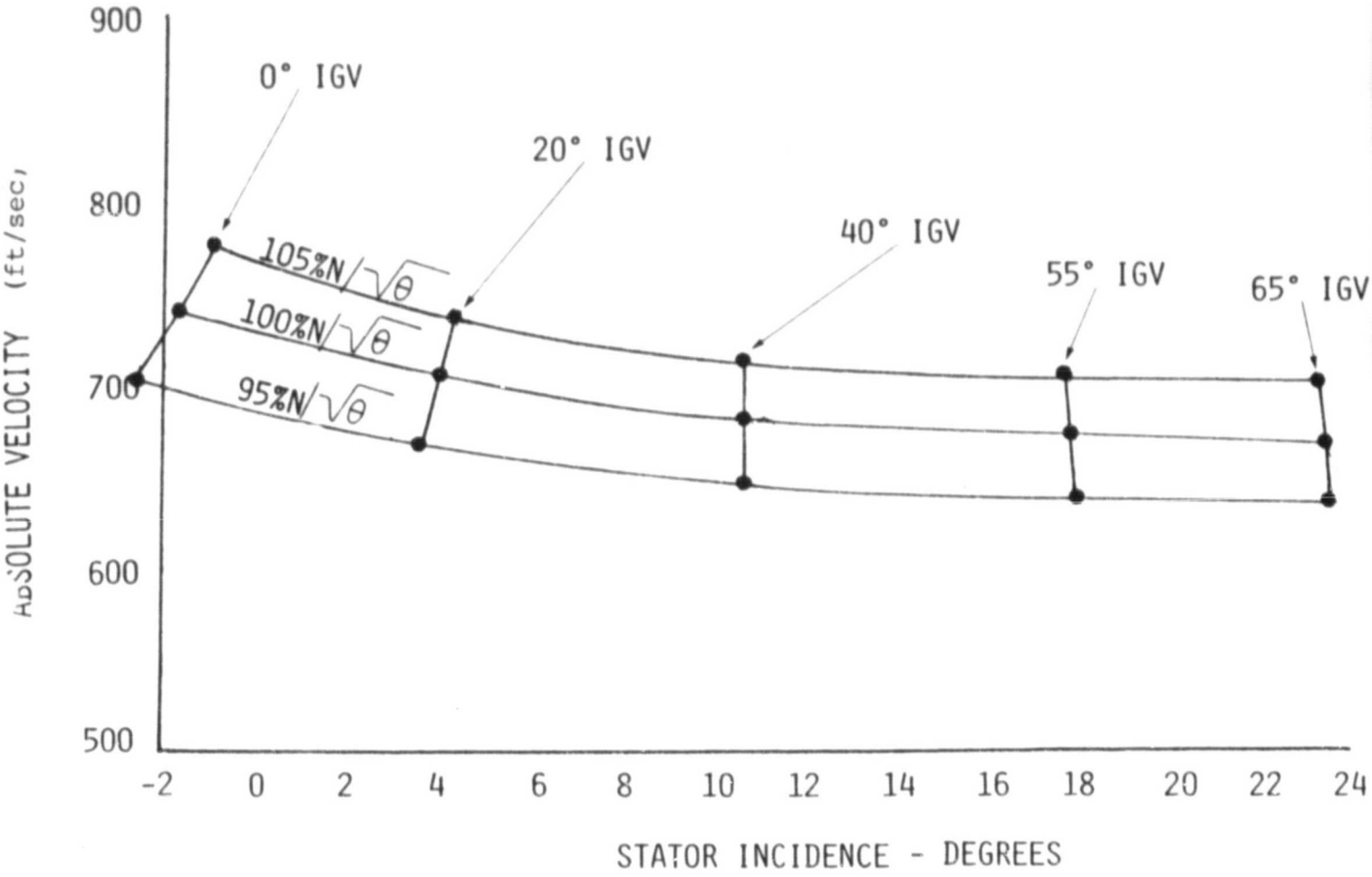

Figure 24. Exit Guide Vane Incidence as a Function of IGV Angle

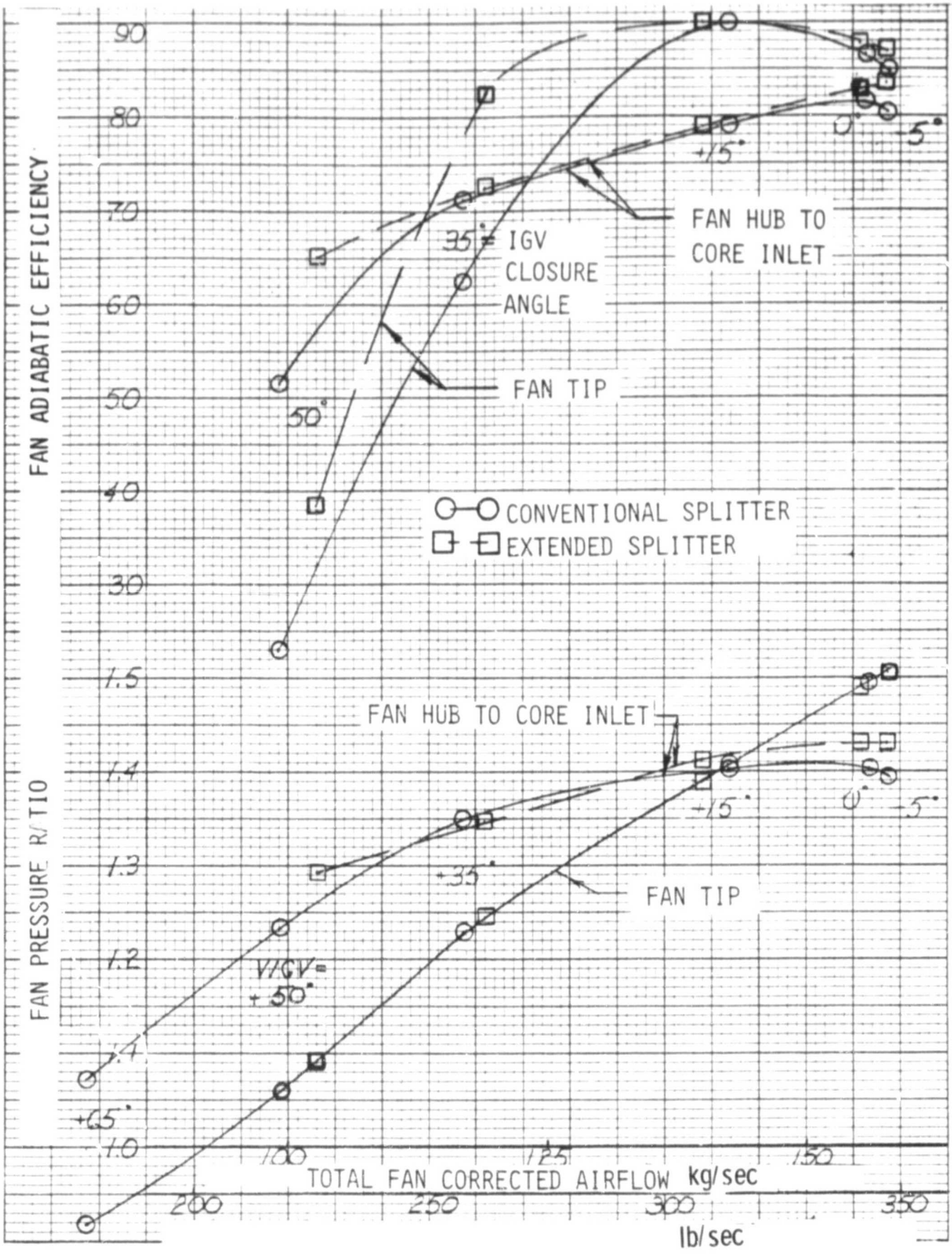

Figure 25. Conventional vs. Extended Splitter
Sea Level Operating Line 100% Fan Corr. Speed

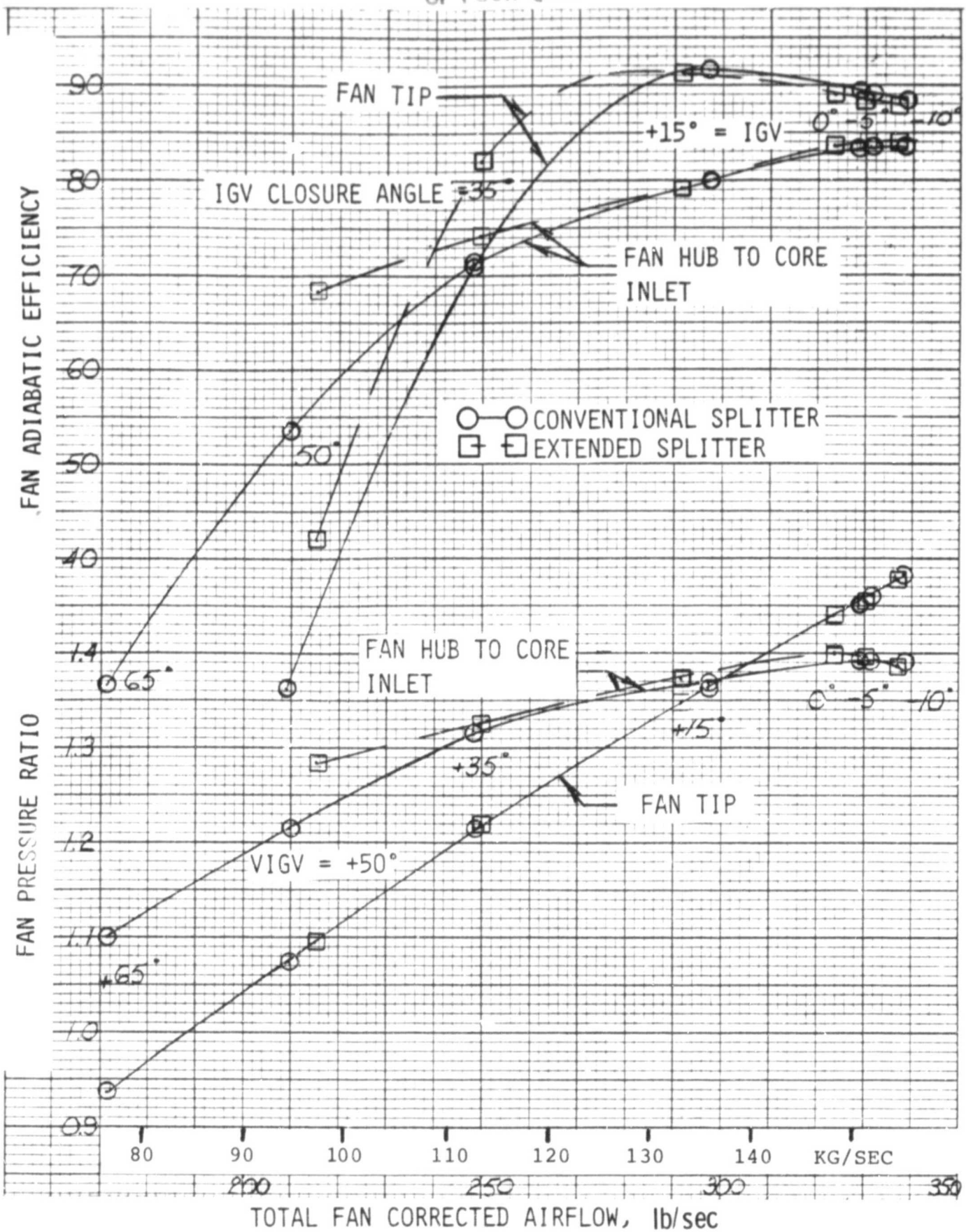

Figure 26. Conventional vs. Extended Splitter
Sea Level Operating Line 95% Corr. Fan Speed

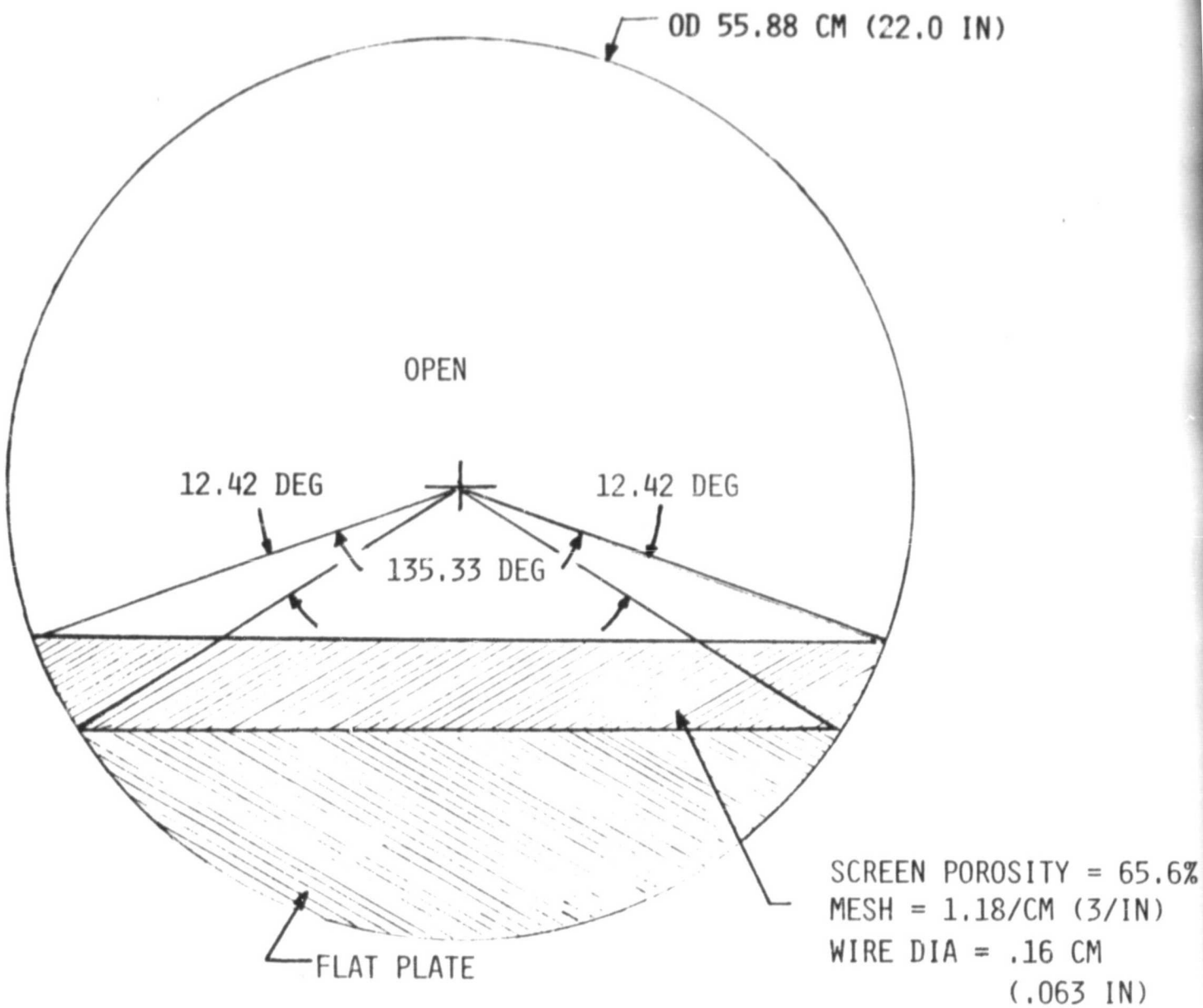

Figure 27. TF34 Fan Crosswind Distortion Screen No. 1

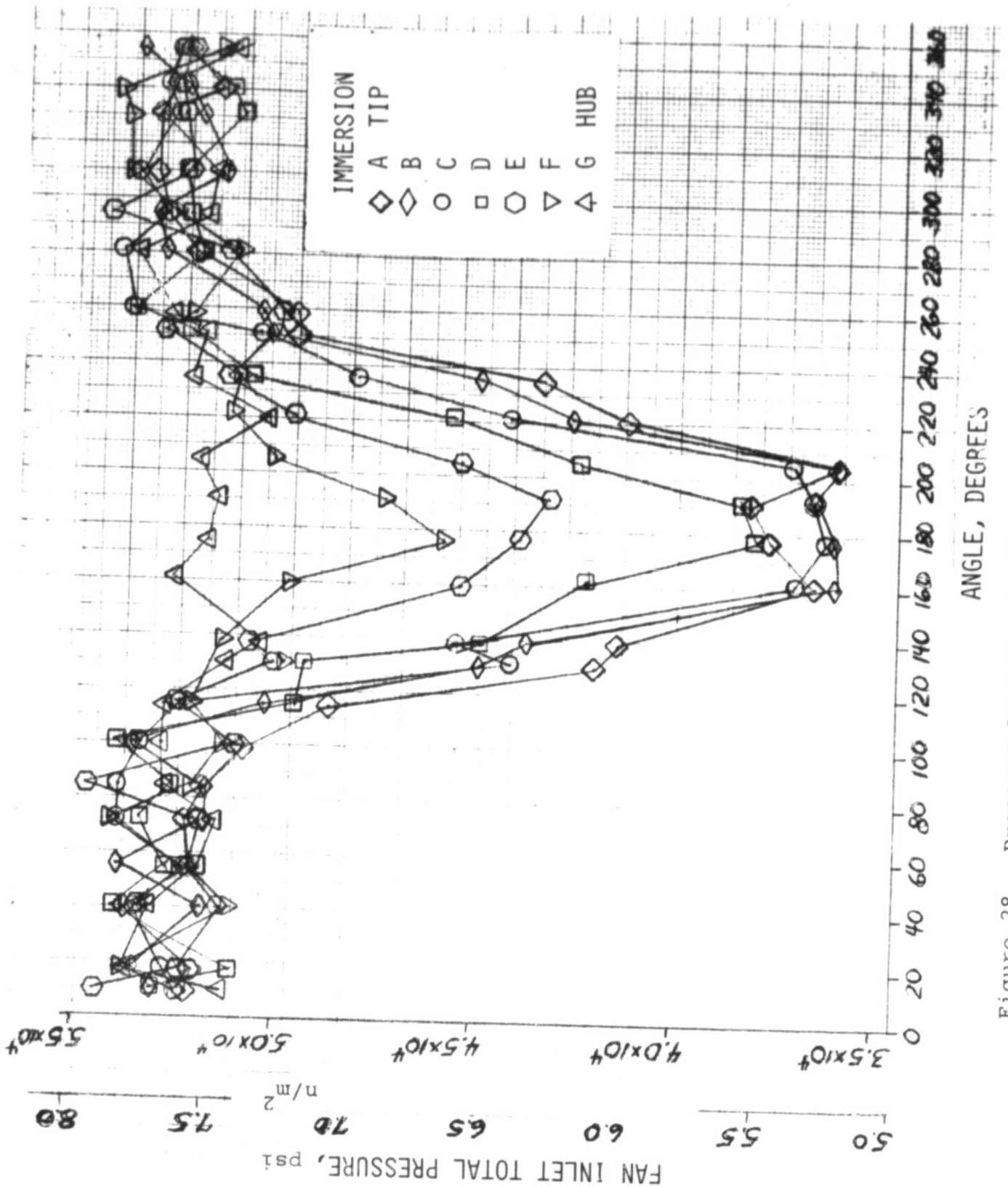

Figure 28. Pressure Loss Due to Distortion at the Fan Inlet
TF34 Crosswind Distortion Screen #1

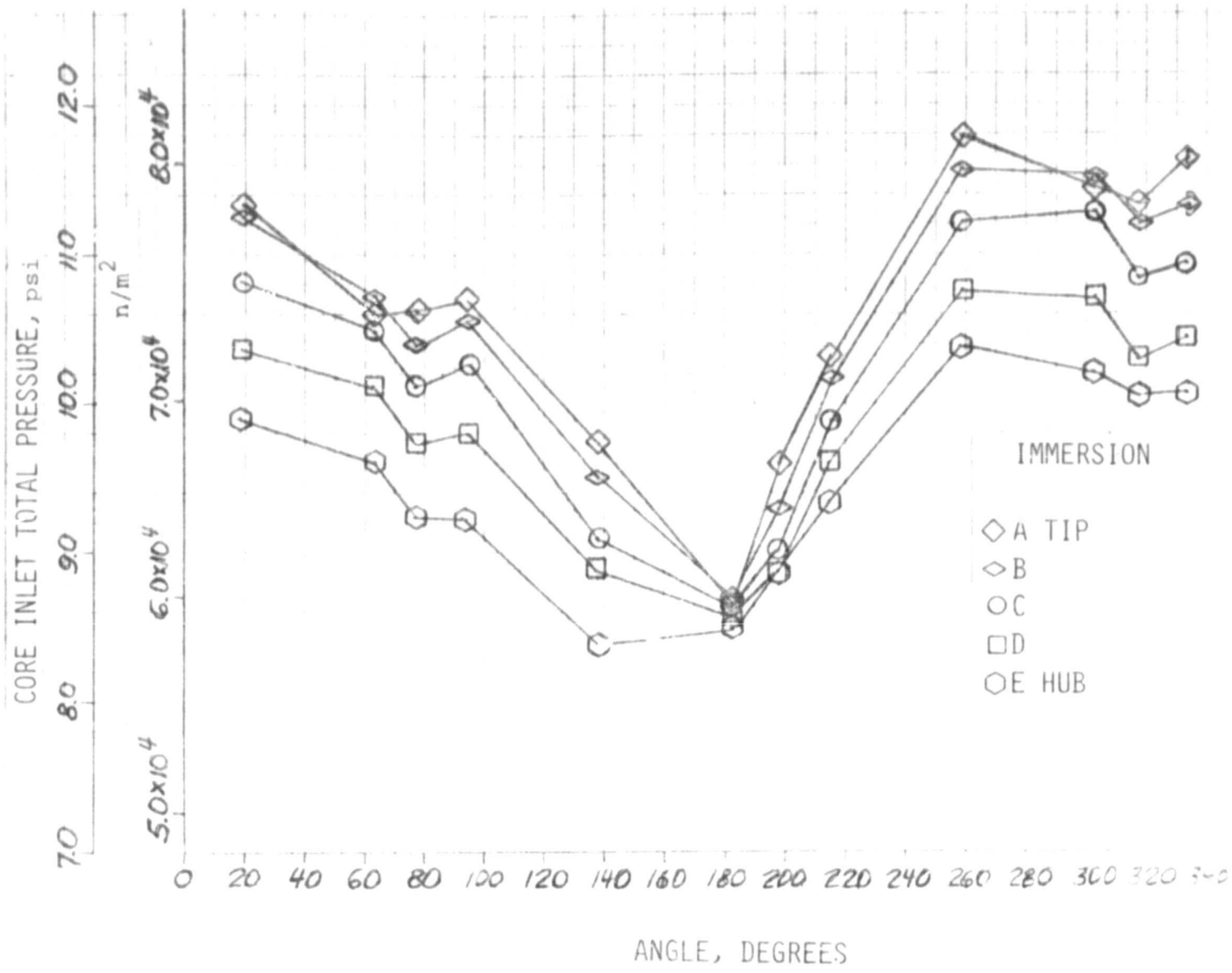

Figure 29. Pressure Loss Due to Distortion at the Core Inlet
TF34 Crosswind Distortion Screen #1

$$IDC = \frac{P_{RING\ AVG} - P_{RING\ MIN}}{P_{FACE\ AVG}}$$ FOR EACH OF THE FIVE RINGS

$$IDC_{HUB} = \frac{IDC_1 + IDC_2}{2}$$

$$IDC_{TIP} = \frac{IDC_4 + IDC_5}{2}$$

$$IDC_{MAX} = \text{GREATER OF } IDC_{HUB} \text{ OR } IDC_{TIP}$$

$$IDR = \frac{P_{FACE\ AVG} - P_{RING\ AVG}}{P_{FACE\ AVG}}$$ FOR EACH OF THE FIVE RINGS

$$IDR_{TIP} = IDR_5 \text{ (TIP RING)}$$

$$IDR_{HUB} = IDR_1 \text{ (HUB RING)}$$

INSTRUMENTATION PLANE (FIVE EQUAL AREA RINGS)

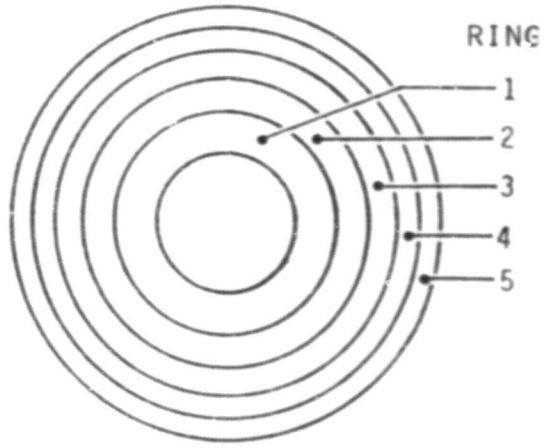

Figure 30. Distortion Definitions

DISTORTION TRANSFER = $IDC_{MAX\ CORE\ INLET}/IDC_{MAX\ FAN\ INLET}$

STALL SENSITIVITY = Δ PRS/$IDC_{MAX\ FAN\ INLET}$

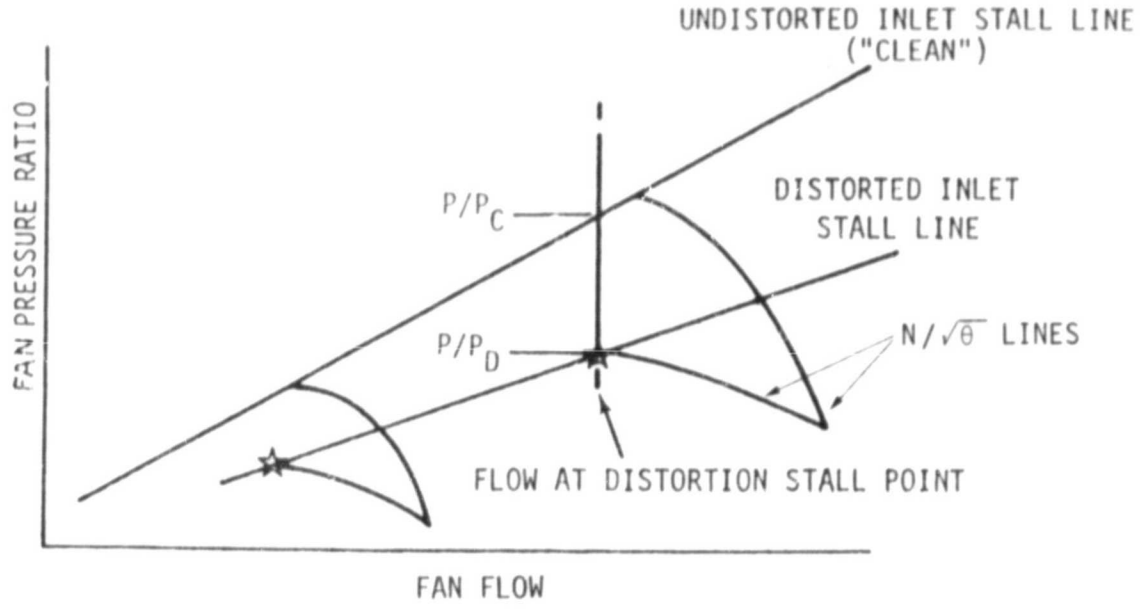

WHERE $\Delta PRS = \dfrac{P/P_{CLEAN\ STALL\ LINE} - P/P_{DISTORTED\ STALL\ LINE}}{P/P_{CLEAN\ STALL\ LINE}}$

AT FLOW OF DISTORTION STALL POINT AND IDC_{MAX} = MAXIMUM CIRCUMFERENTIAL DISTORTION AT DISTORTION STALL POINT FLOW.

Figure 31. Distortion Transfer and Stall Sensitivity Definitions

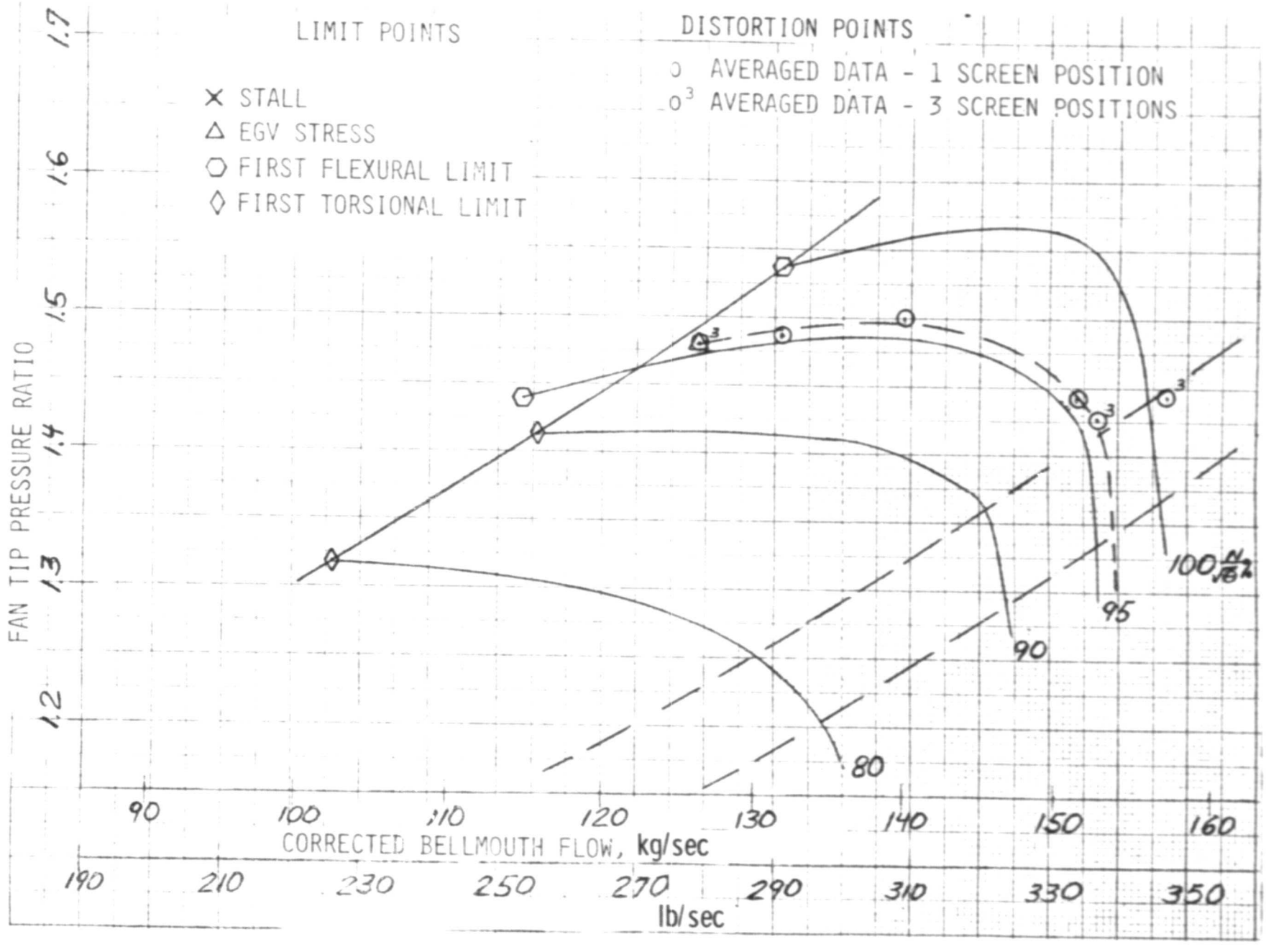

Figure 32. Fan Map Conventional Splitter, IGV Angle = 0°

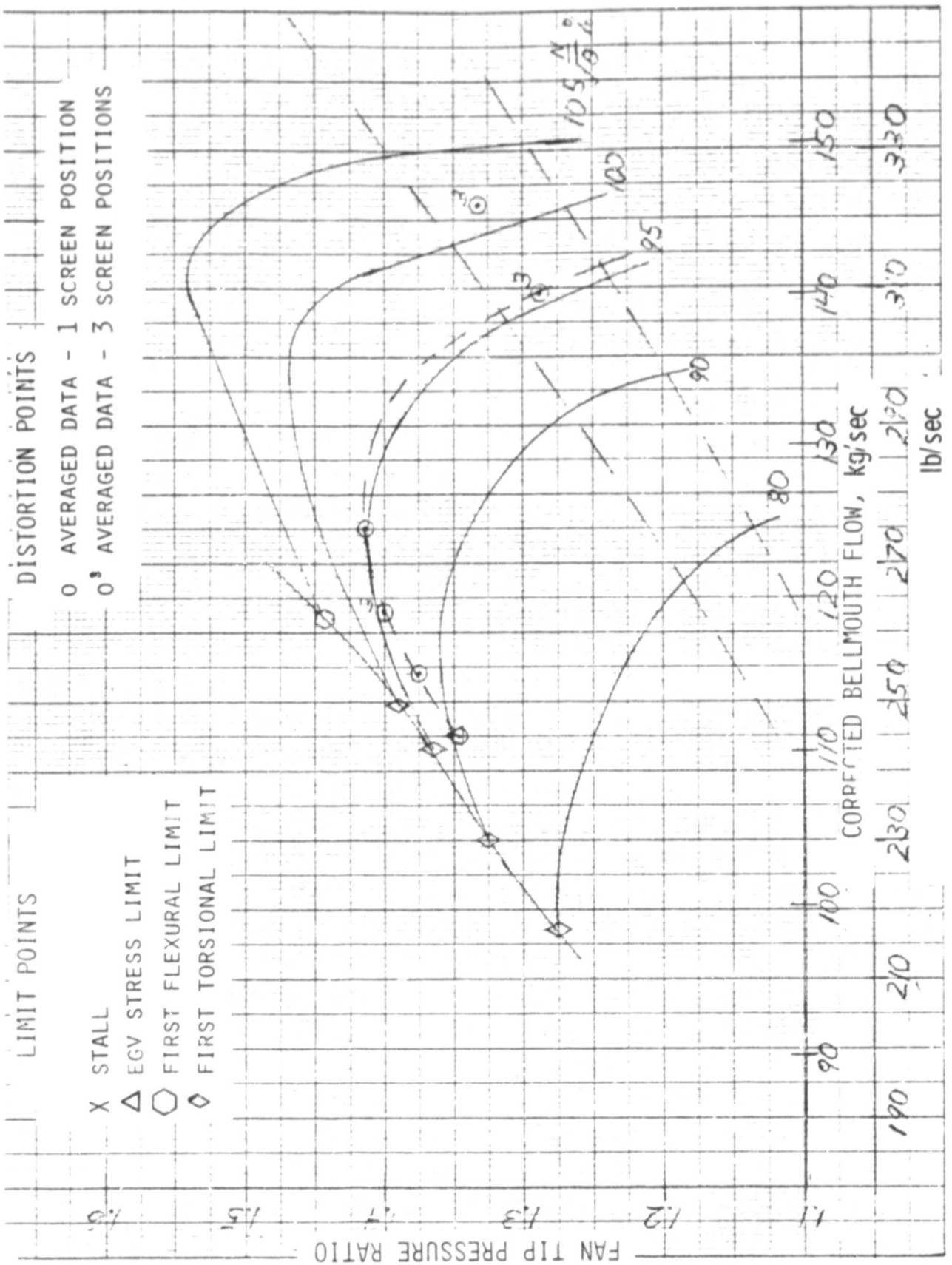

Figure 33. Fan Map Conventional Splitter, IGV Angle = 15°

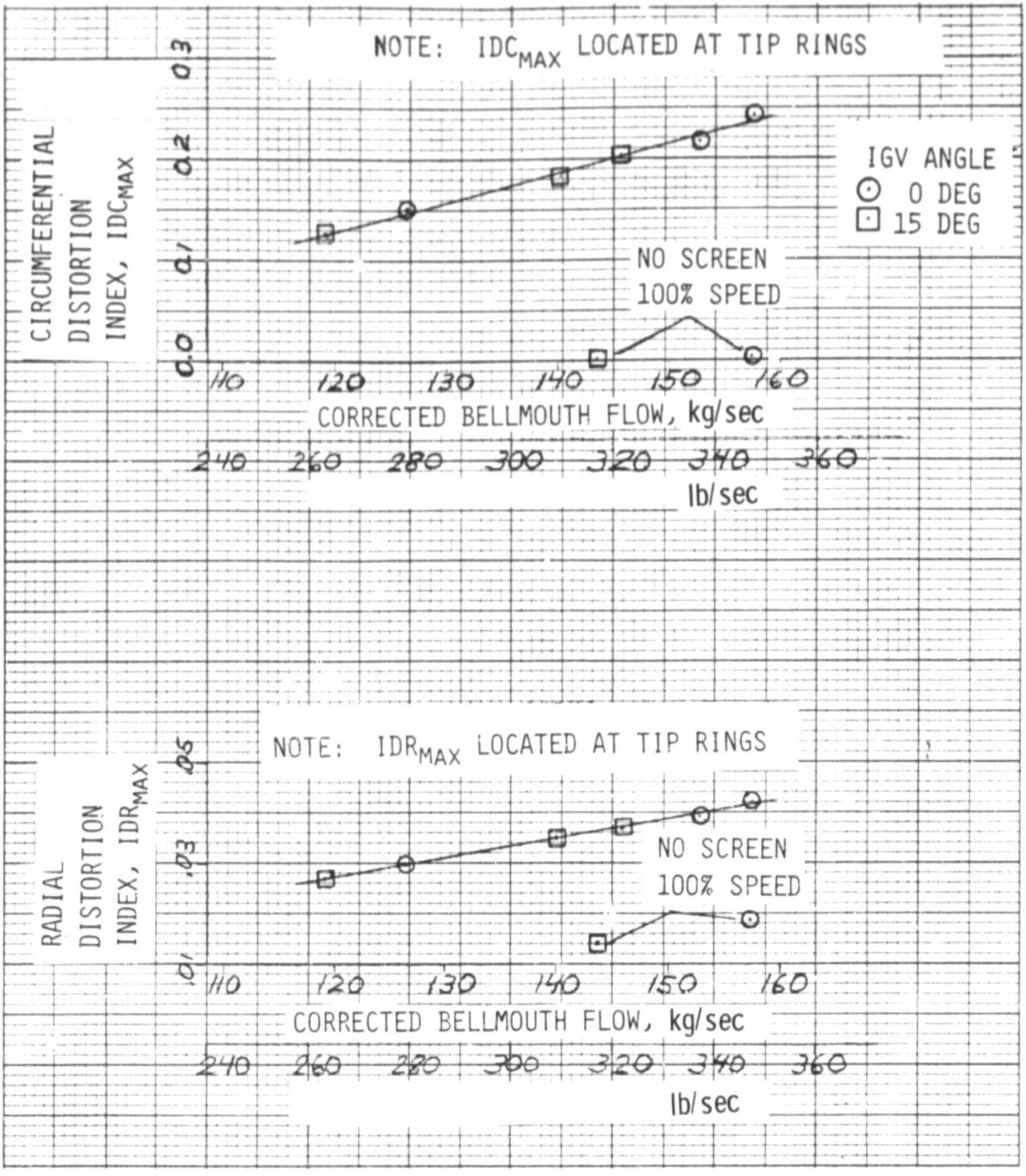

Figure 34. Fan Inlet Distortion
Crosswind Distortion Screen

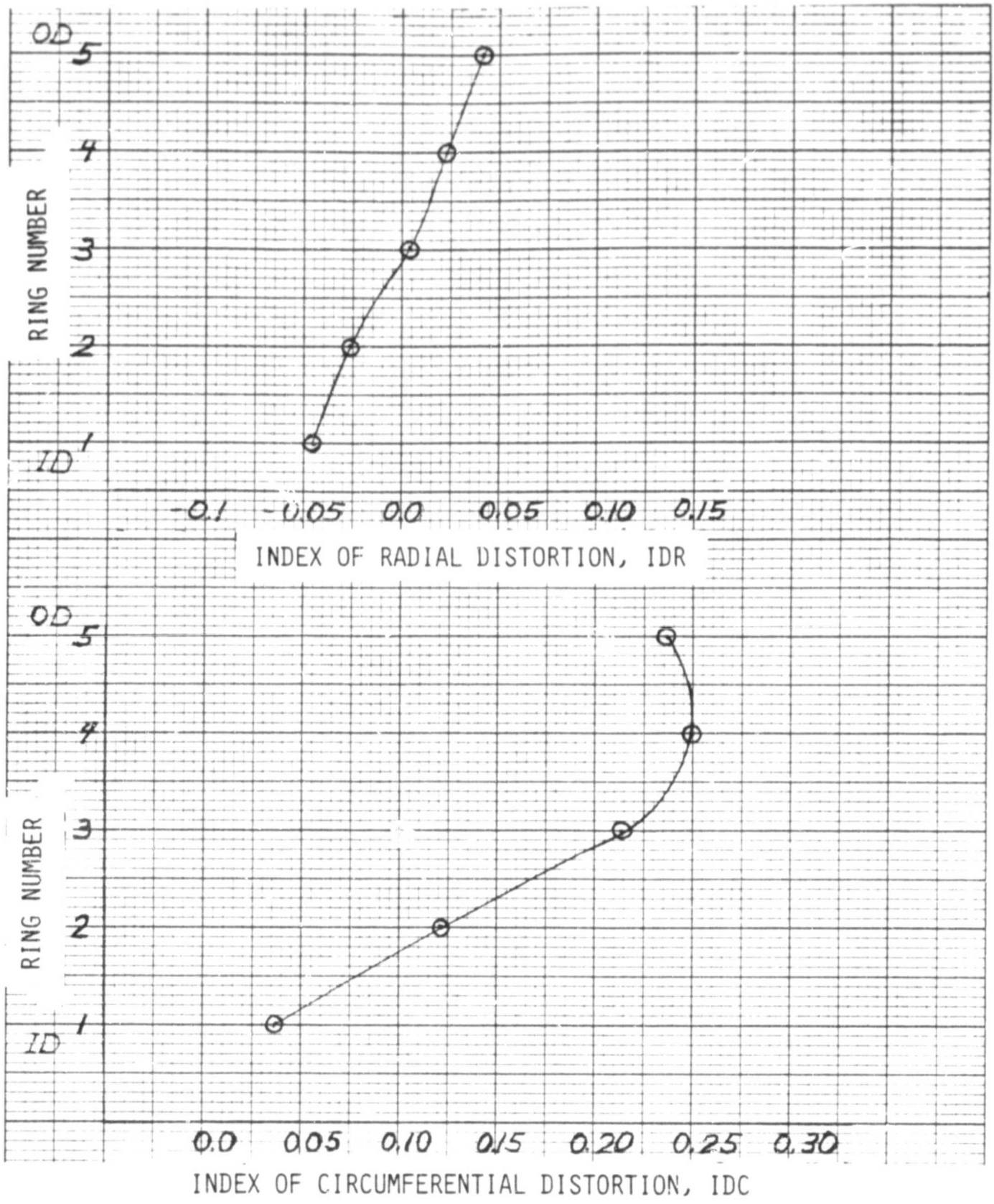

Figure 35. NASA TF34 Distortion Testing, 0° IGV 100% $\sqrt{\frac{N}{\theta}}$ Distortion Index vs. [illegible] g Fan Inlet

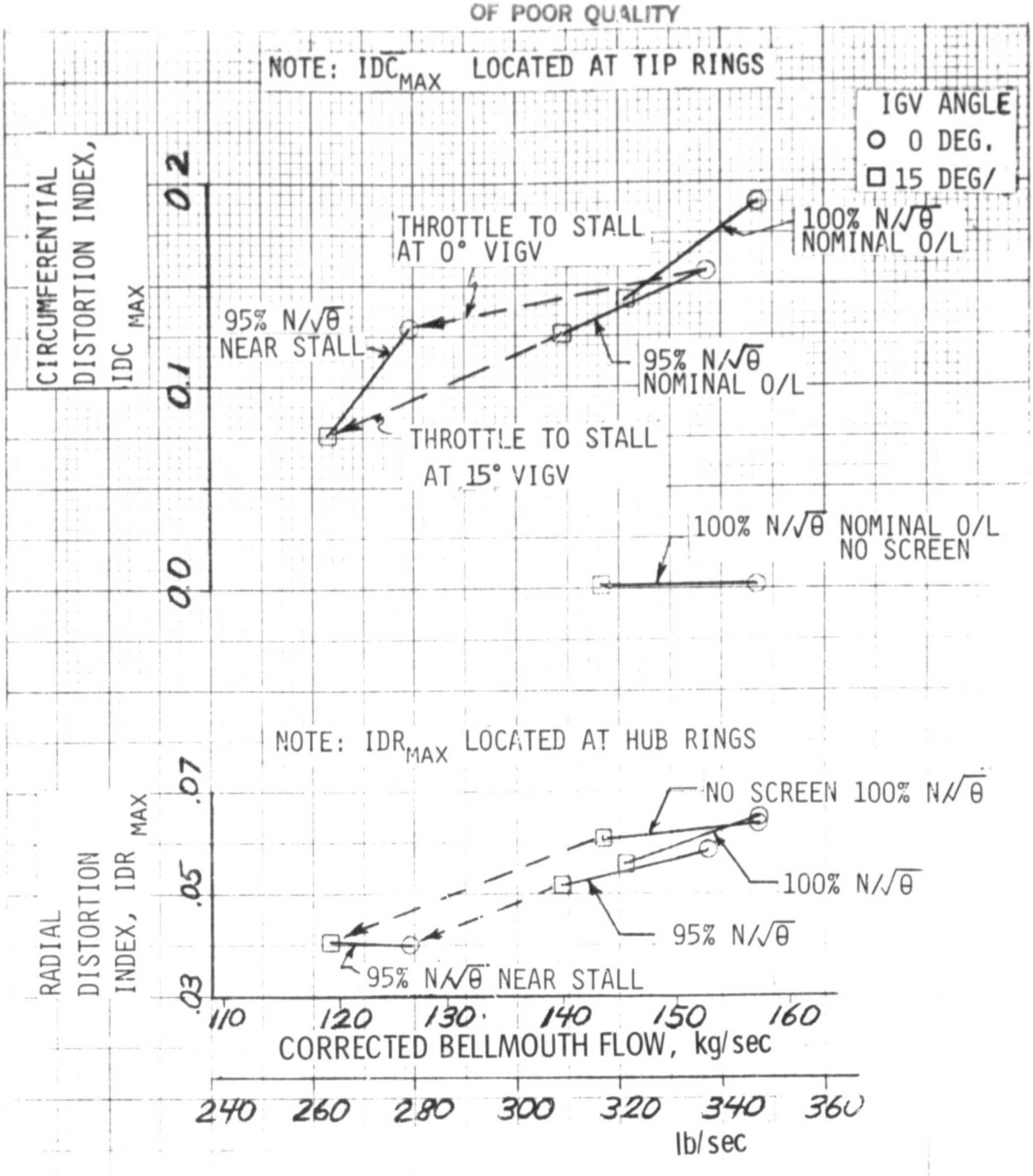

Figure 36. Core Compressor Inlet with Crosswind Distortion Screen

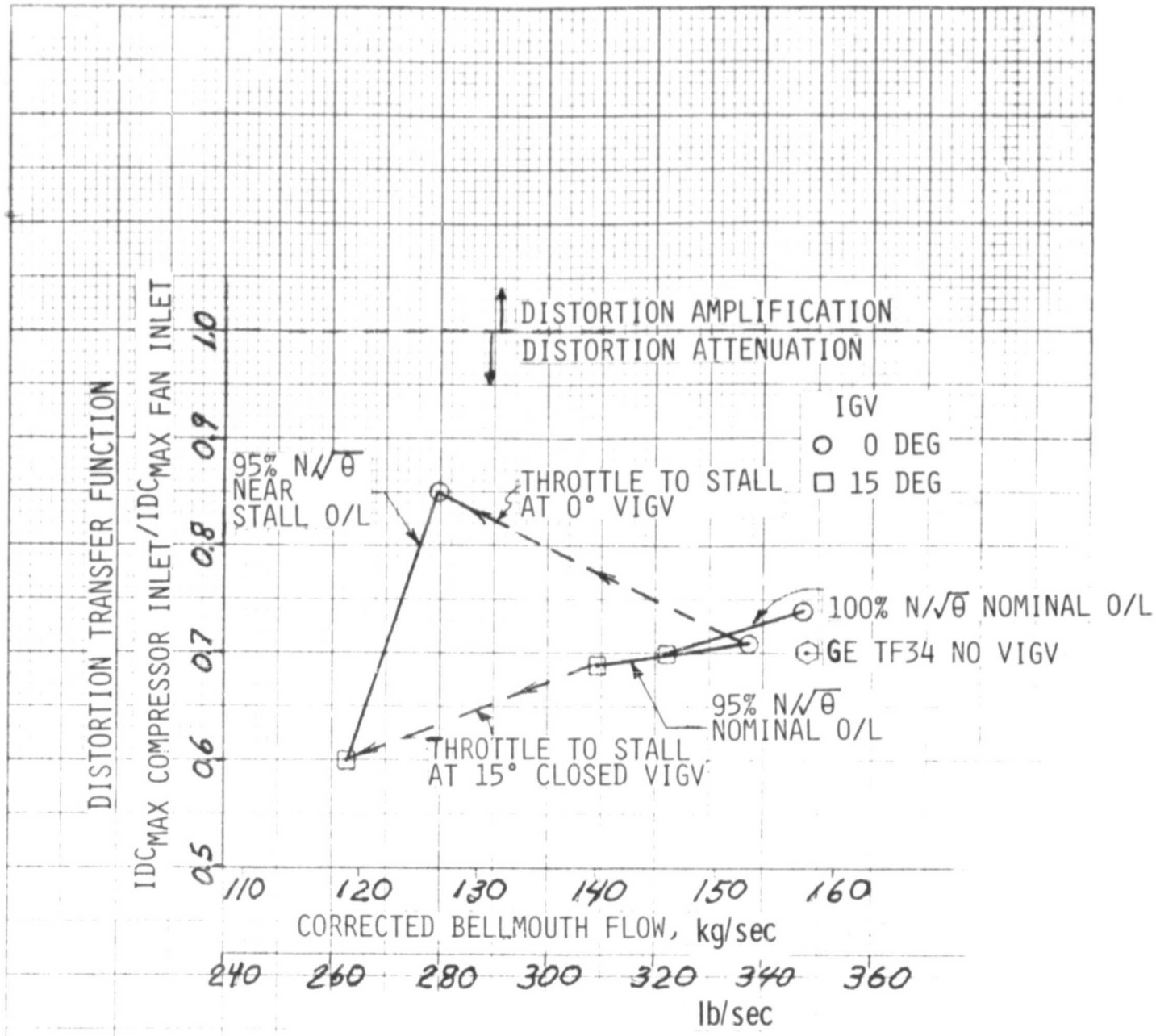

Figure 37. TF34 VIGV Distortion Transfer

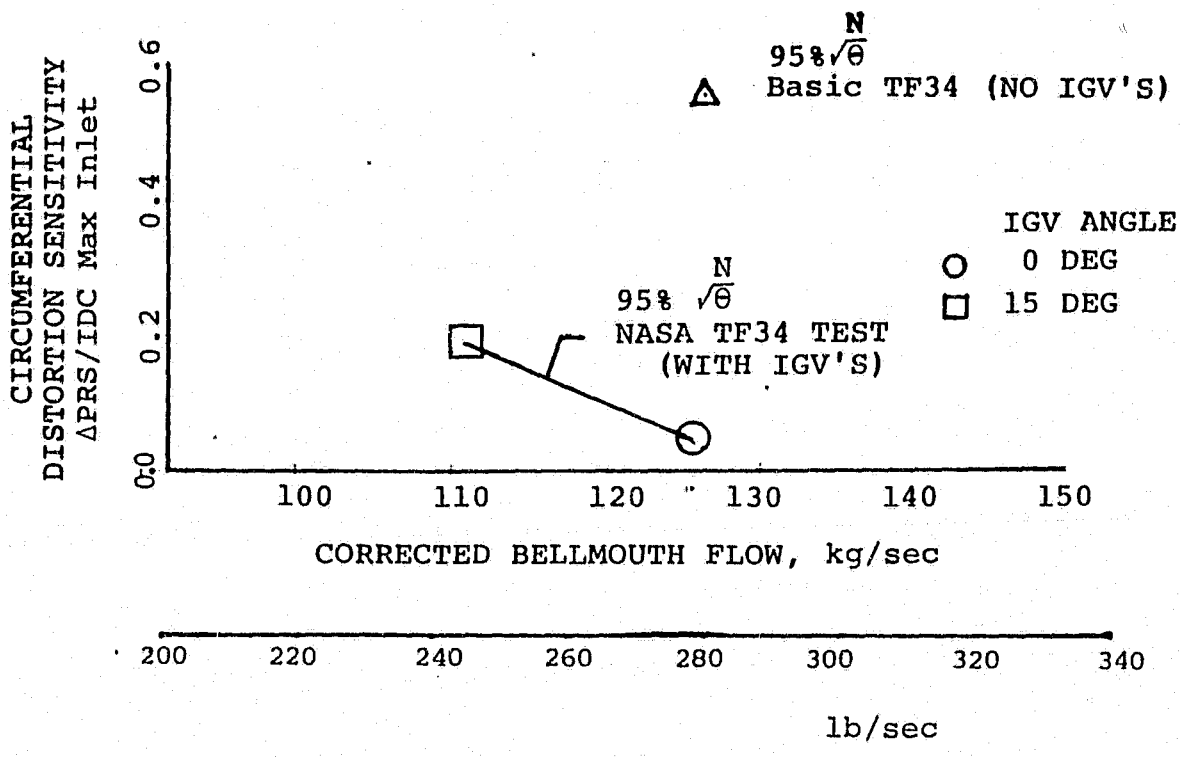

Figure 38. Fan Distortion Sensitivity Reduction Due to Part Span Variable IGV's

ENGINE PERFORMANCE AND SYSTEMS ANALYSIS

Background

Data obtained from this fan engine test provided information for representing product level engine performance, both at Sea Level Takeoff and at 4.57 km, (15k ft)/.6 Mach number cruise.

A comparison of overall performance against prediction was made with part span VIGV's set at zero degrees and along a nominal fan tip operating line. The matching of engine and facility limits at NASA/Lewis precluded sea level testing. Therefore, examination of thrust measurements was made at 4.57km (15k ft) and .6 Mach number. Data for the VTOL takeoff conditions was generated from a cycle model with the revised fan characteristics obtained from the altitude component mapping.

Instrumentation

The fan exit and core inlet were well instrumented. Sufficient additional instrumentation was installed at NASA/Lewis for the determination of internal component performance. Figure 39 shows the station designations together with a key showing where airstream data was collected. Figure 40 summarizes the quantity and types of probes used at each location.

Component Performance

In order to appropriately explain engine performance, assessment of actual component performance is required. Figures 41 through 44 show the general trend between the measured performance levels and those of the baseline TF34 engine. This data is matched to the tested altitude condition, physical geometries and fan speed. The measured efficiency of the low pressure turbine appears to be six points too high, probably due to interturbine instrumentation error. This effect trades off with the high pressure turbine resulting in too low an HPT efficiency. However, the combination of the two turbine levels results in appropriate exiting gas conditions when applied to the model.

In addition, higher than predicted fan duct losses, as indicated in Figure 45, and a slightly different core stream suppression effect result in differences between model and test engine thrust as seen in Figure 46.

Overall Performance

The problem is better defined by examining the actual exhaust gas properties. With the availability of pressure and temperature measurements, gross thrust calculations for a conic nozzle can be made. (Appendix I details the approach used.) It becomes apparent in calculating net thrust that due to the high ram thrust term a large error in net performance may result. Figure 47 shows the results using 4.57km (15k ft)/.6 Mn nominal op line data. The levels of calculated net thrust come from using the "as measured" airflow obtained for each point shown. In developing Figure 47, the TF34-100 product engine thrust coefficients were incorporated (Cv_{bypass} = .99; Cv_{core} = .9944). The effect of varying thrust coefficients is shown on Figure 48, establishing a range of estimated performance. It appears as if thrust levels may be explained within an allowable tolerance. However, any further analysis of the exhaust system is beyond the scope of this report.

VTOL Operation

Since no actual testing at sea level static standard day conditions was conducted, it was necessary to predict the sea level operation of the fan along some operating line resulting from inlet guide vane movement at constant fan speed. The decrease of fan pressure ratio and airflow were thus based on the trends exhibited by the engine at 4.57km (15k ft). On the basis of the higher fan performance achieved with the extended splitter, as shown in the fan component section, this configuration was chosen for our sample vehicle. Table 2 contains the fan characteristics read from the component map and used to obtain the thrust modulation characteristic shown in Figure 49. Note, that TF34 product level components are assumed. Also, average thrust levels are shown without margins since these data are considered direct results from testing at 4.57km, but computationally rematched at sea level static.

A comparison between the new thrust modulation estimates and previous prediction is shown in Figure 50. The average slope of thrust loss to VIGV closure at 100 percent fan speed, (about 1.37 percent thrust per degree), is stronger than predicted due to higher incidence angle losses occurring across the fan tip system. The levels of thrust shown at 100 percent fan speed and 0° VIGV angle result with the relaxation of the present TF34 turbine temperature limits.

In the case of a twin engine application, modulation of fan thrust is not only important for the conversion of available gas thrust power to fan shaft power, but also for attitude control of the aircraft during critical maneuvers, such as takeoff and landing.

Because of this requirement, fast response of thrust to geometry change (in this case VIGV movement) is necessary.

Figure 51 is a replot of the thrust data generated, including gas generator characteristics, with the critical VTOL points superimposed. The levels of thrust chosen are based on earlier studies which required:

1. ±20 percent thrust modulation for takeoff

2. Safe One Engine Inoperative (OEI) emergency landing (@ 95 percent fan speed) also with ±20 percent thrust modulation.

Figure 51 addresses the considerations of the systems discussed in Reference 1.

For the stated requirements, it is shown that VIGV movement can be limited to only 40°. This smaller control movement may be desirable from a control and hardware standpoint.

Subsequent studies for some VTOL airframe applications suggest that only ±9 percent modulation may be necessary with nominal takeoff thrust at about 9000 pounds thrust per engine.

TABLE 2

TF34 FAN CHARACTERISTICS WITH VIGV CLOSURE - SLS STD. DAY
(Based on Predicted Operating Line Migration and Extended Splitter)

Fan Speed	VIGV Degrees	Airflow KG/Sec (#/sec)	Efficiency Tip	Efficiency Hub*	Pressure Ratio Tip	Pressure Ratio Hub*
100%	-5	157.4 (347)	.870	.861	1.51	1.45
	0	154.7 (341)	.878	.856	1.49	1.45
	15	139.7 (308)	.900	.812	1.39	1.43
	35	118.8 (262)	.825	.746	1.25	1.36
	50	102.5 (226)	.388	.667	1.09	1.30
95%	0	147.0 (324)	.890	.865	1.44	1.42
	15	132.5 (292)	.912	.814	1.35	1.39
	35	113.4 (250)	.820	.762	1.22	1.33
	50	97.5 (215)	.420	.685	1.10	1.29

*Levels of hub performance are based on conditions excluding the inter-compressor duct loss for purpose of cycle deck manipulation.

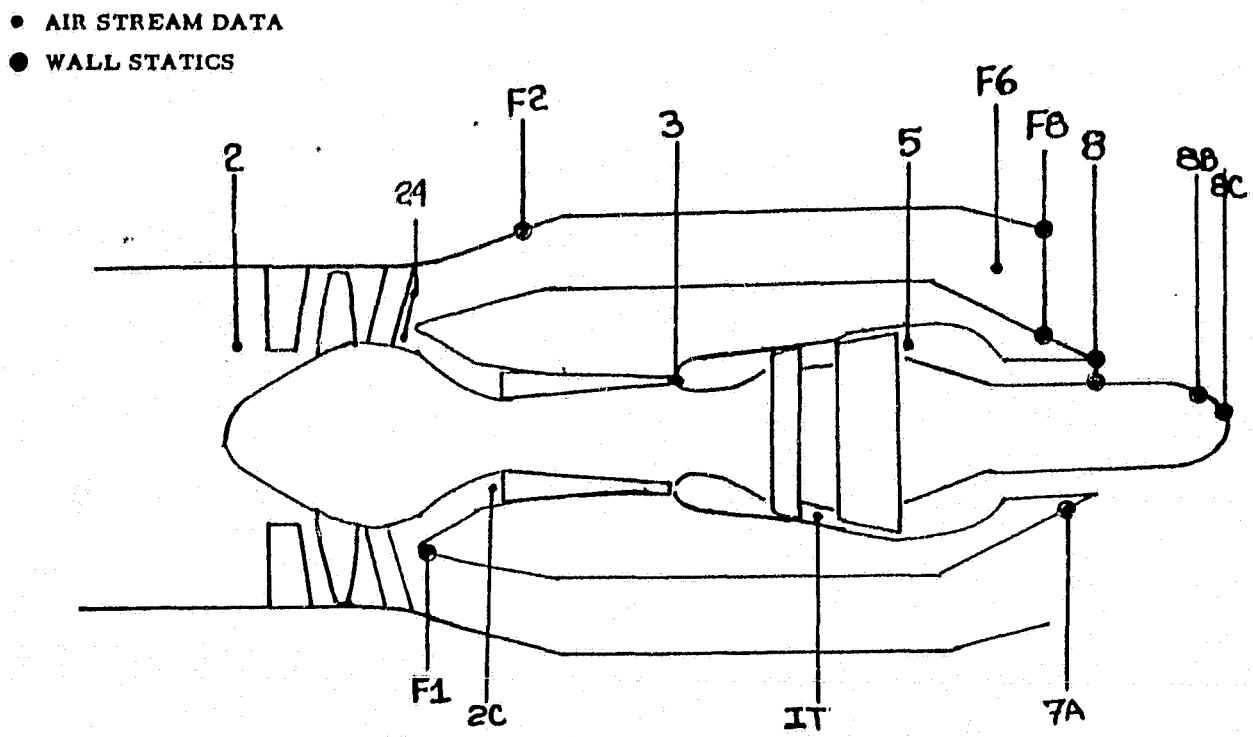

Figure 39. Station Diagram

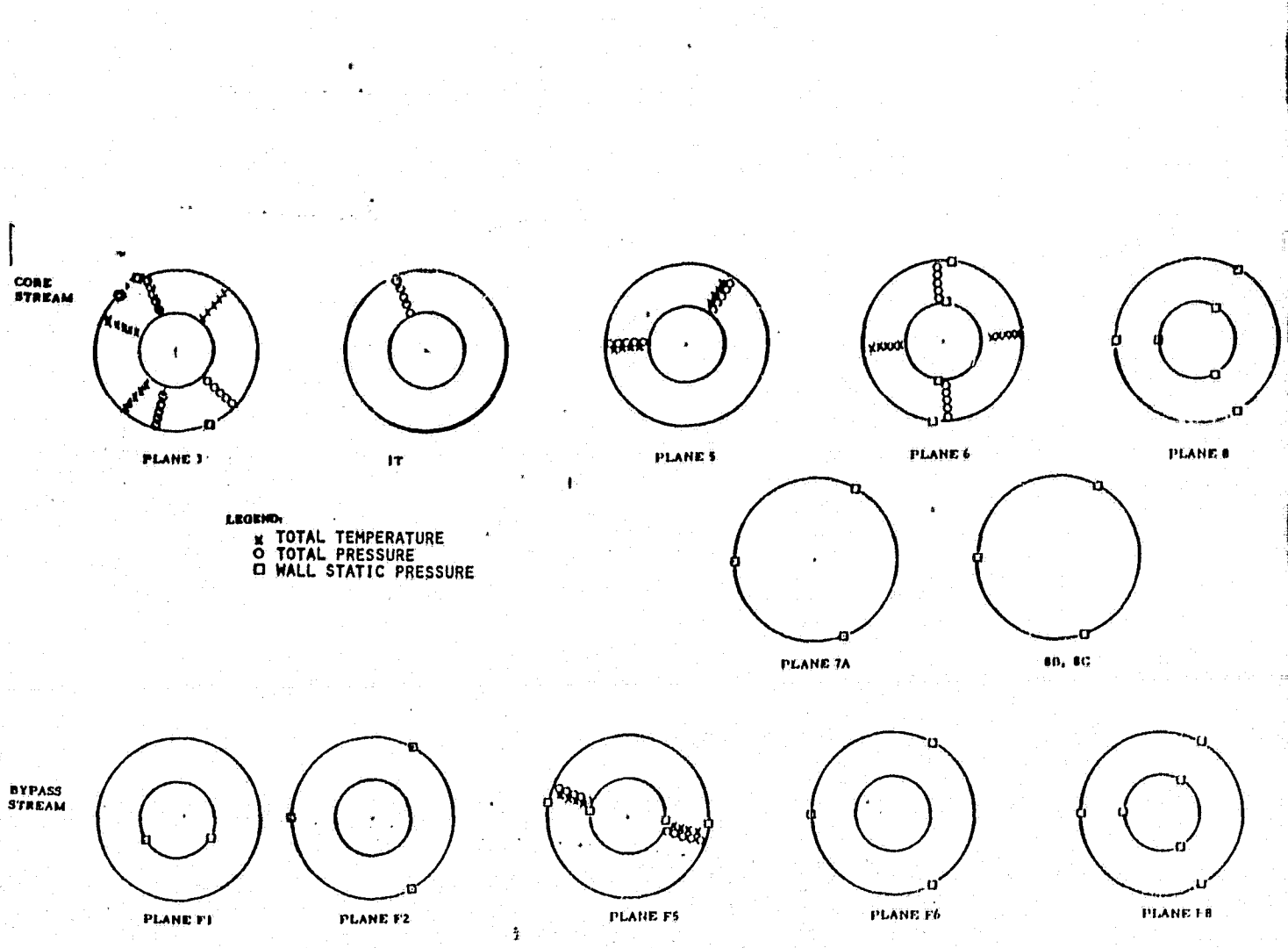

Figure 40. Steadystate Internal Performance Instrumentation (Aft Looking Forward)

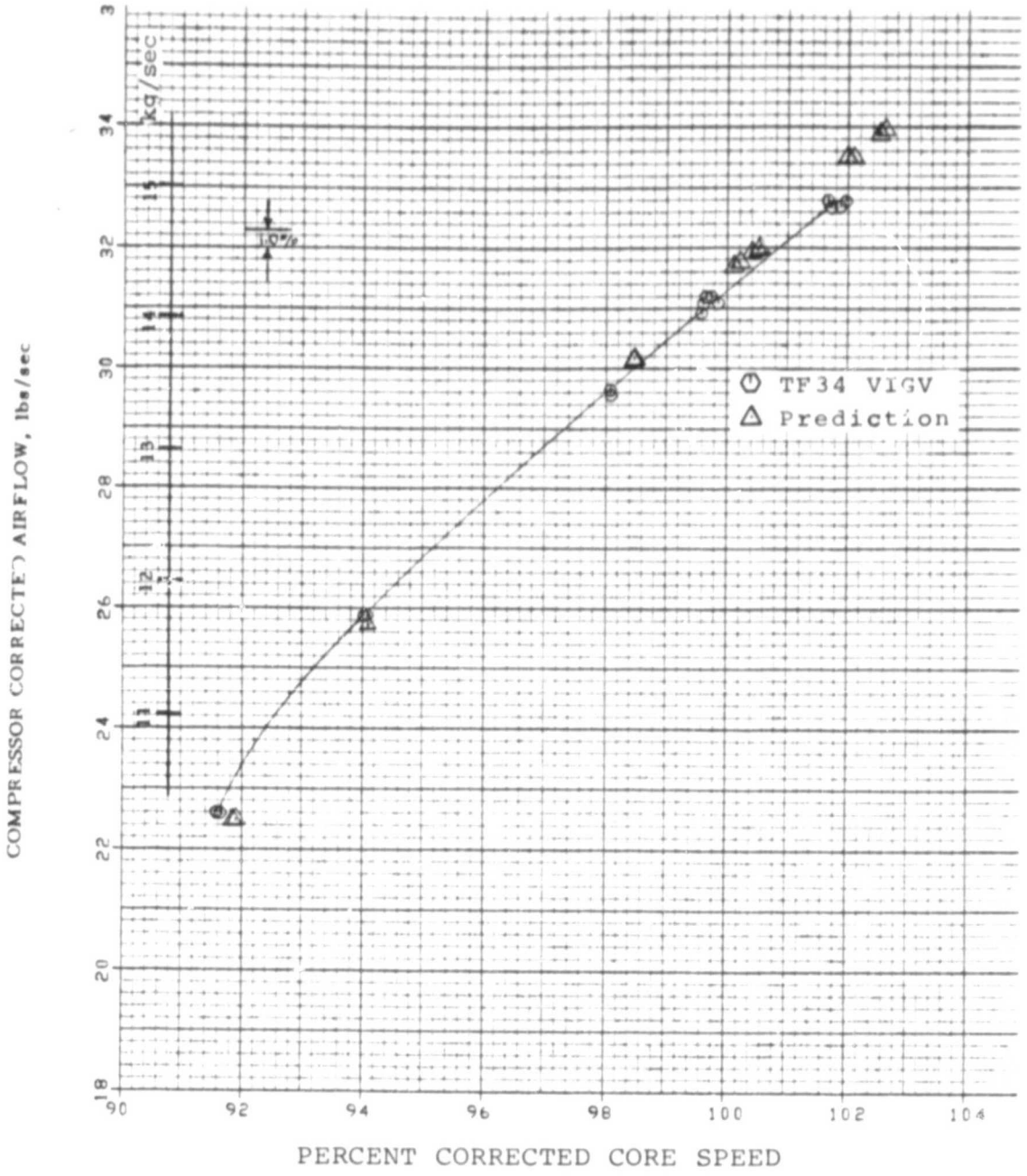

Figure 41. Core Compressor Flow vs. Speed

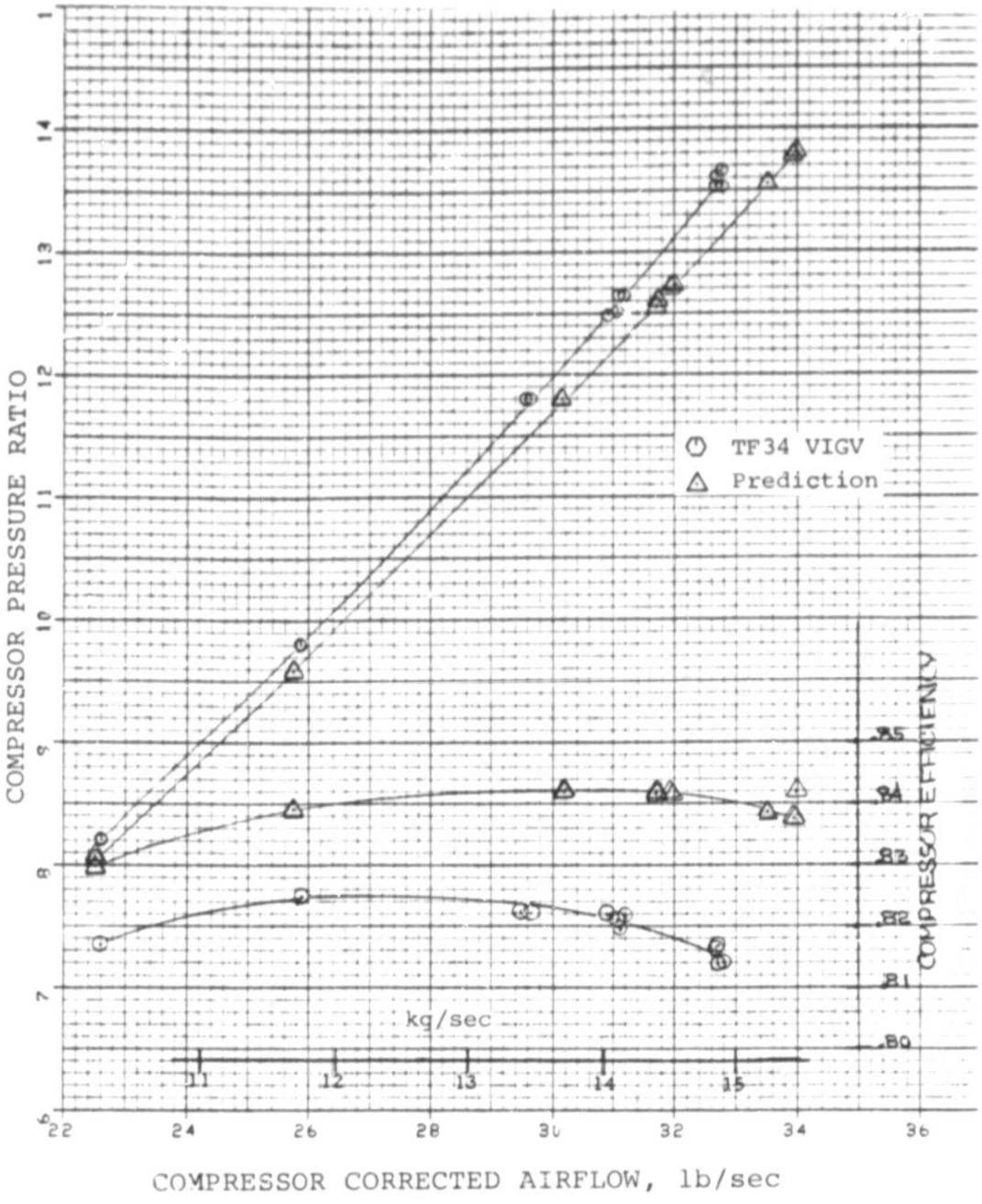

Figure 42. Core Compressor Pressure Ratio vs. Airflow (Core)

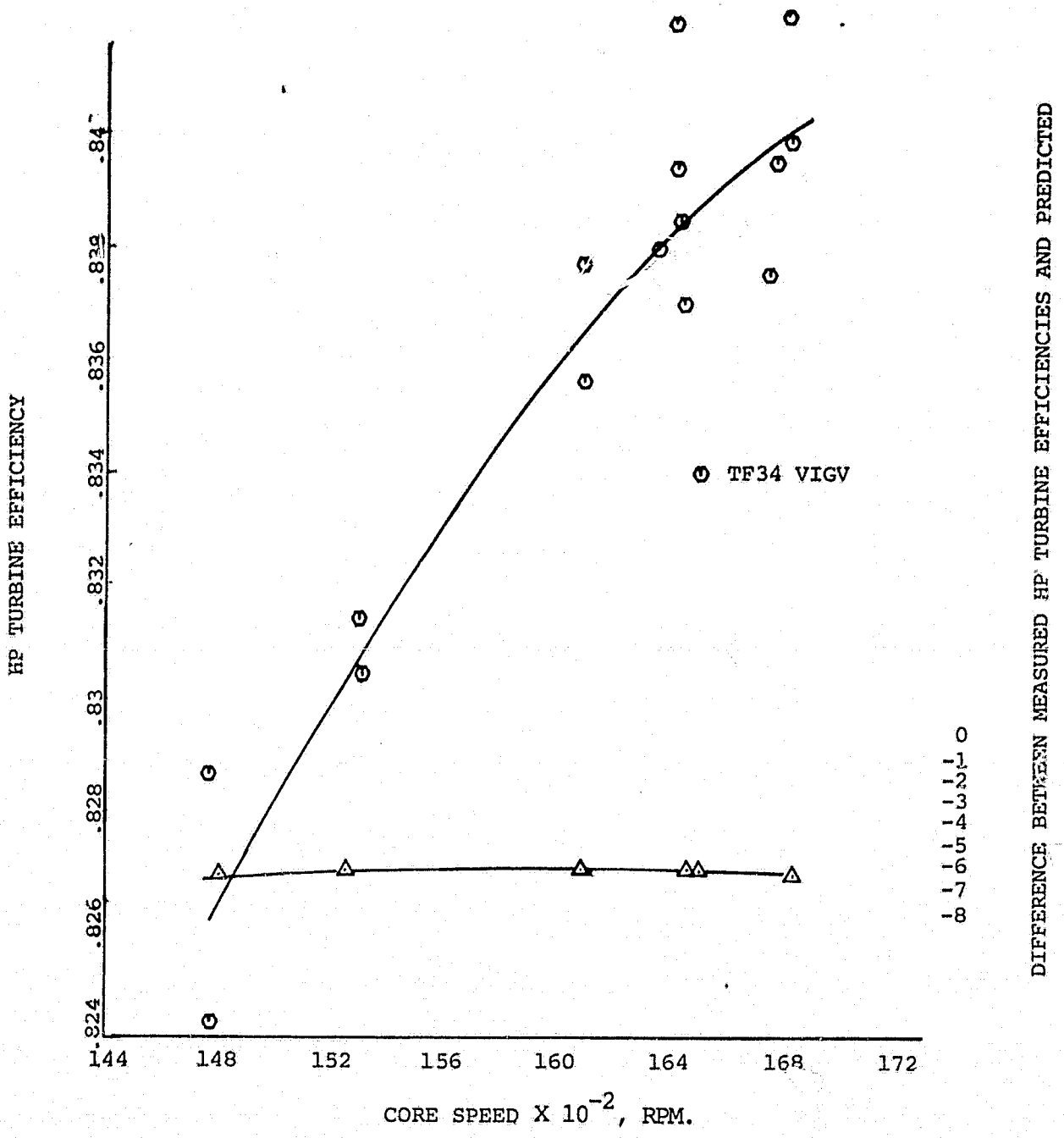

FIGURE 43. High Pressure Turbine Efficiency vs. Core Speed

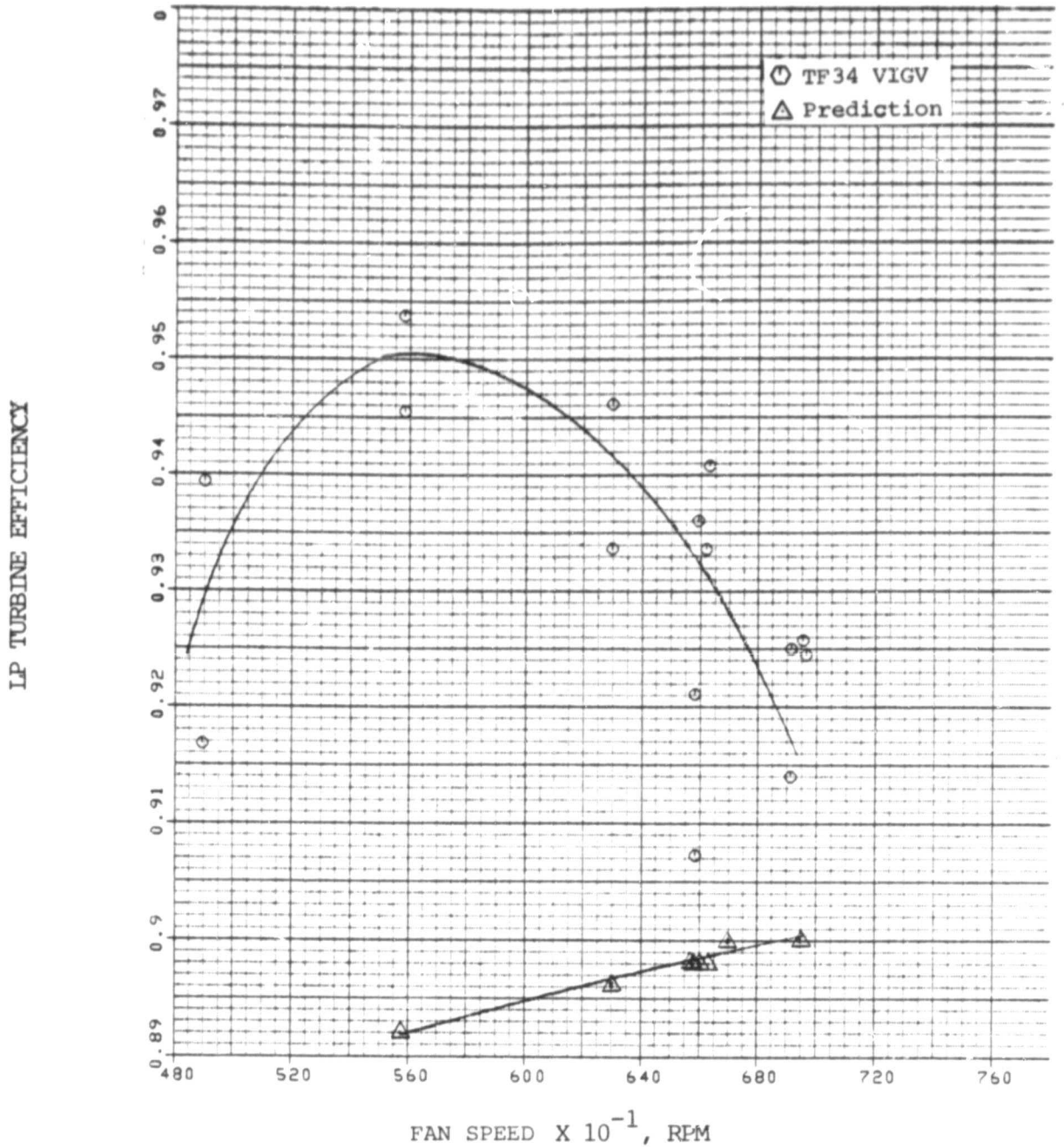

Figure 44. Low Pressure Turbine Efficiency vs. Fan Speed

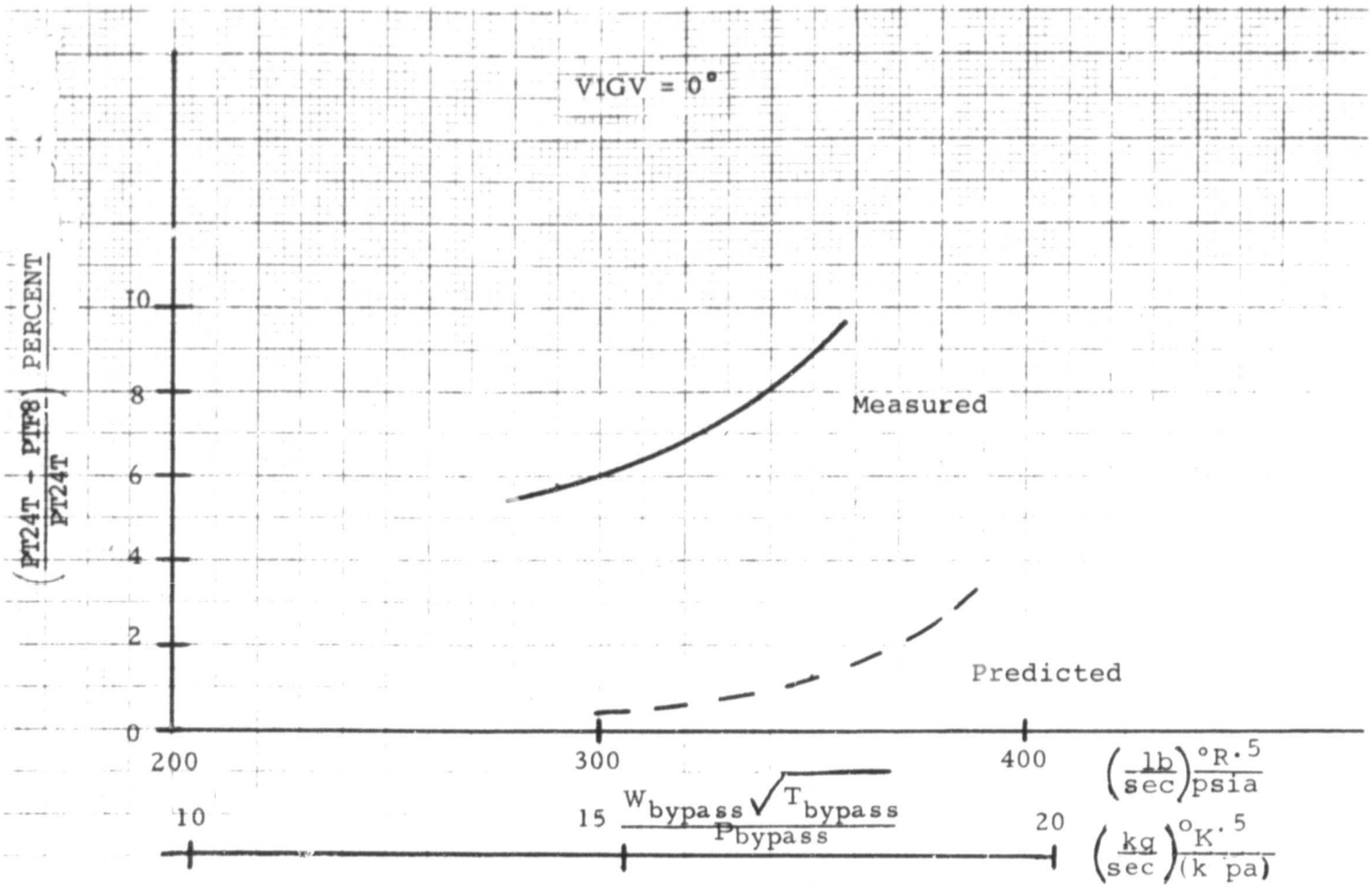

Figure 45. Fan Duct Pressure Loss
(Based on Fan Tip Exit Pressure)

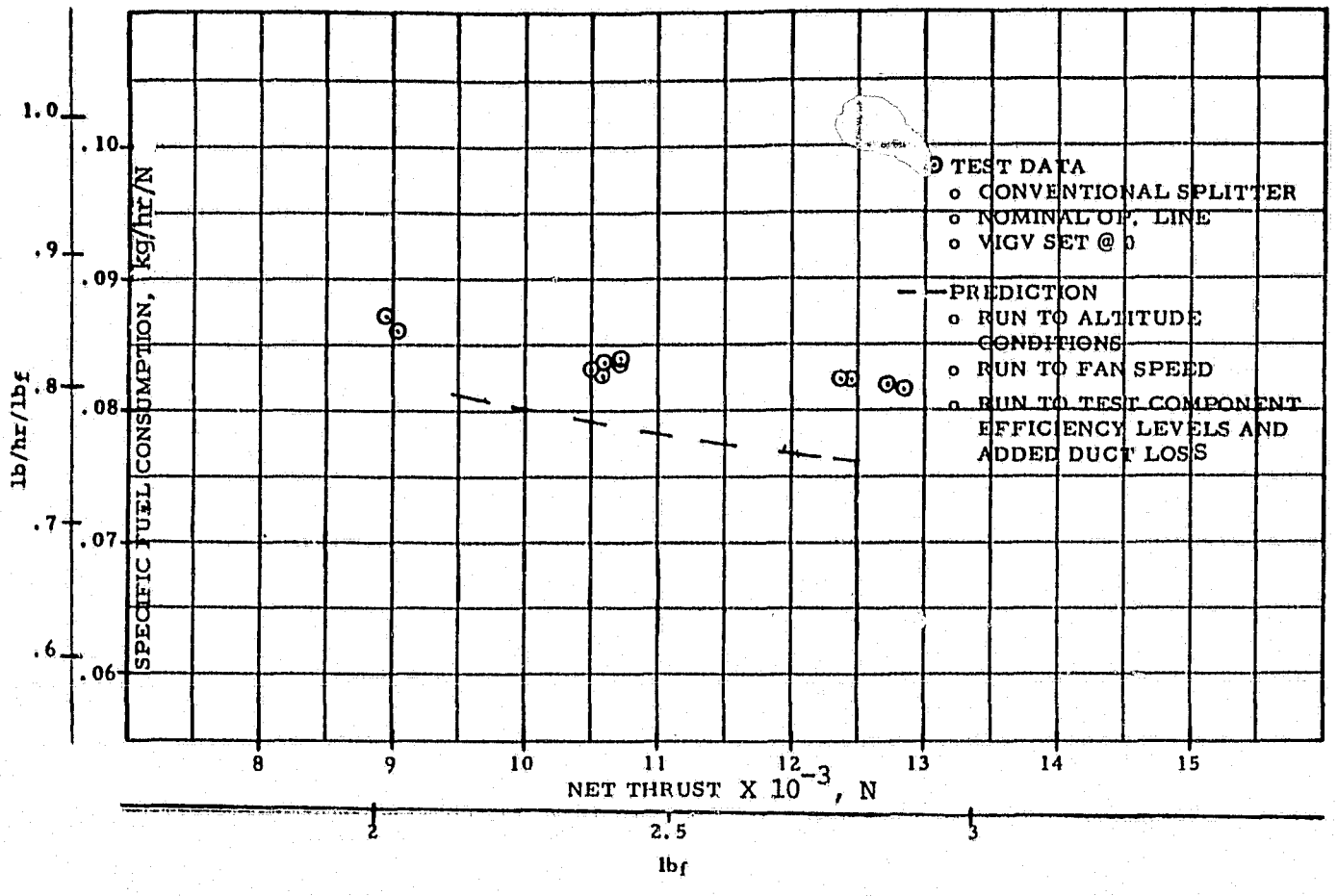

Figure 46. SFC vs. Net Thrust
Test Data Compared to Predicted at 15k ft and 0.6Mn

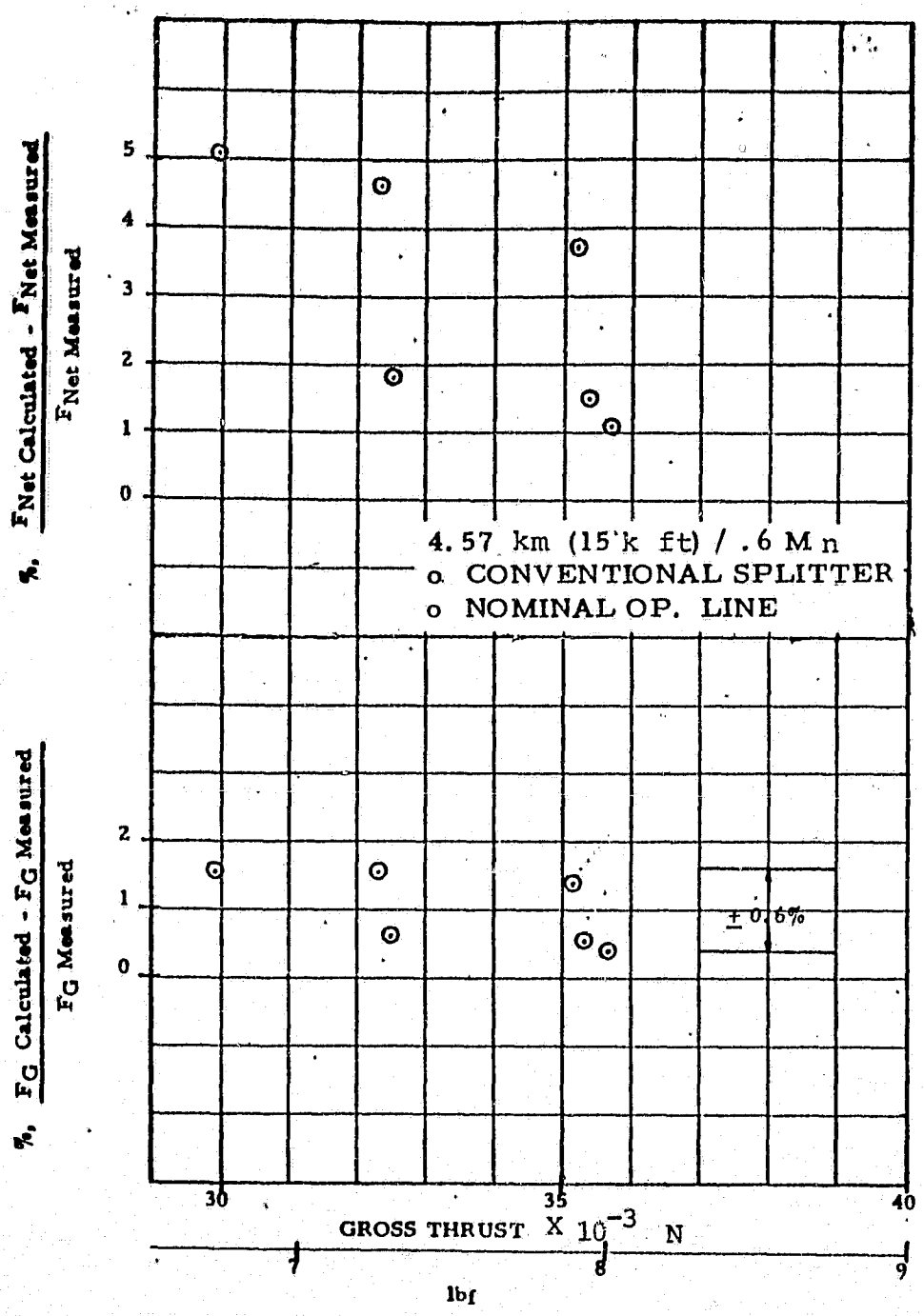

Figure 47. Comparison of Calculated F_G with Measured Thrust Data and the Tolerance Effect on Resulting Net Thrust

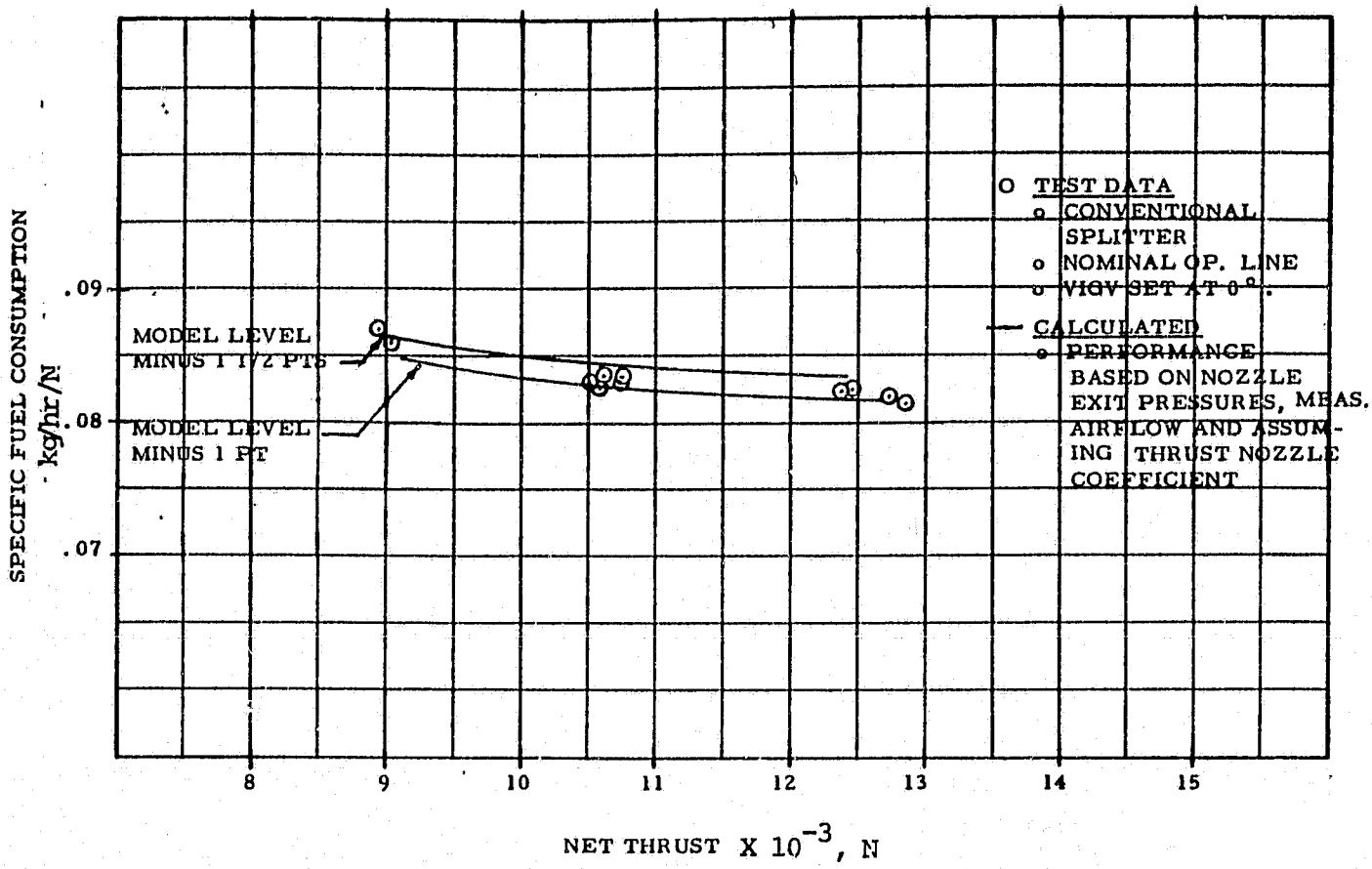

Figure 48. SFC vs. Net Thrust for 15k ft/0.6Mn

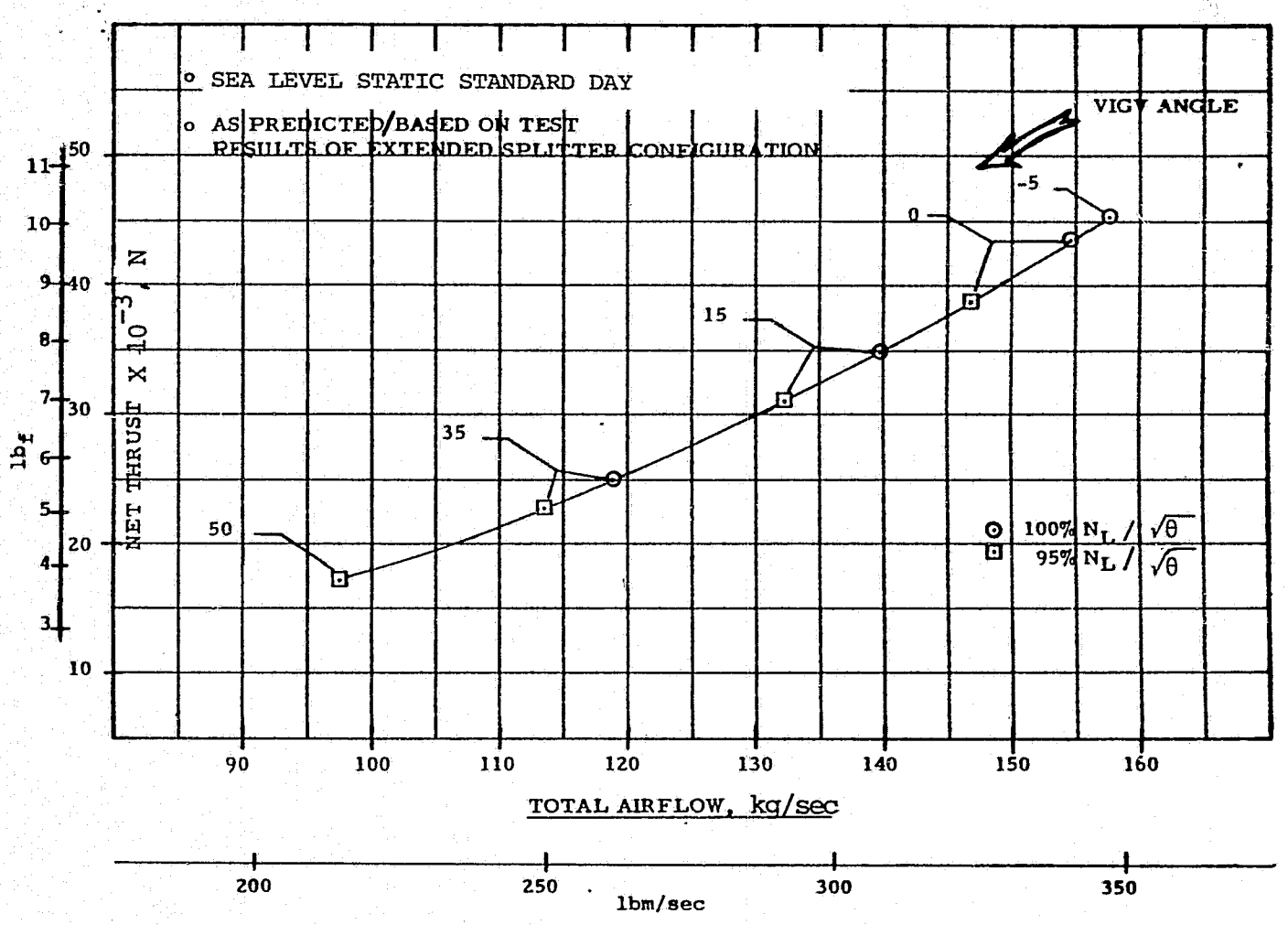

Figure 49. Average Thrust and Flow Variation With VIGV Closure

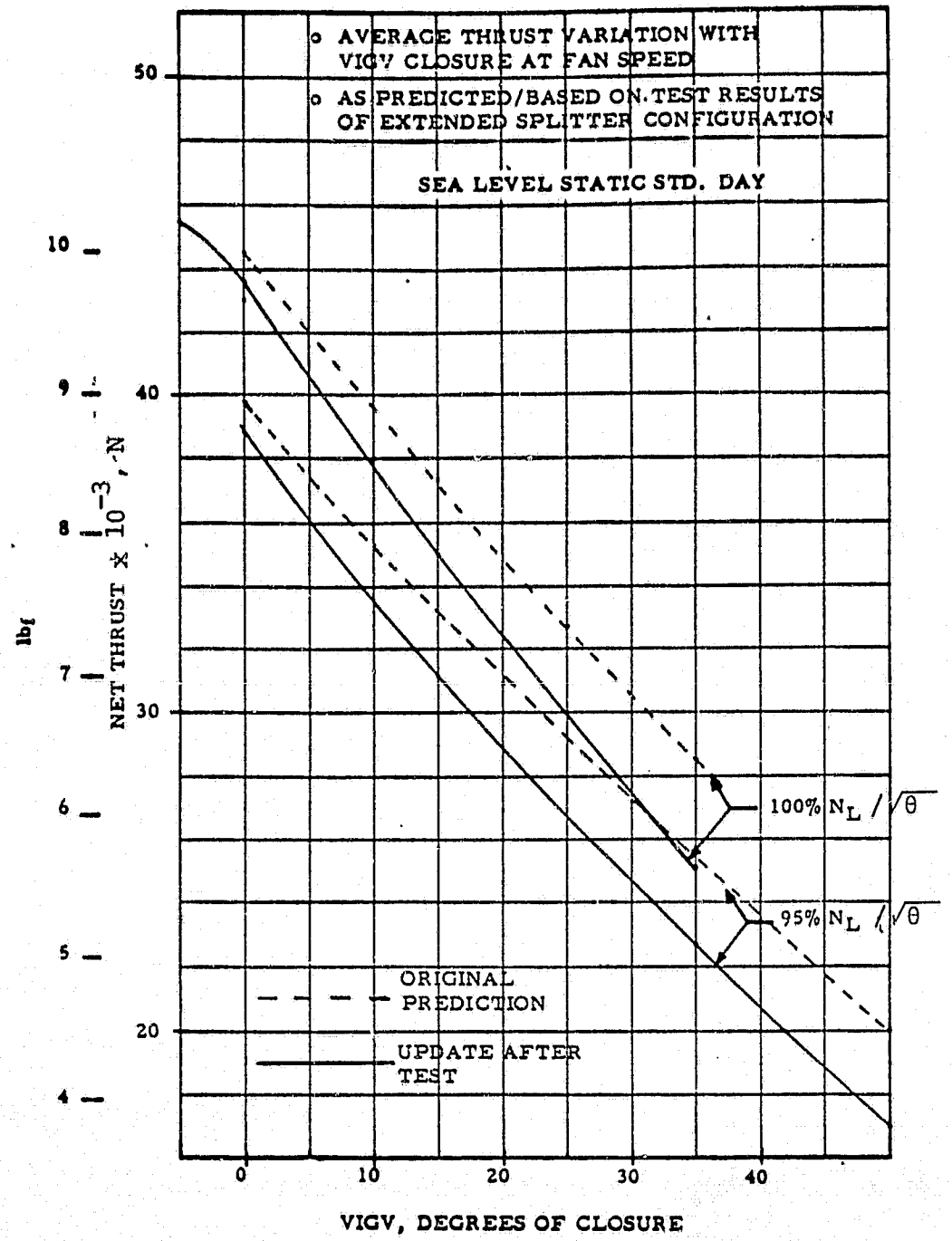

Figure 50. Net Thrust vs. VIGV - Test vs. Prediction

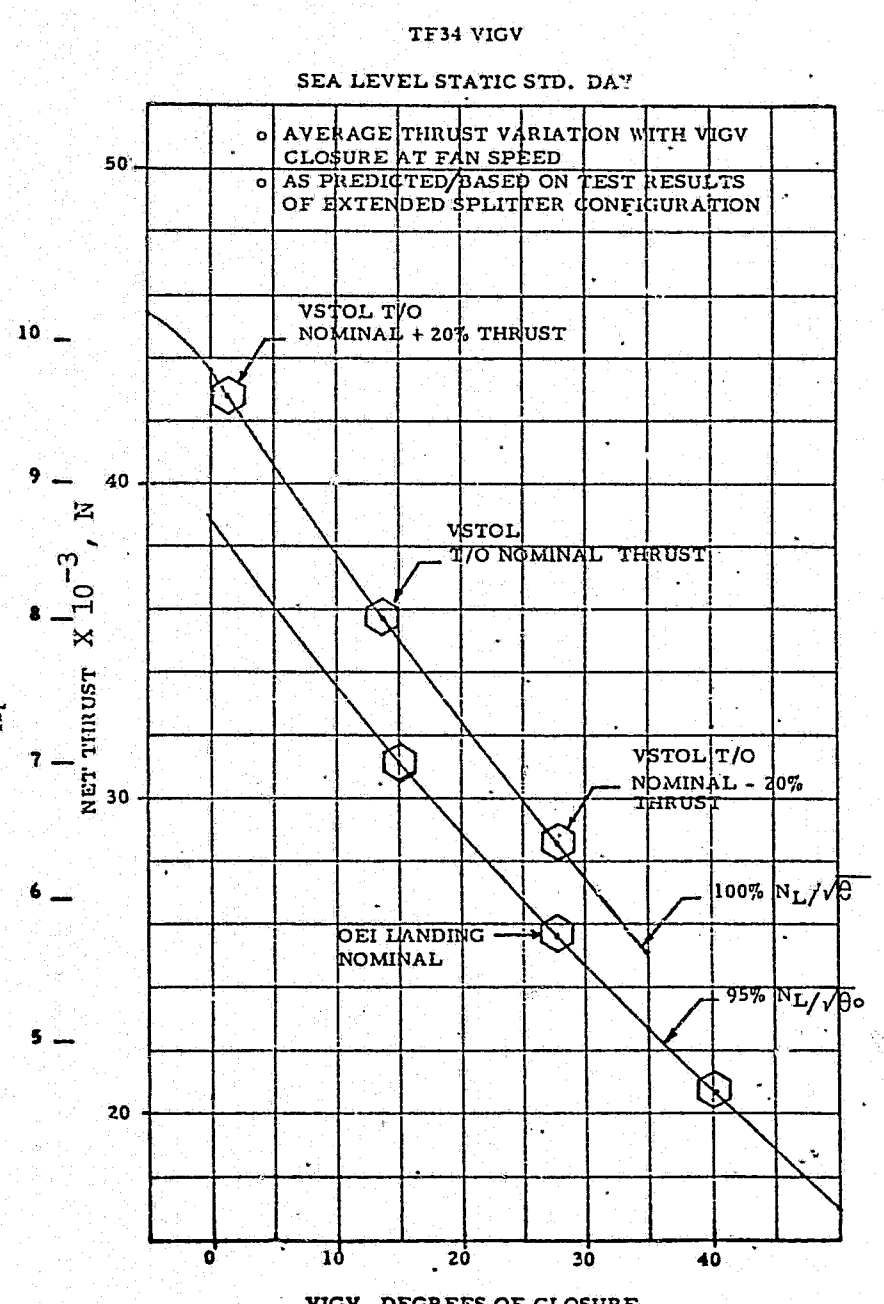

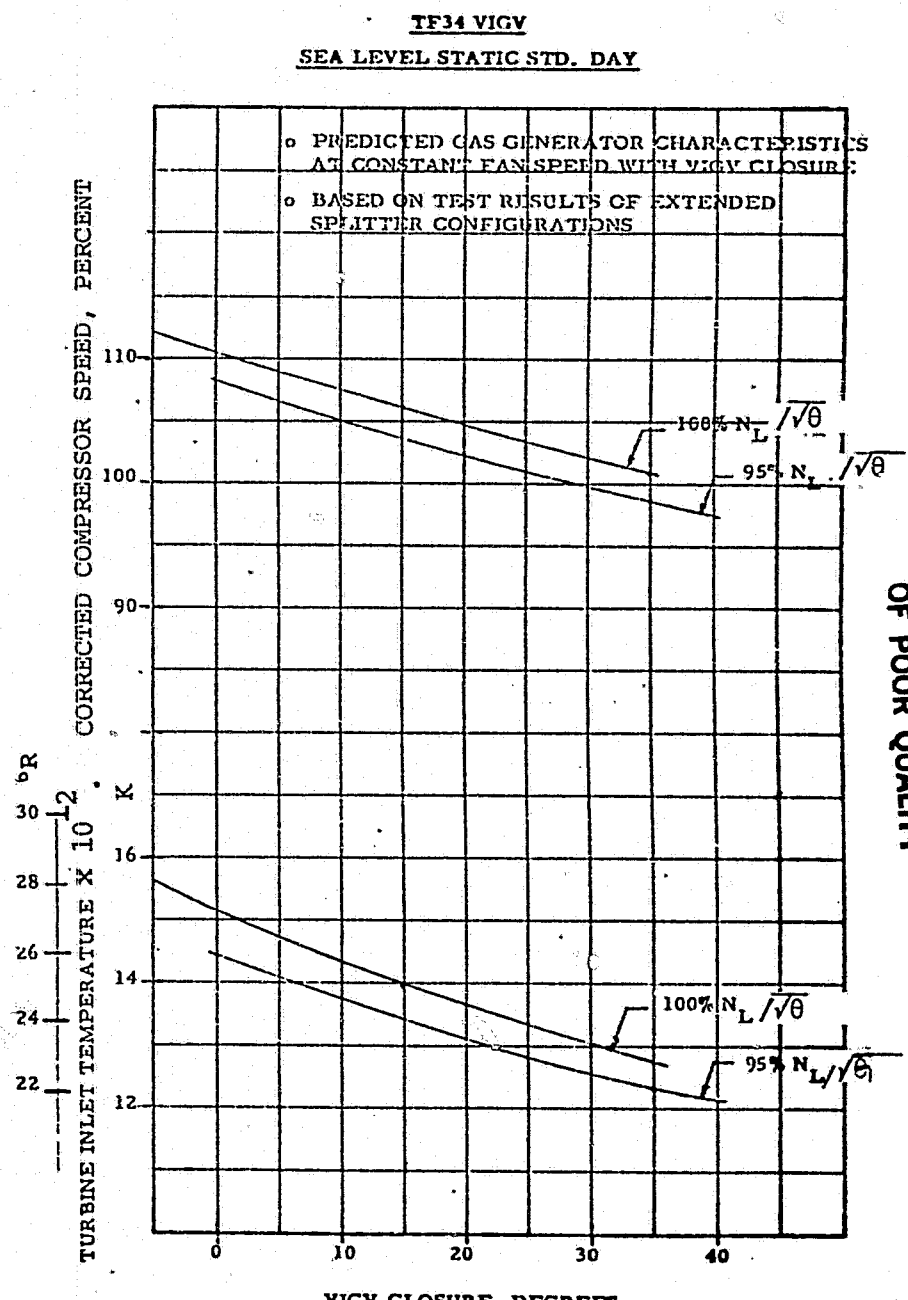

Figure 51. VTOL Take Off Conditions

CONCLUSIONS AND RECOMMENDATIONS

1. The concept of using a fan part span VIGV for flow and thrust modulation on a TF34 has been successfully validated.

2. A VIGV closure of 40° resulted in 30 percent flow reduction and 53 percent thrust reduction.

3. VIGV closure reduced thrust as a result of the combined mechanisms of reduction of airflow and increased losses in the fan tip region.

4. A data base for future variable IGV and VTOL applications is available from this test program.

5. The performance of the PET TF34 fan with VIGV at 0° is consistent with the basic TF34 fan without VIGV with no measurable effect on limit line, flow at speed, or efficiency.

6. Relative to the conventional splitter, the extended splitter shows improvements:

   a) In VTOL sea level takeoff performance (Minor SFC penalties for the low altitude cruise condition may occur depending on the mission).

   b) In fan efficiency above 95 percent speed and core inlet pressure at 0° IGV angle at both sea level and 15K 0.6 MN.

   c) In fan efficiency and core inlet pressure at varying IGV angle at all flight conditions.

7. With the presence of VIGV's , fan distortion sensitivity is less than 8 percent of the sensitivity without VIGV's.

8. The distortion transfer from fan inlet to core is the same as the basic TF34 on the nominal fan operating line; but distortion transfer with the fan on a high operating line is significantly reduced with IGV closure.

REFERENCES

1. Reed, V. L. and Schneider, P. W., "V/STOL Thrust Modulation through the use of Variable Inlet Guide Vanes," AIAA-80-1248, June 1980.

2. Biesiadny, Thomas J., "Test Techniques for Obtaining Off-Nominal Compressor Data during Engine Tests" NASA TMX-71597, 1974.

3. Bobula, G. A., Soeder, R. H., and Burkardt, L. A., "Effect of a Part Span Variable Inlet Guide Vane on the Performance of a High Bypass Turbofan Engine," AIAA-81-1362, July 1981.

APPENDIX I

NOZZLE THRUST CALCULATION

Calculations of nozzle thrust were made by applying a thrust coefficient, C_V to the ideally expanded gross thrust for a conic nozzle based on exit gas measurements. It was considered that the nozzles exhaust to different local ambient pressures represented by the outer static pressure in both gas streams. This is due to different air velocities passing each nozzle and slight turning of the bypass stream. The static pressure at the control boundary surface was considered the average of inner and outer wall static measurements. Therefore, the following diagram applies:

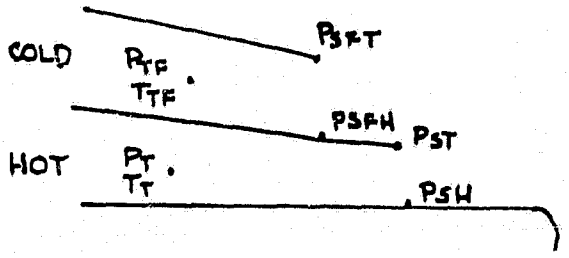

$$FGI_{cold} = f(T_{TF},\ P_{TF}/P_{SFT})$$

$$FGI_{hot} = f(T_T,\ P_T/P_{ST})$$

$$FG = C_{V\,cold}\, FGI_{cold} + Ac\,(\overline{P_{SF}} - P_{SFT}) + C_{V\,hot}\, FGI_{hot} + AH\,(\overline{P_S} - P_{ST})$$

Where $C_{V\,cold} = .99$ & $C_{V\,hot} = .9944$, initially

The results are shown in Figure 47.

Note: Additional force component results from a plug thrust from the rear external core. By using an average static pressure and appropriate physical area, it is estimated that this would contribute only ~ .5% to the calculated F_G's shown.

APPENDIX II - FAN PERFORMANCE DATA

List of Figures

All Figures are plotted with CORRECTED BELLMOUTH FLOW as the abscissa

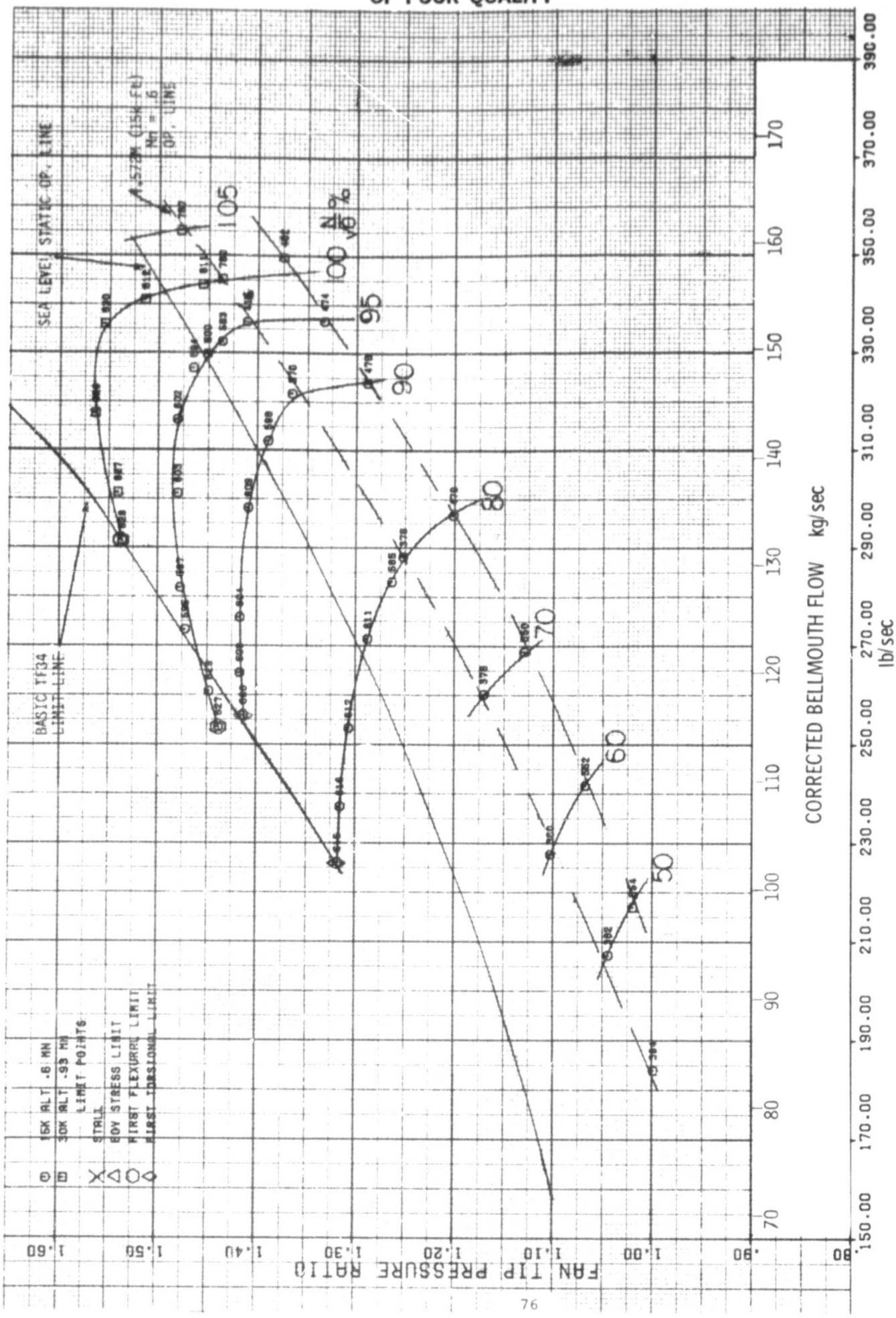

FIGURE II-1 TIP PRESSURE RATIO AT IGV ANGLE OF 0° (CONVENTIONAL SPLITTER)

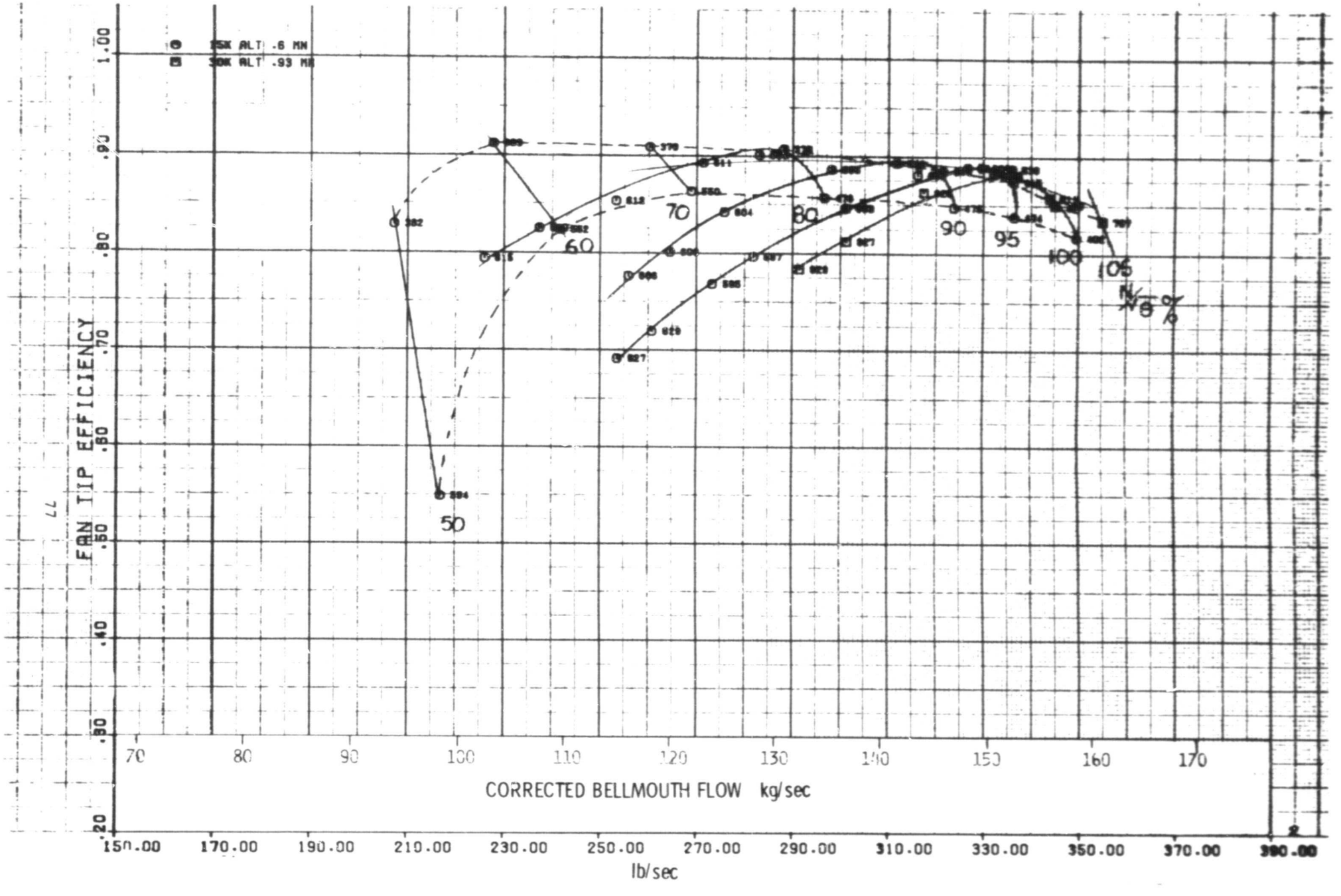

FIGURE II-2 TIP EFFICIENCY AT IGV ANGLE OF 0° (CONVENTIONAL SPLITTER)

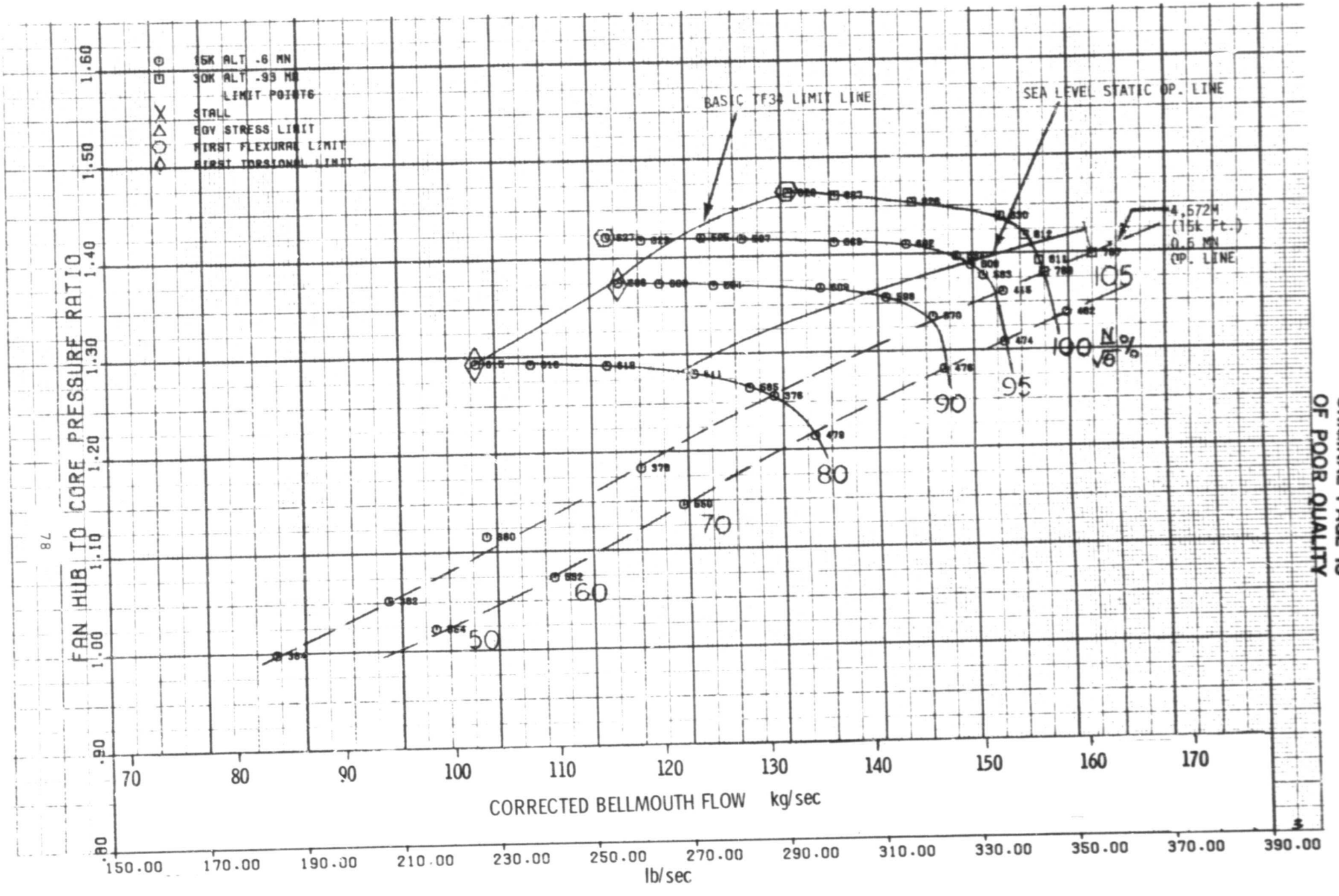

FIGURE II-3 HUB PRESSURE RATIO AT IGV ANGLE OF 0° (CONVENTIONAL SPLITTER)

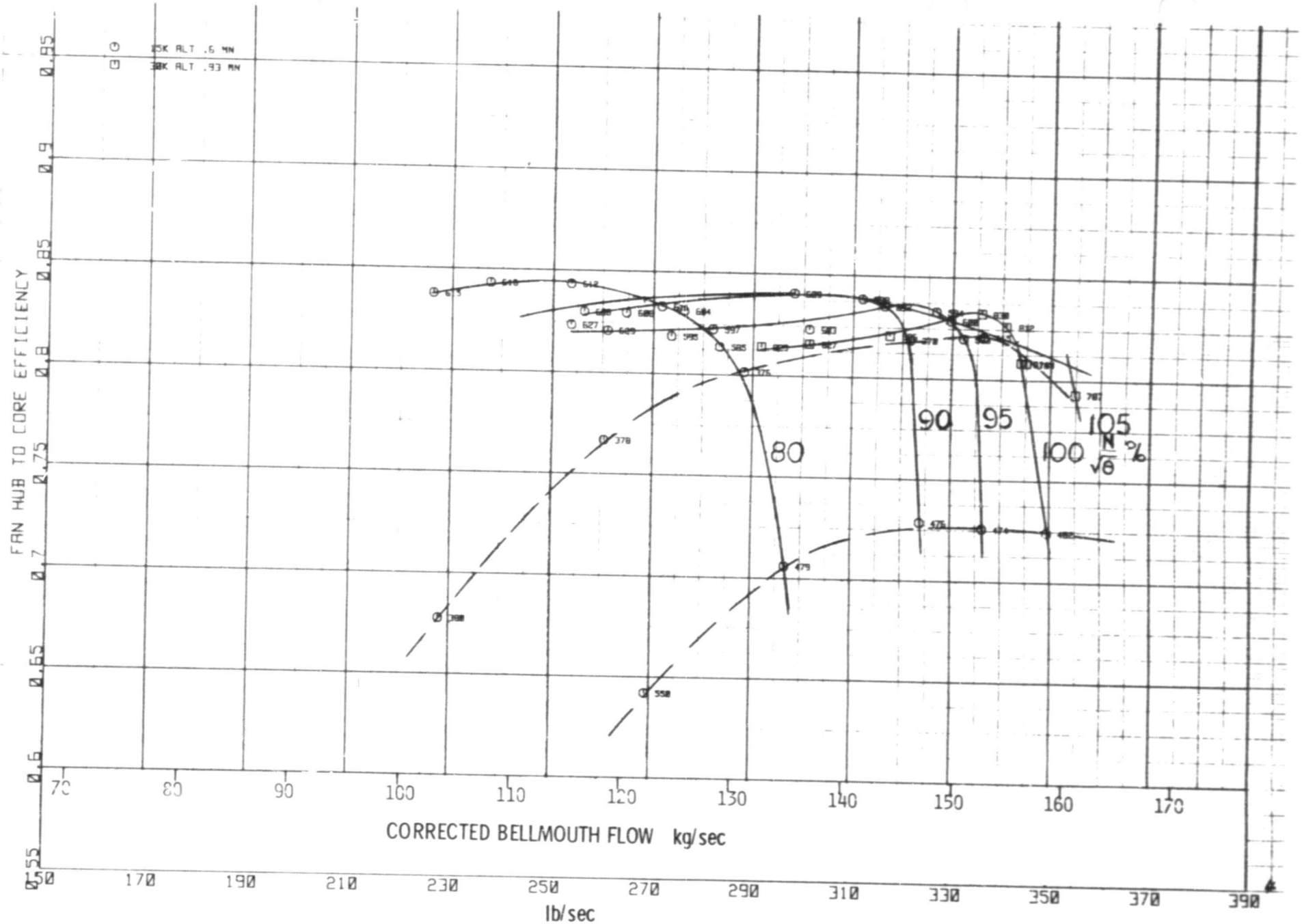

FIGURE II-4 HUB EFFICIENCY AT IGV ANGLE OF 0° (CONVENTIONAL SPLITTER)

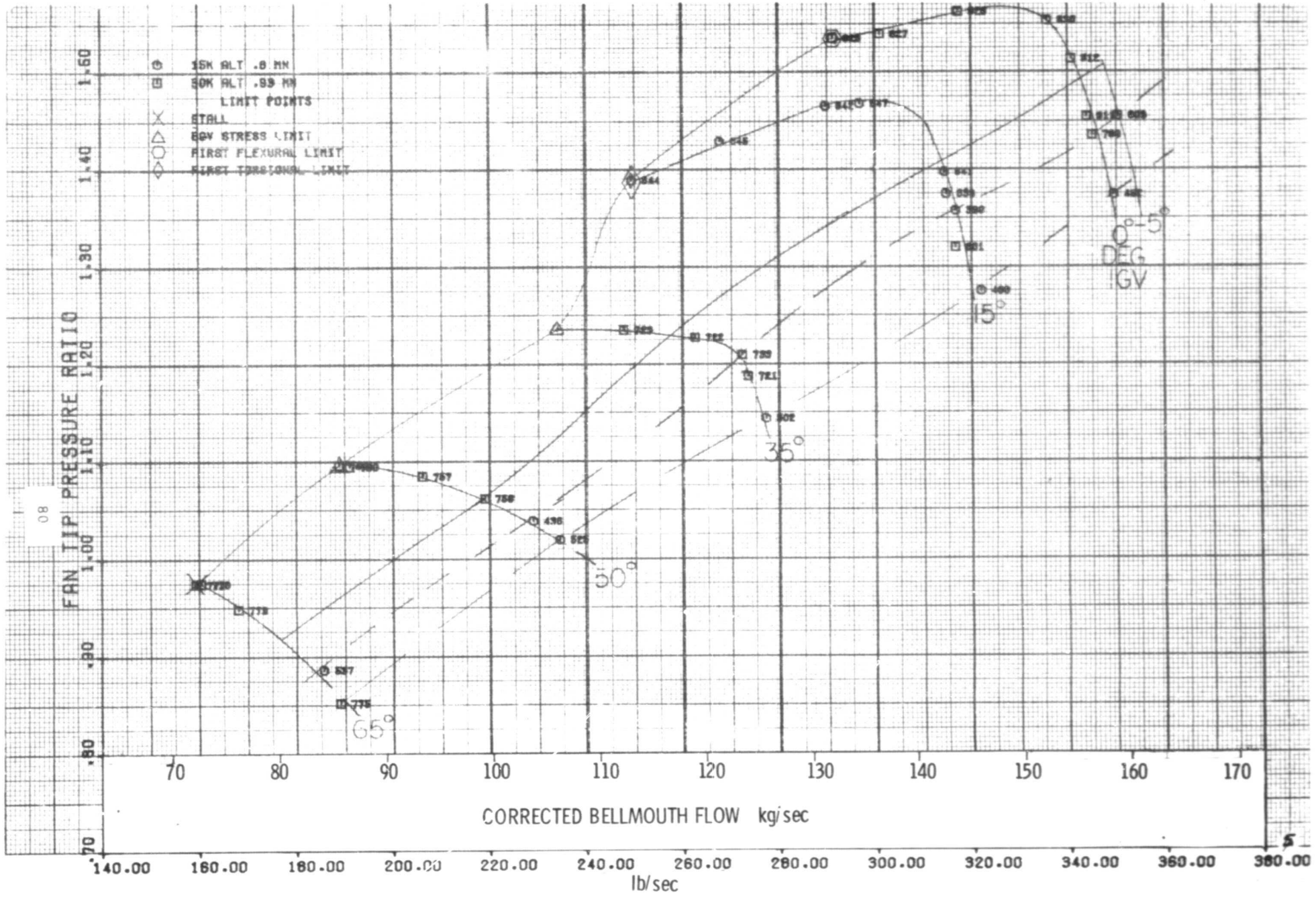

Figure 11-5 Tip Pressure Ratio at 100 Percent Speed (Conventional Splitter)

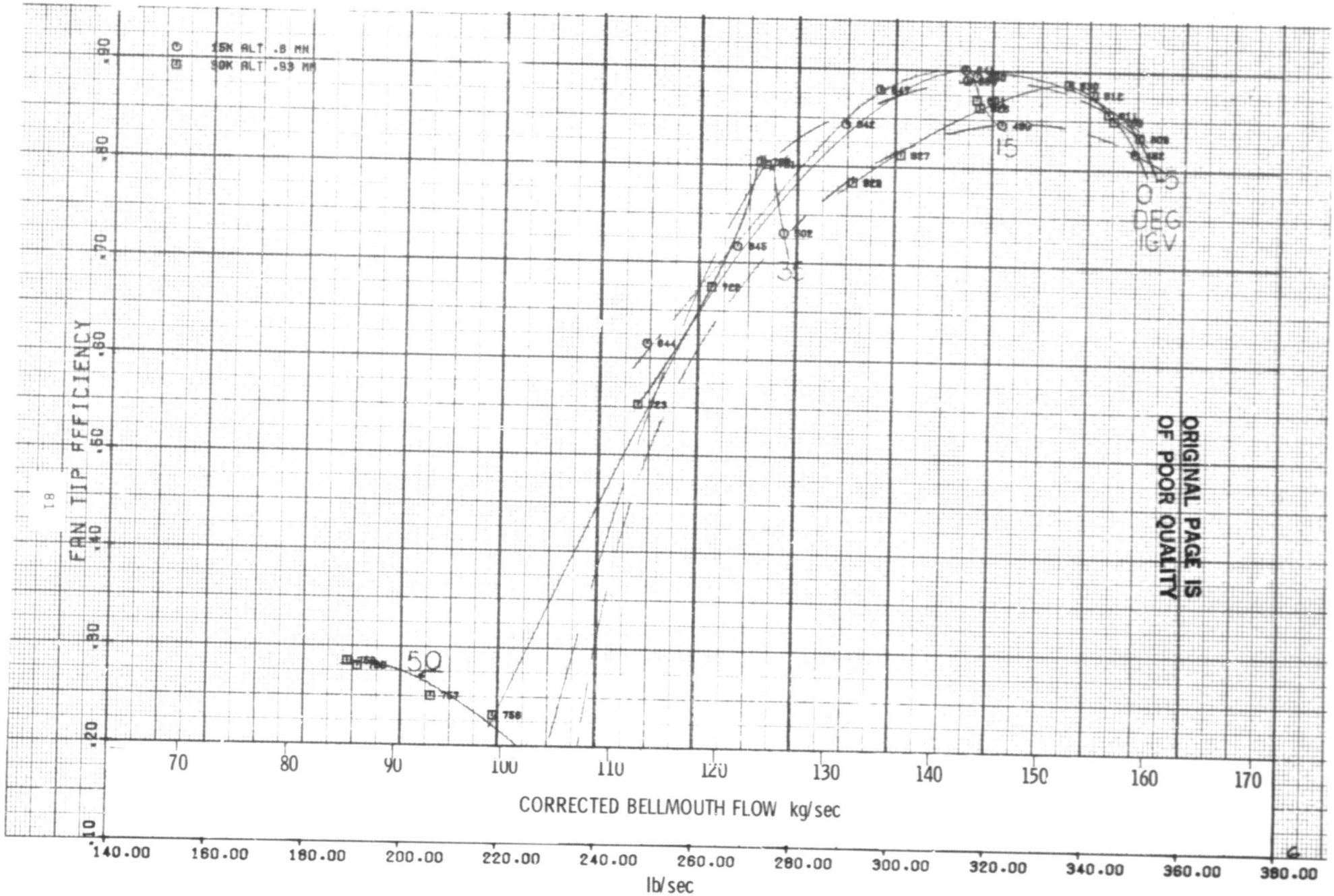

Figure 11-6 Tip Efficiency at 100 Percent Speed (Conventional Splitter)

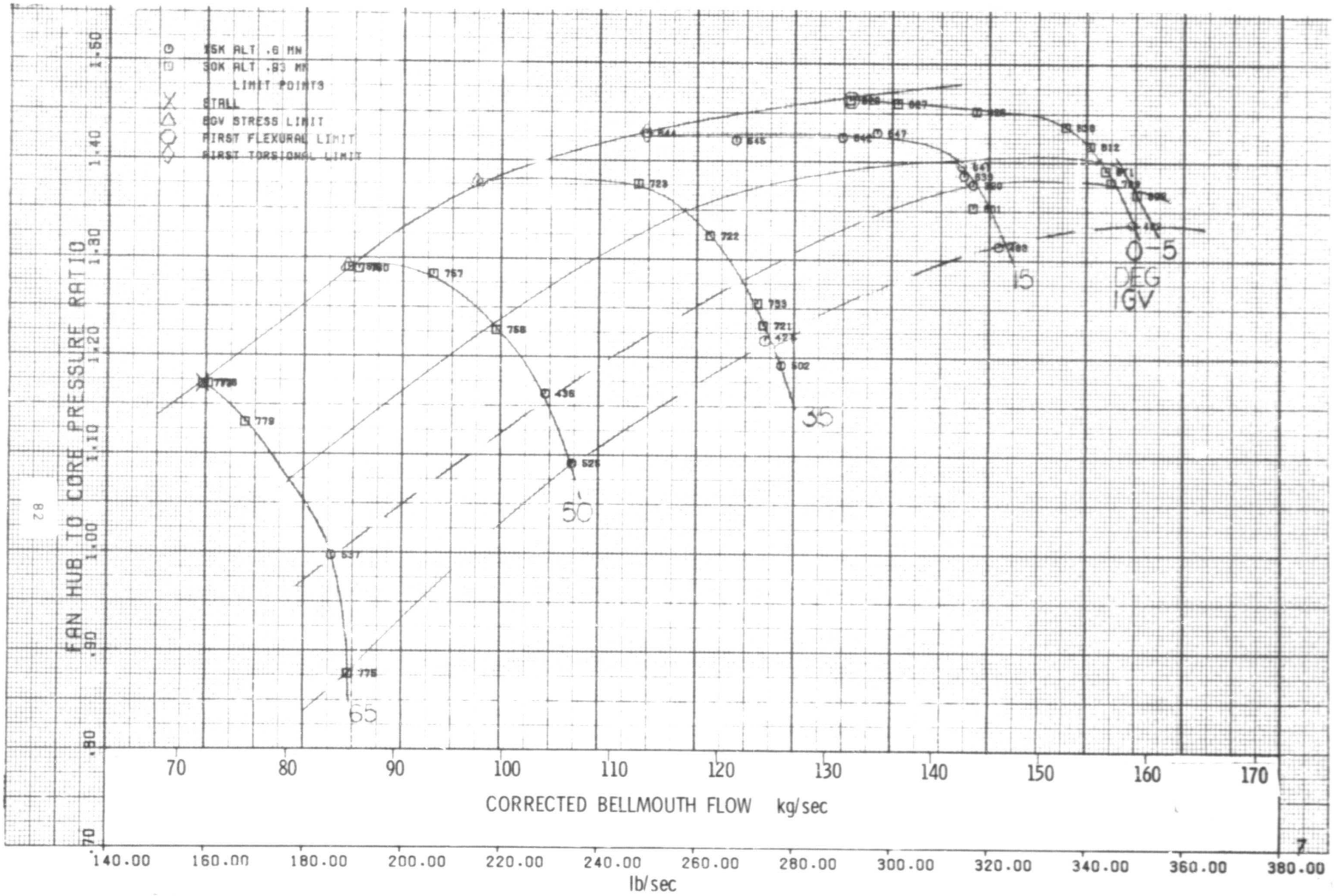

Figure II-7 Hub Pressure Ratio at 100 Percent Speed (Conventional Splitter)

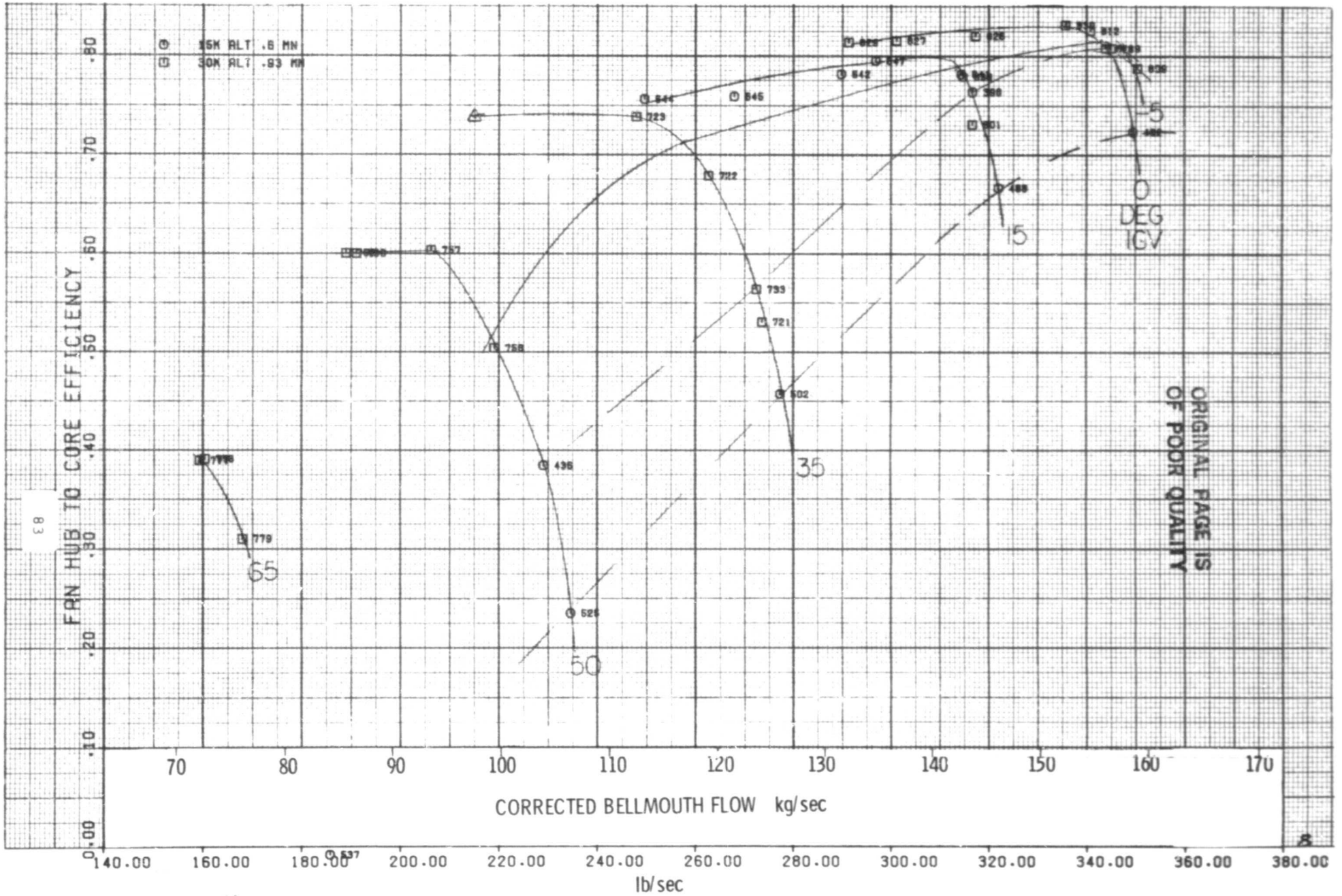

Figure II-8 Hub Efficiency at 100 Percent Speed (Conventional Splitter)

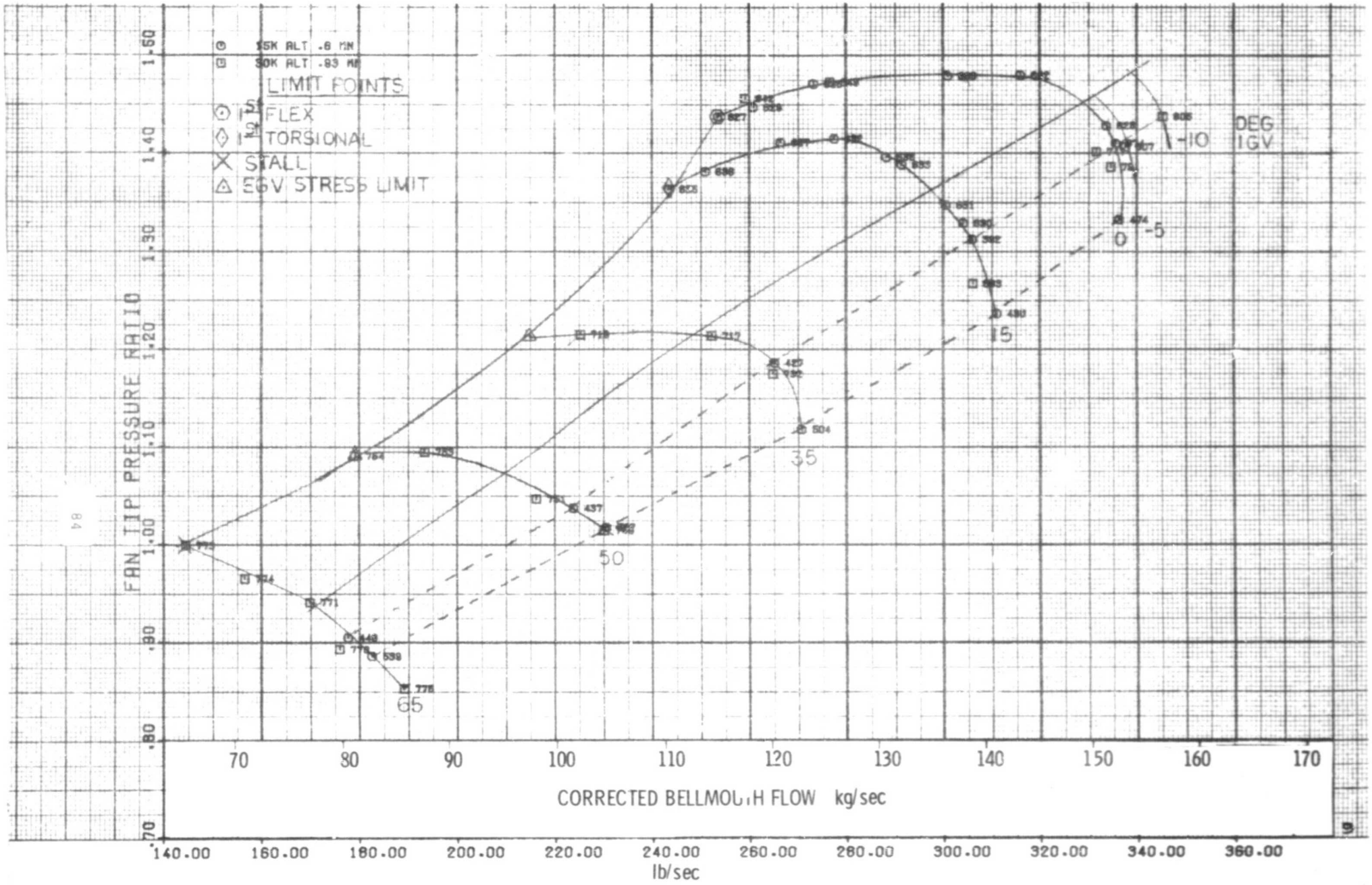

Figure II-9 Tip Pressure Ratio at 95 Percent Speed (Conventional Splitter)

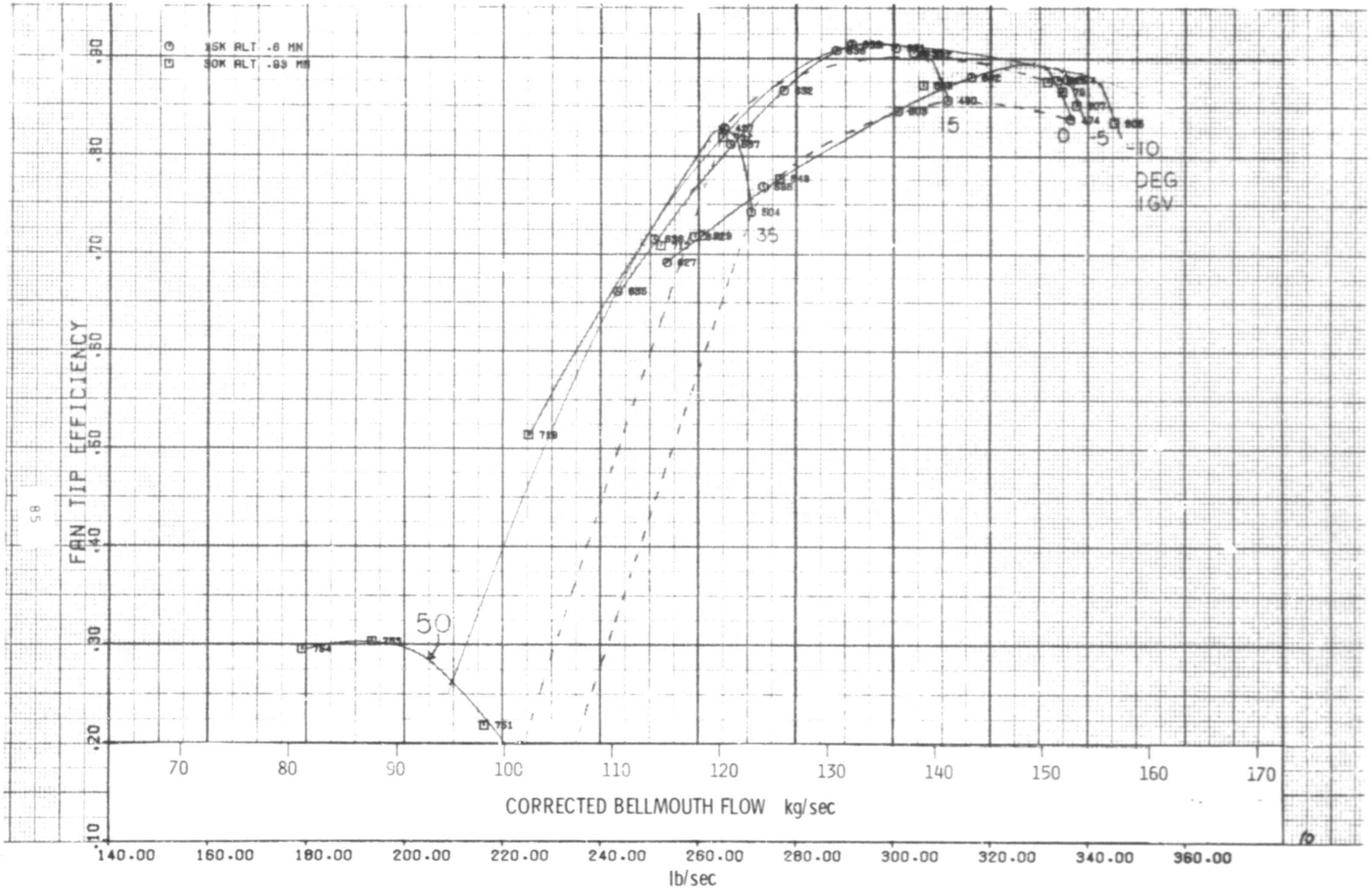

Figure 11-10 Tip Efficiency at 95 Percent Speed (Conventional Splitter)

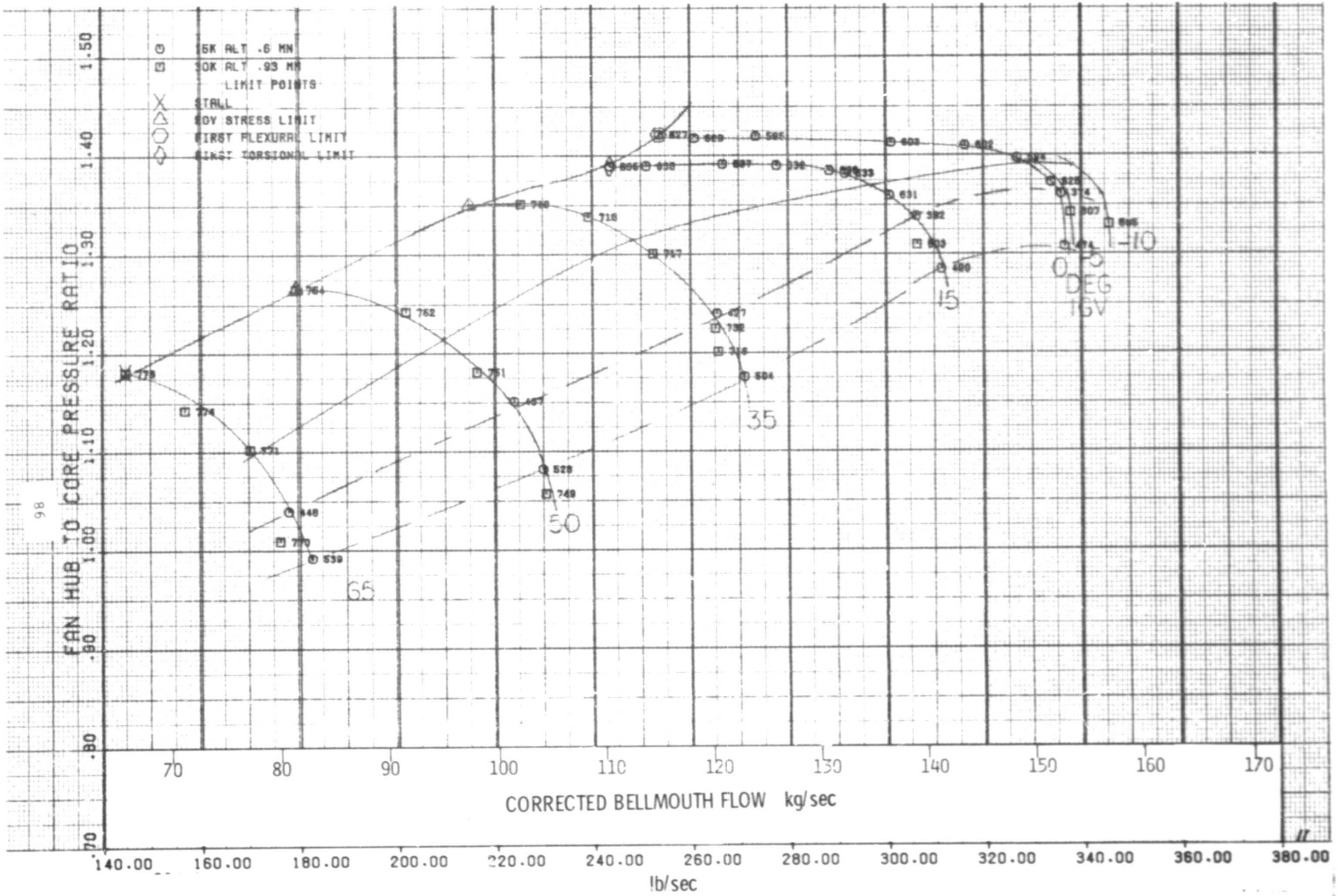

Figure 11-11 Hub Pressure Ratio at 95 Percent Speed (Conventional Splitter)

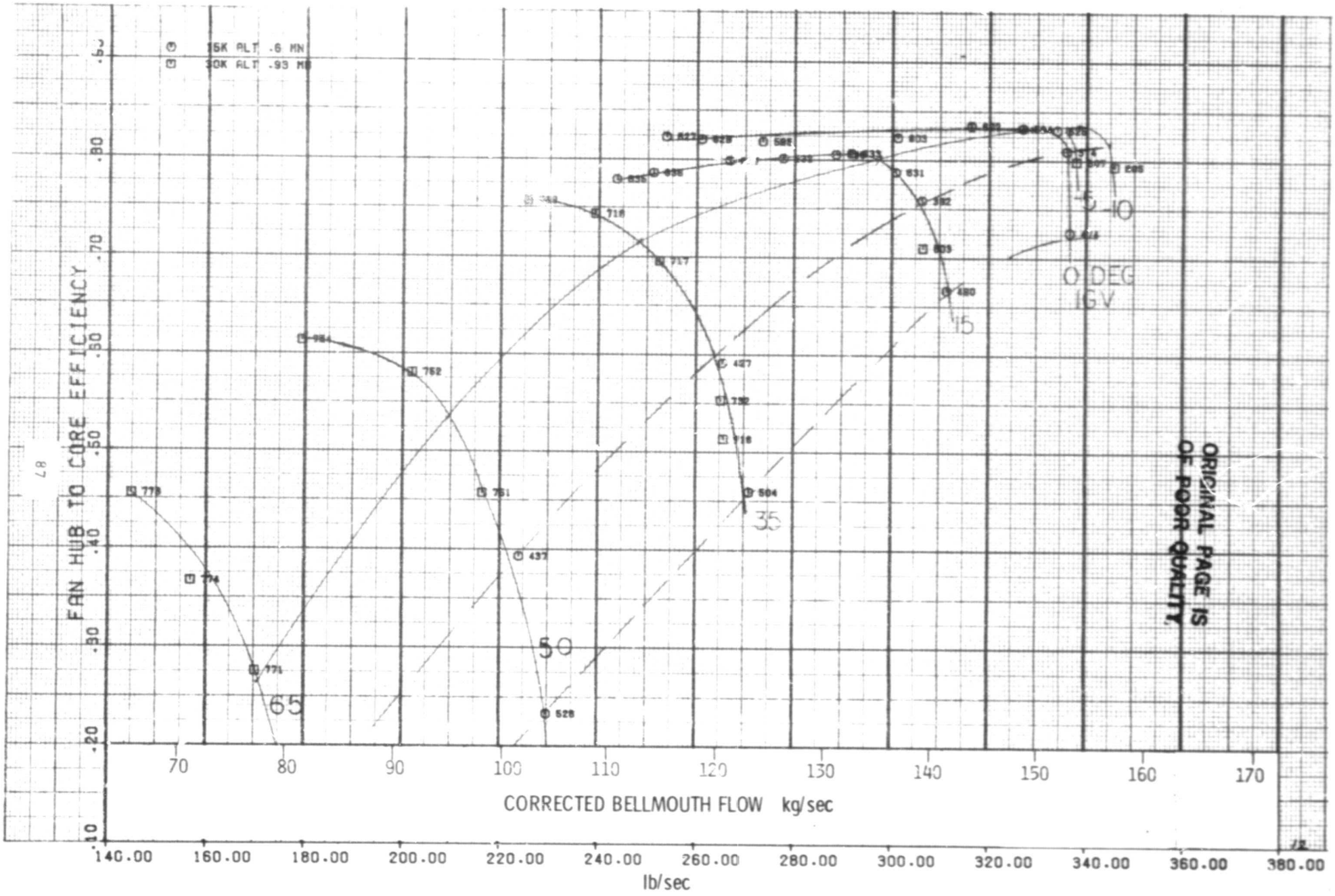

Figure 11-12 Hub Efficiency at 95 Percent Speed (Conventional Splitter)

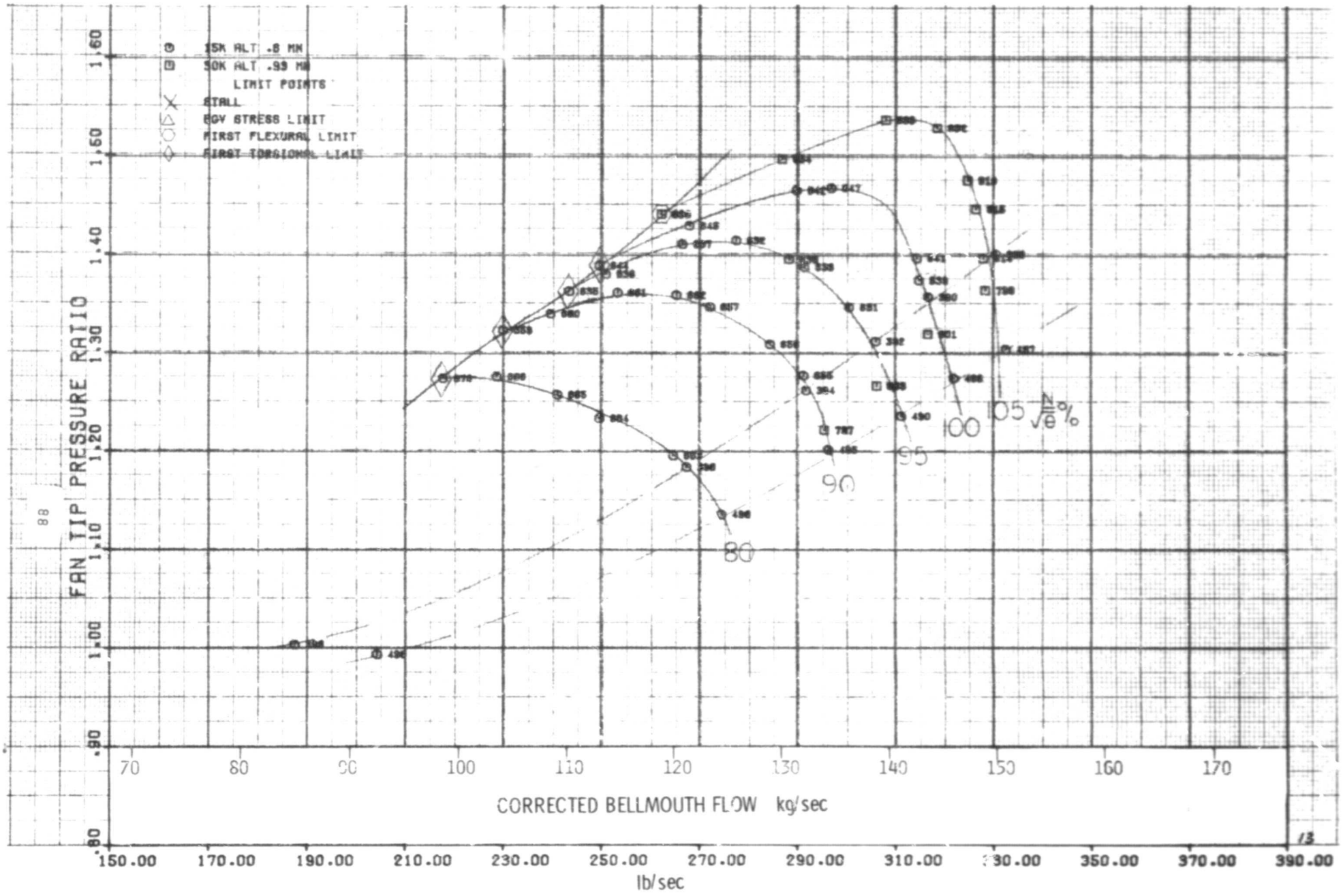

FIGURE II-13 TIP PRESSURE RATIO AT IGV ANGLE OF 15° (CONVENTIONAL SPLITTER)

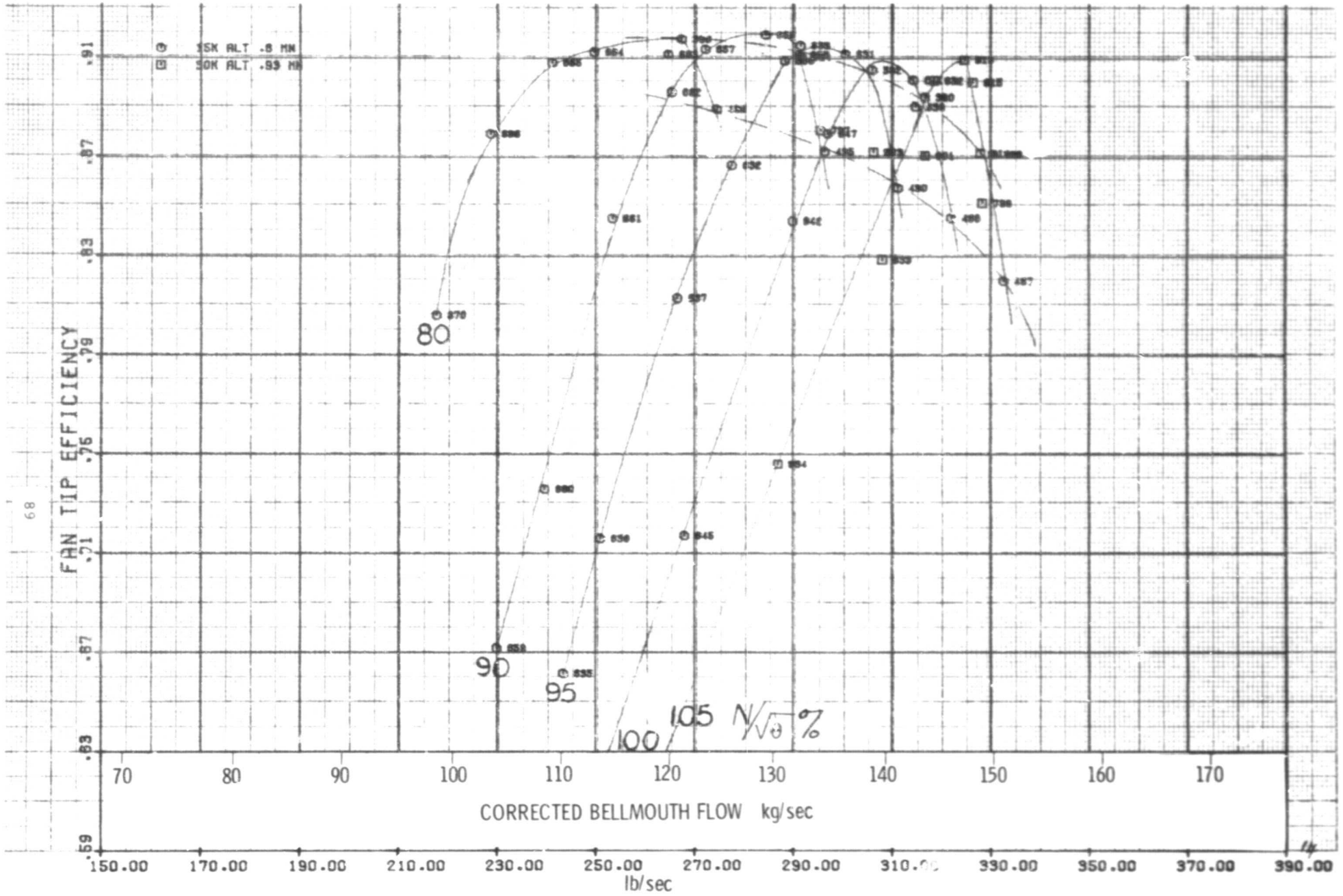

FIGURE II-14 TIP EFFICIENCY AT IGV ANGLE OF 15° (CONVENTIONAL SPLITTER)

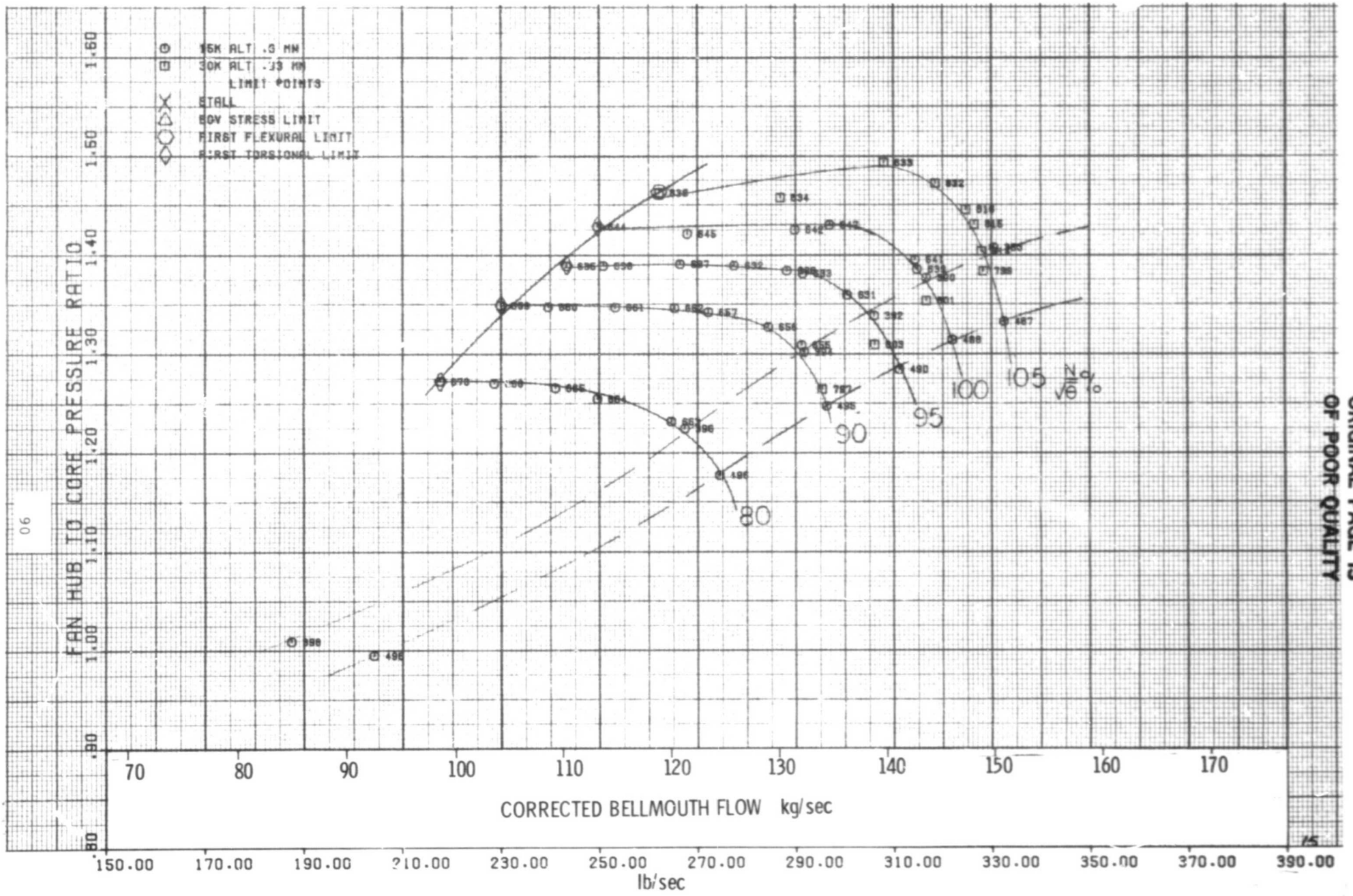

FIGURE II-15 HUB PRESSURE RATIO AT IGV ANGLE OF 15° (CONVENTIONAL SPLITTER)

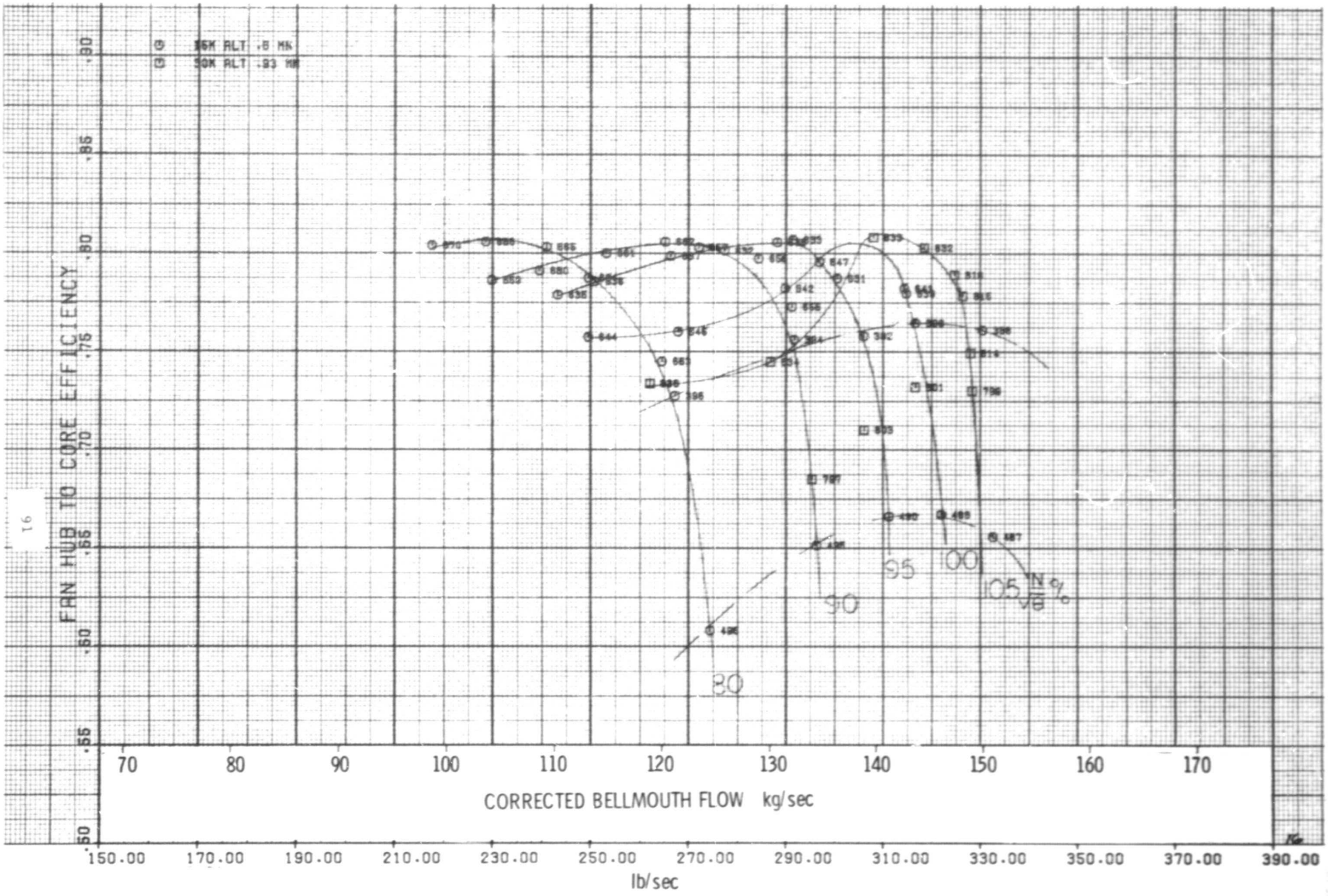

FIGURE II-16 HUB EFFICIENCY AT IGV ANGLE OF 15° (CONVENTIONAL SPLITTER)

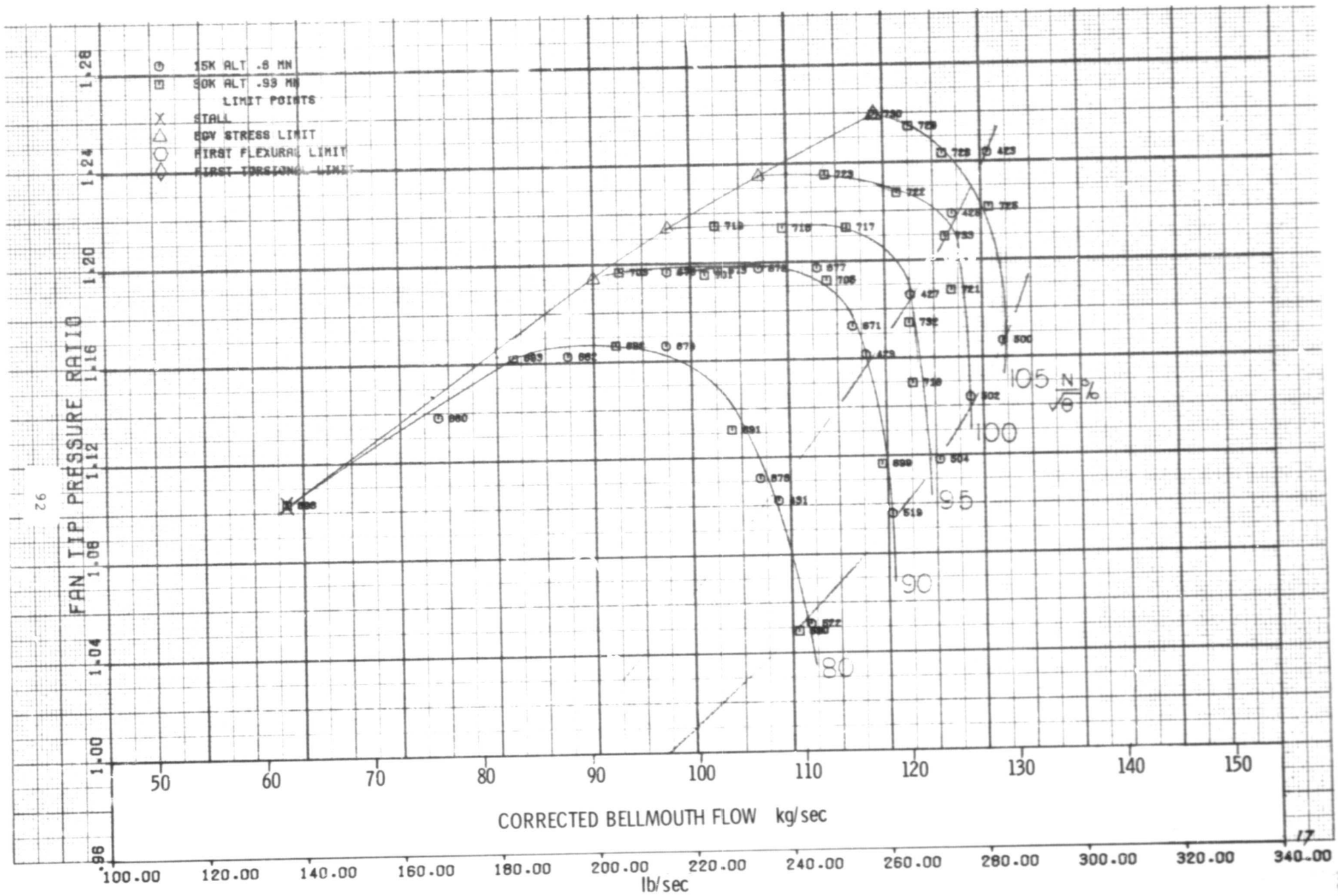

FIGURE II-17 TIP PRESSURE RATIO AT IGV ANGLE OF 35° (CONVENTIONAL SPLITTER)

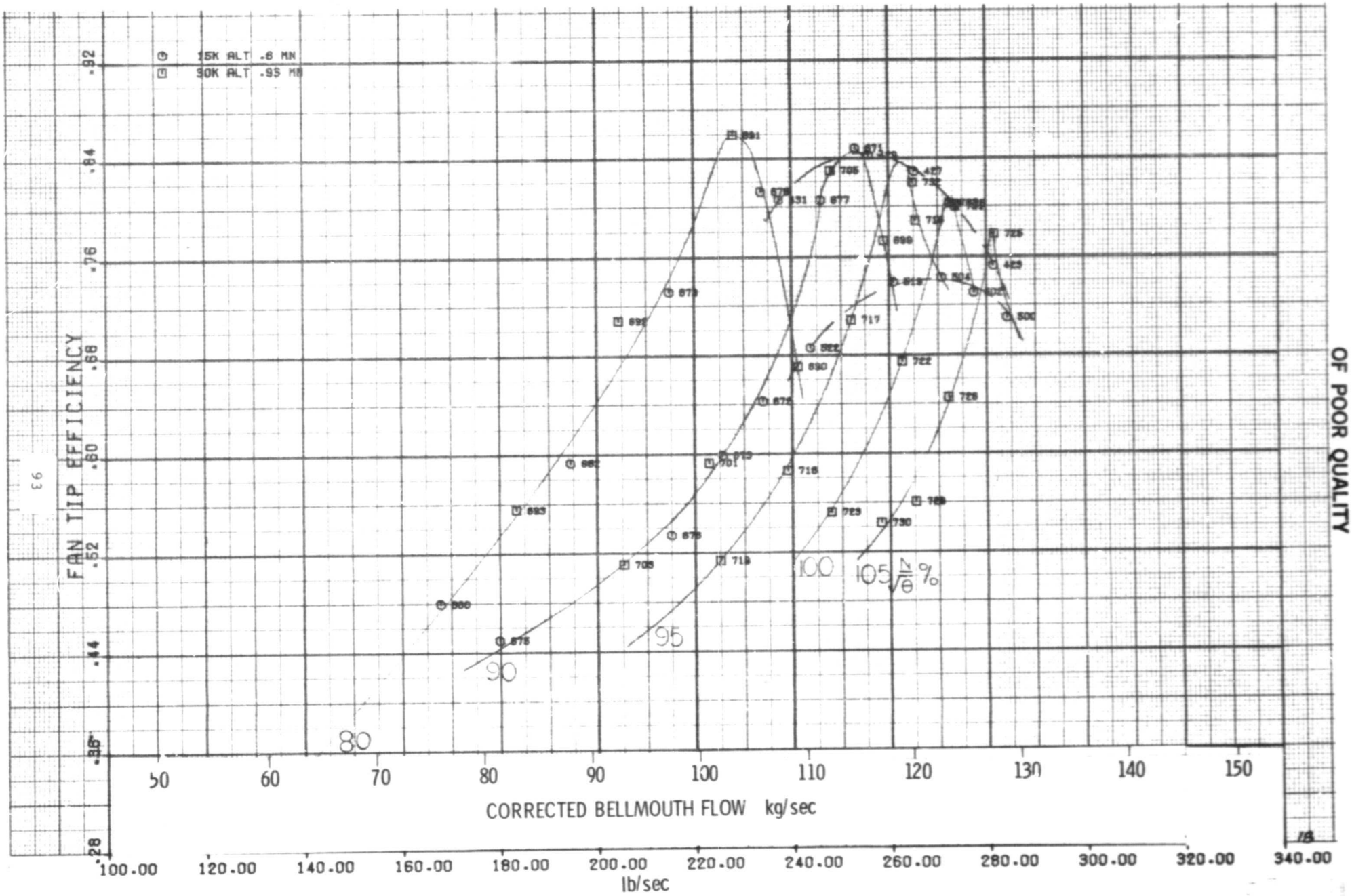

FIGURE II-18 TIP EFFICIENCY AT IGV ANGLE OF 35° (CONVENTIONAL SPLITTER)

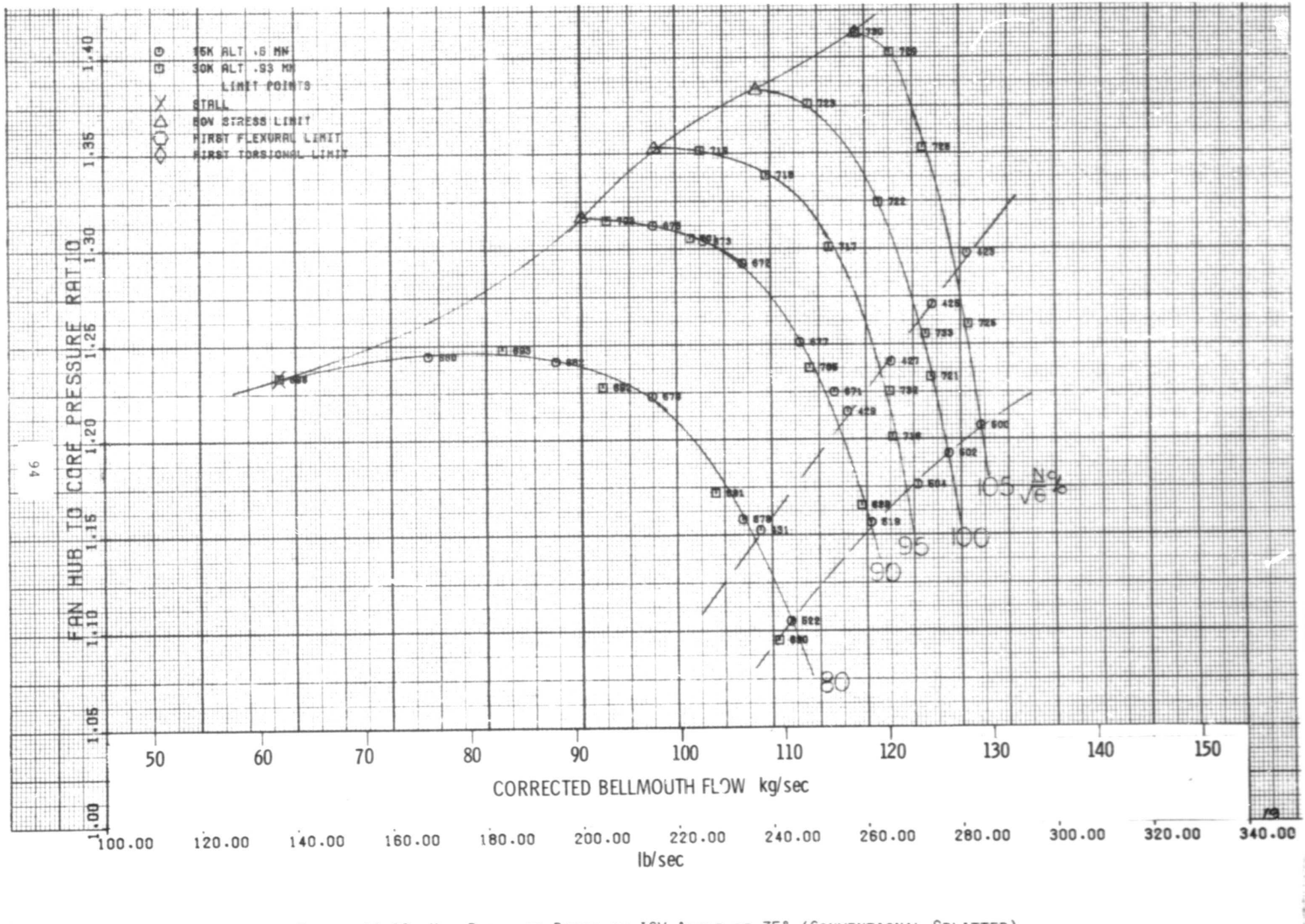

FIGURE II-19 HUB PRESSURE RATIO AT IGV ANGLE OF 35° (CONVENTIONAL SPLITTER)

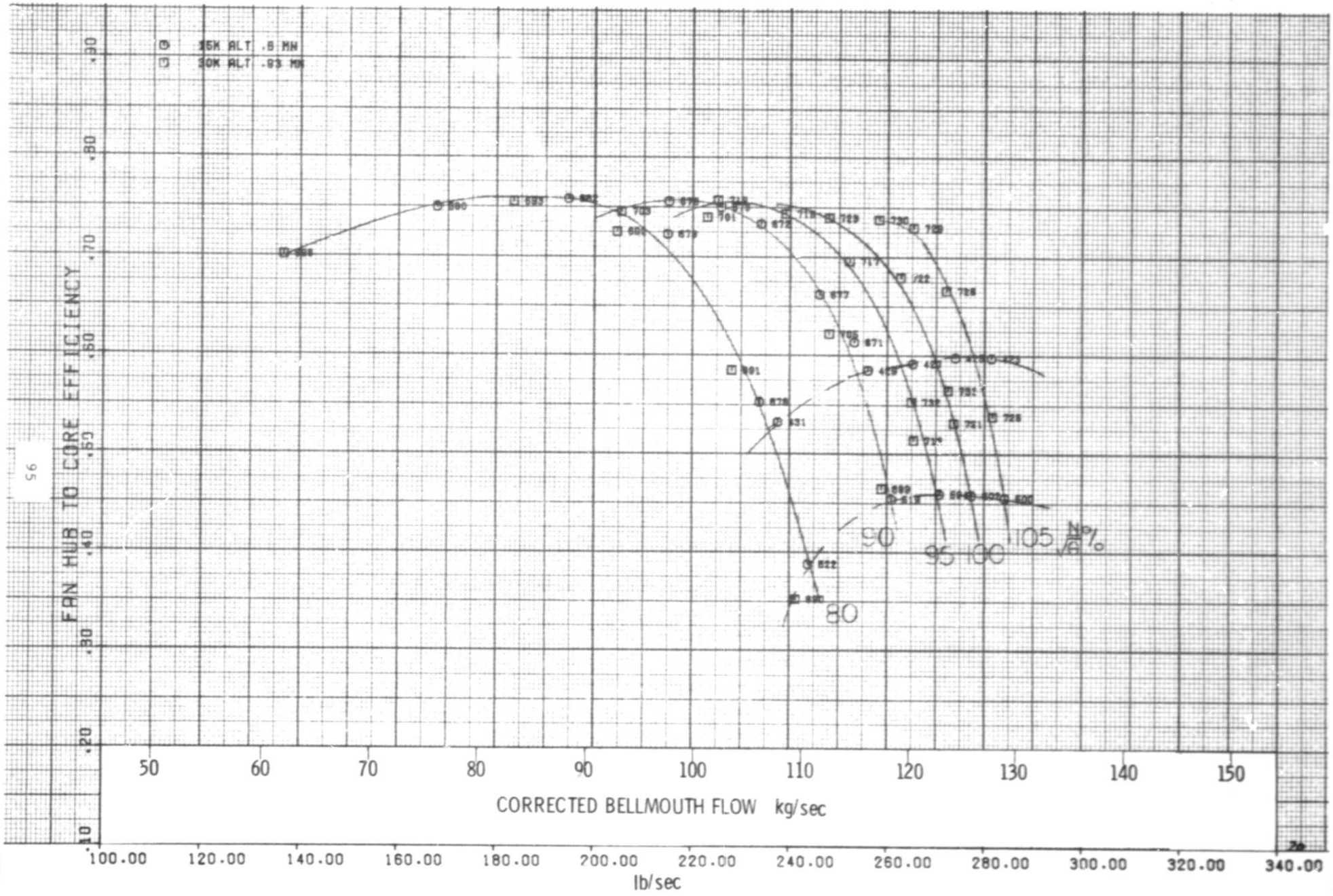

FIGURE II-20 HUB EFFICIENCY AT IGV ANGLE OF 35° (CONVENTIONAL SPLITTER)

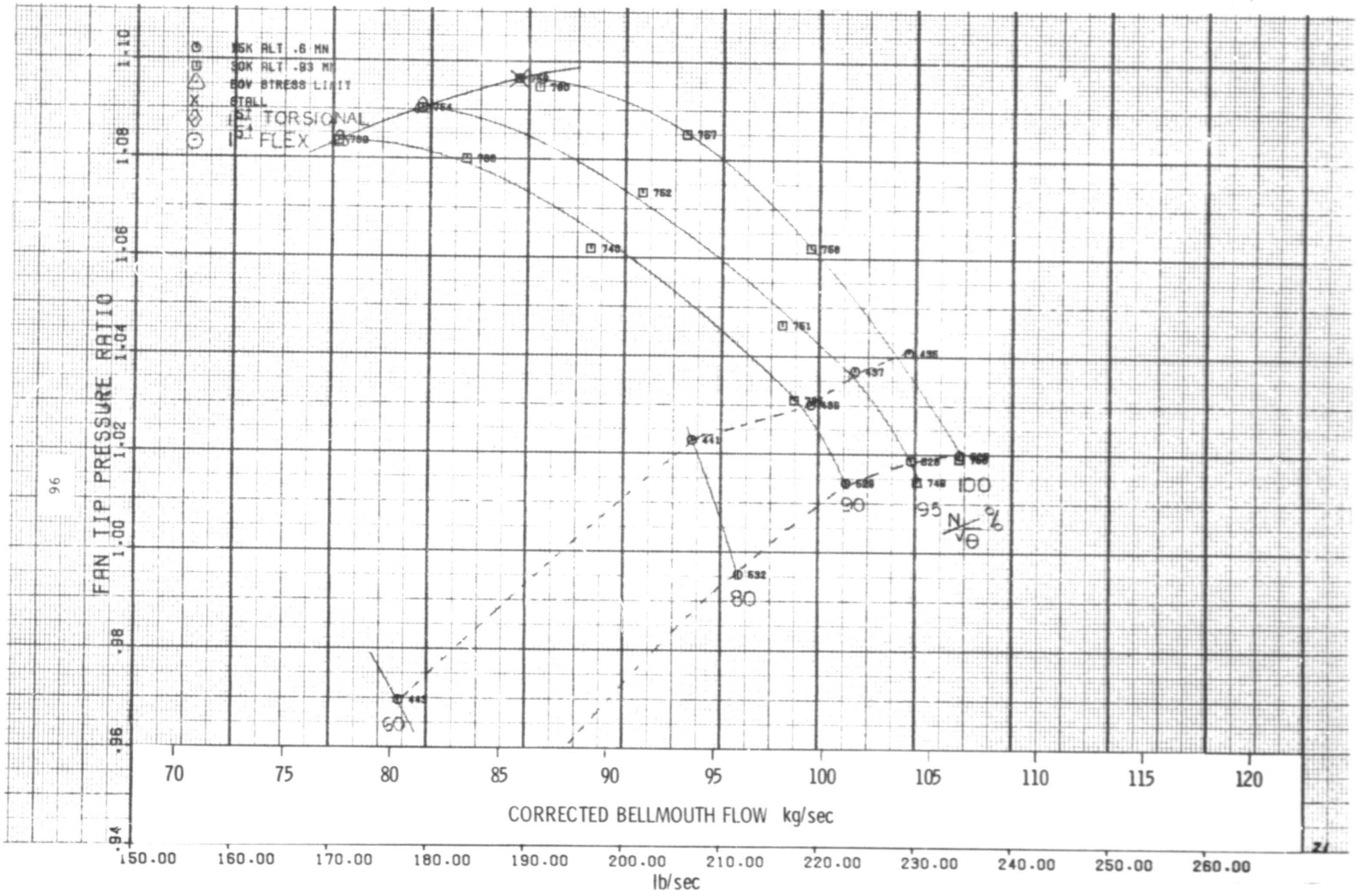

FIGURE II-21 TIP PRESSURE RATIO AT IGV ANGLE OF 50° (CONVENTIONAL SPLITTER)

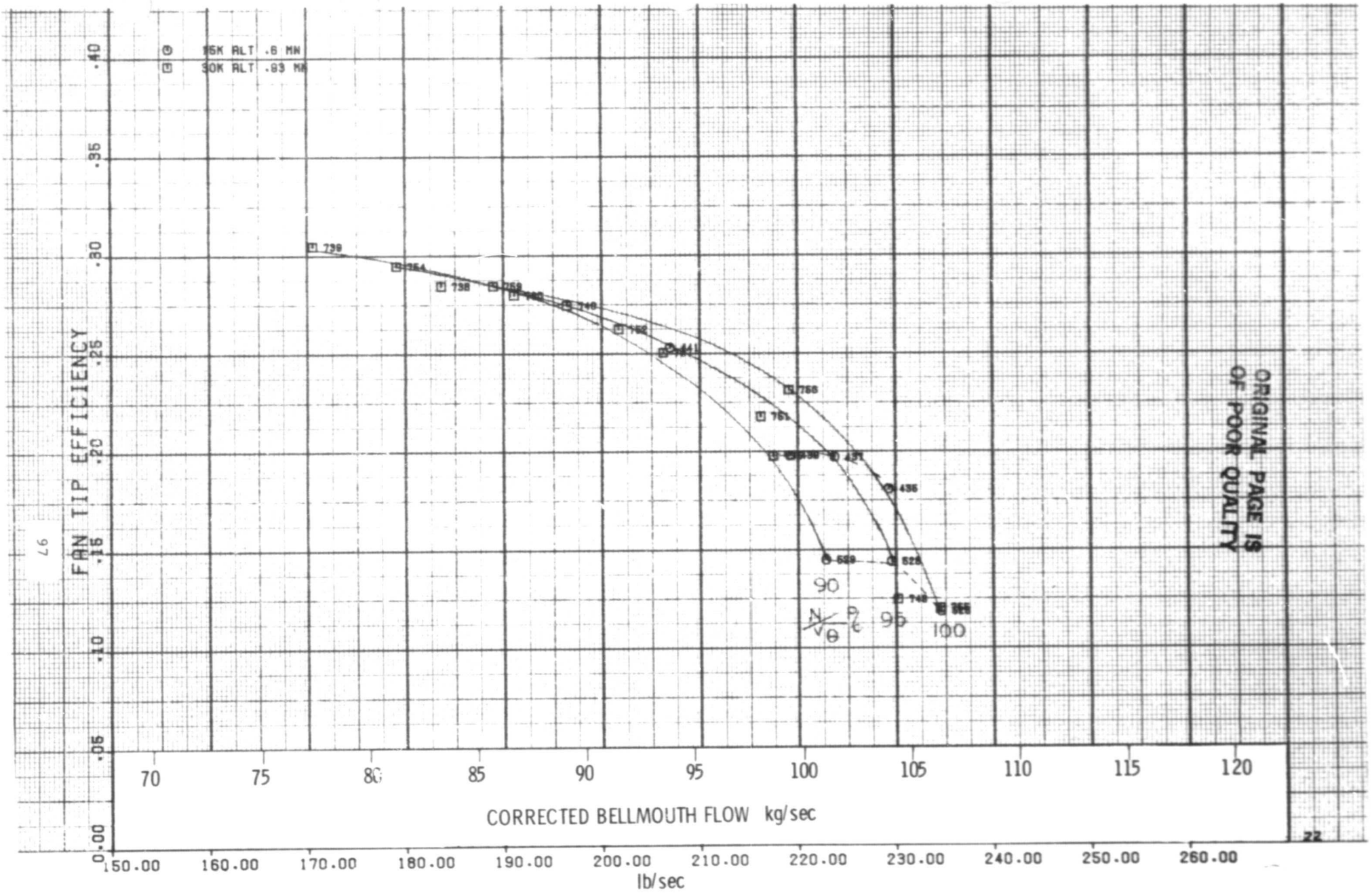

FIGURE II-22 TIP EFFICIENCY AT IGV ANGLE OF 50° (CONVENTIONAL SPLITTER)

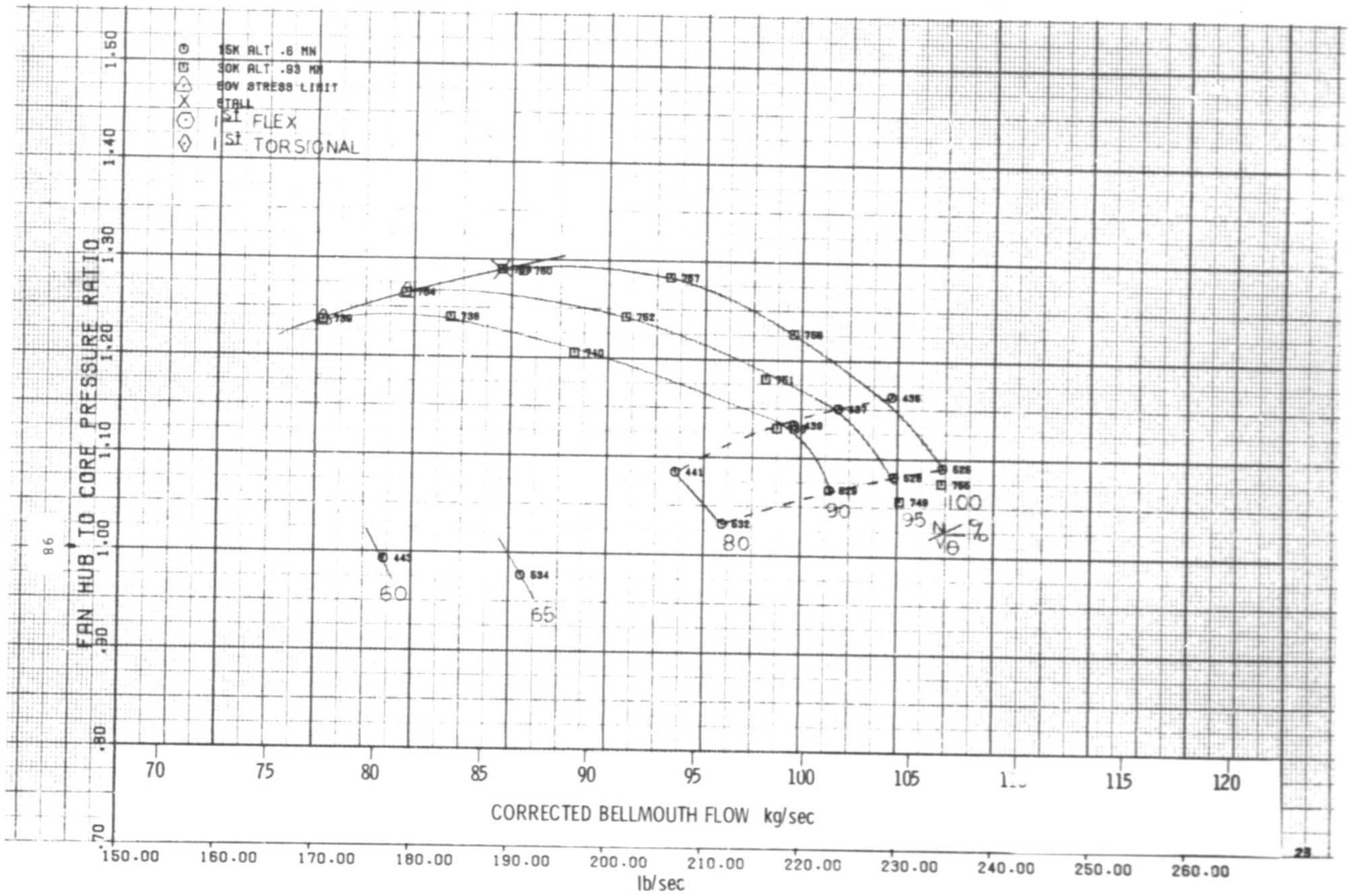

FIGURE II-23 HUB PRESSURE RATIO AT IGV ANGLE OF 50° (CONVENTIONAL SPLITTER)

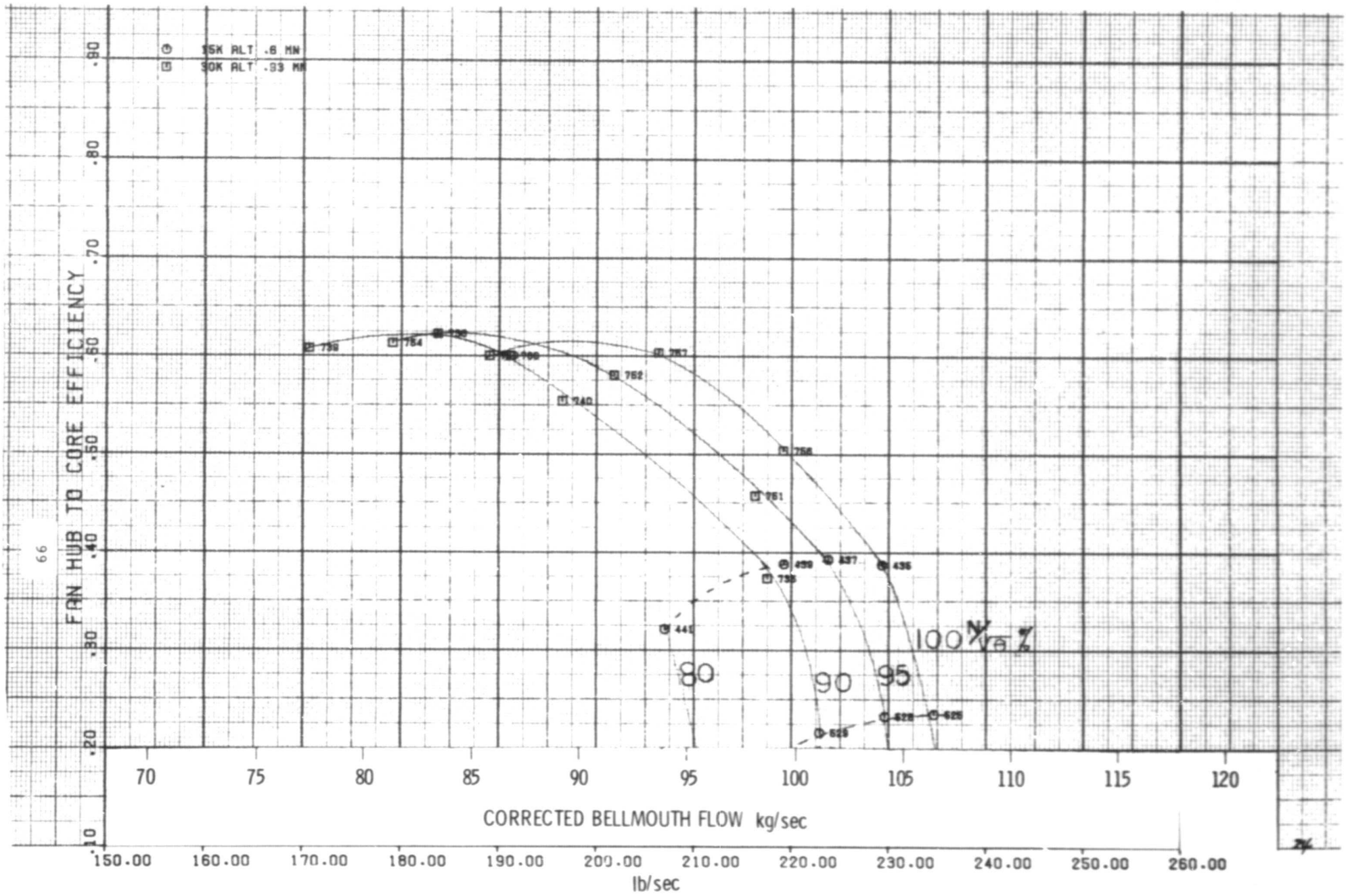

FIGURE II-24 HUB EFFICIENCY AT IGV ANGLE OF 50° (CONVENTIONAL SPLITTER)

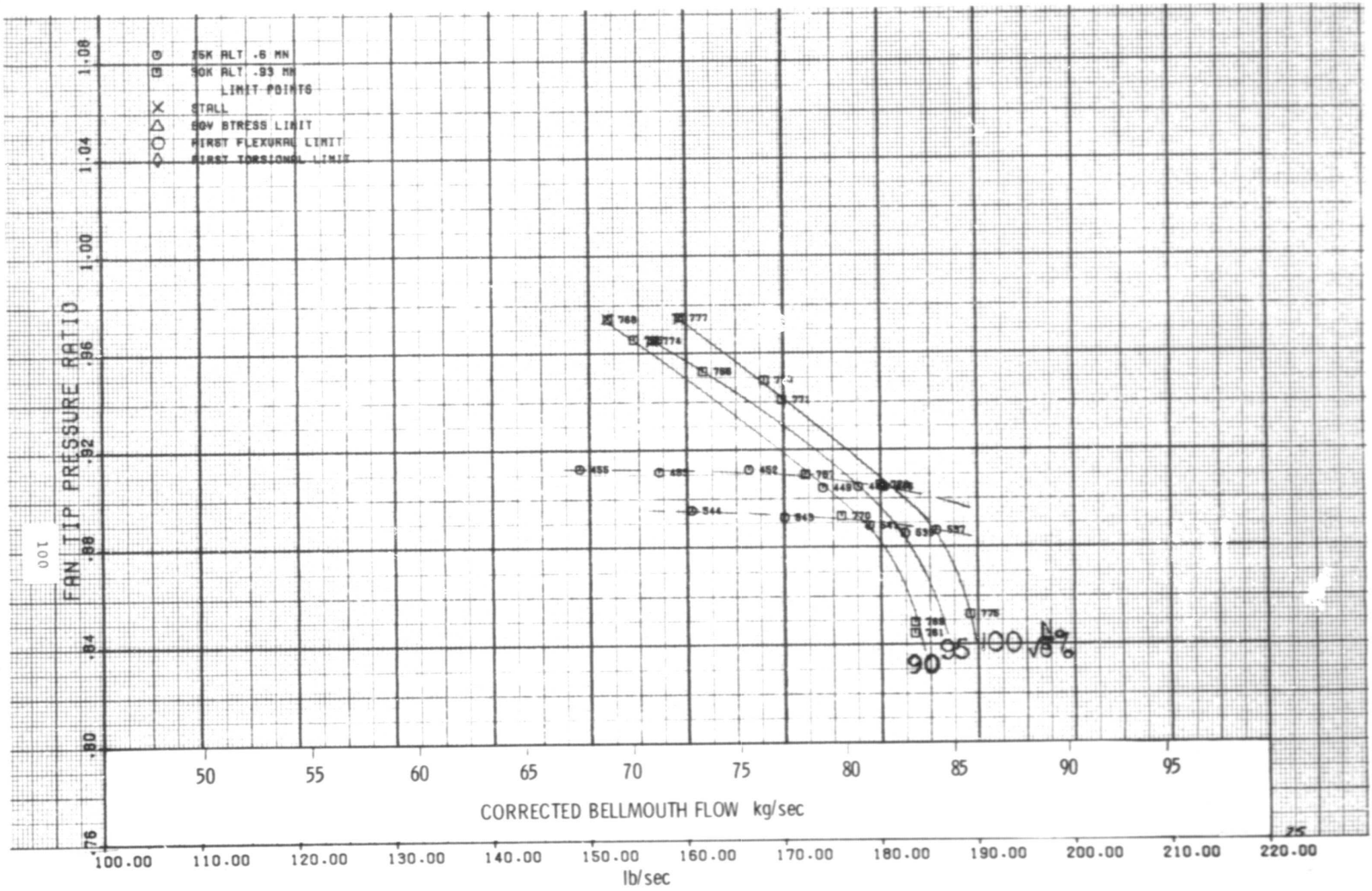

FIGURE II-25 TIP PRESSURE RATIO AT IGV ANGLE OF 65° (CONVENTIONAL SPLITTER)

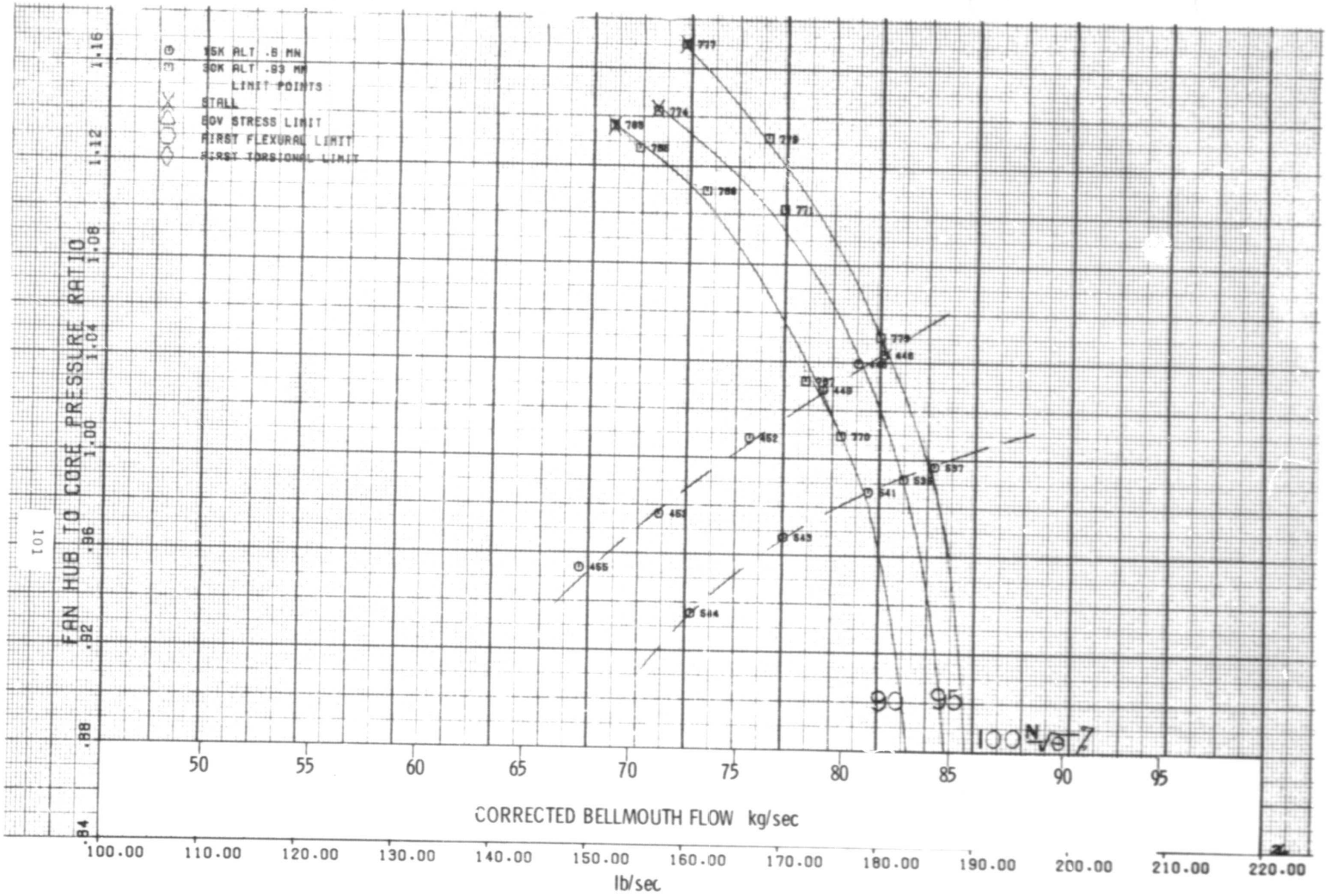

FIGURE II-26 HUB PRESSURE RATIO AT IGV ANGLE OF 65° (CONVENTIONAL SPLITTER)

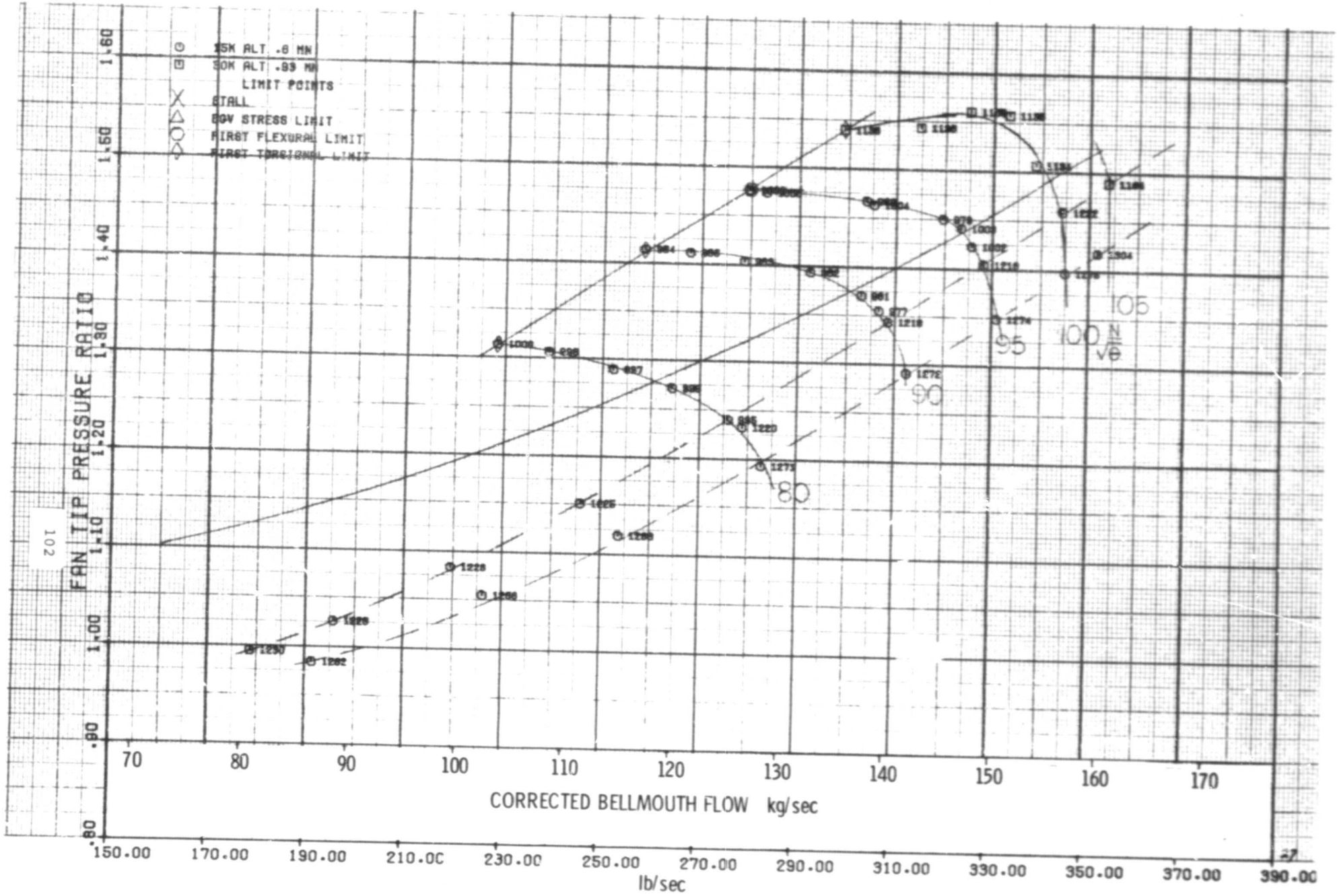

FIGURE II-27 TIP PRESSURE RATIO AT IGV ANGLE OF 0° (EXTENDED SPLITTER)

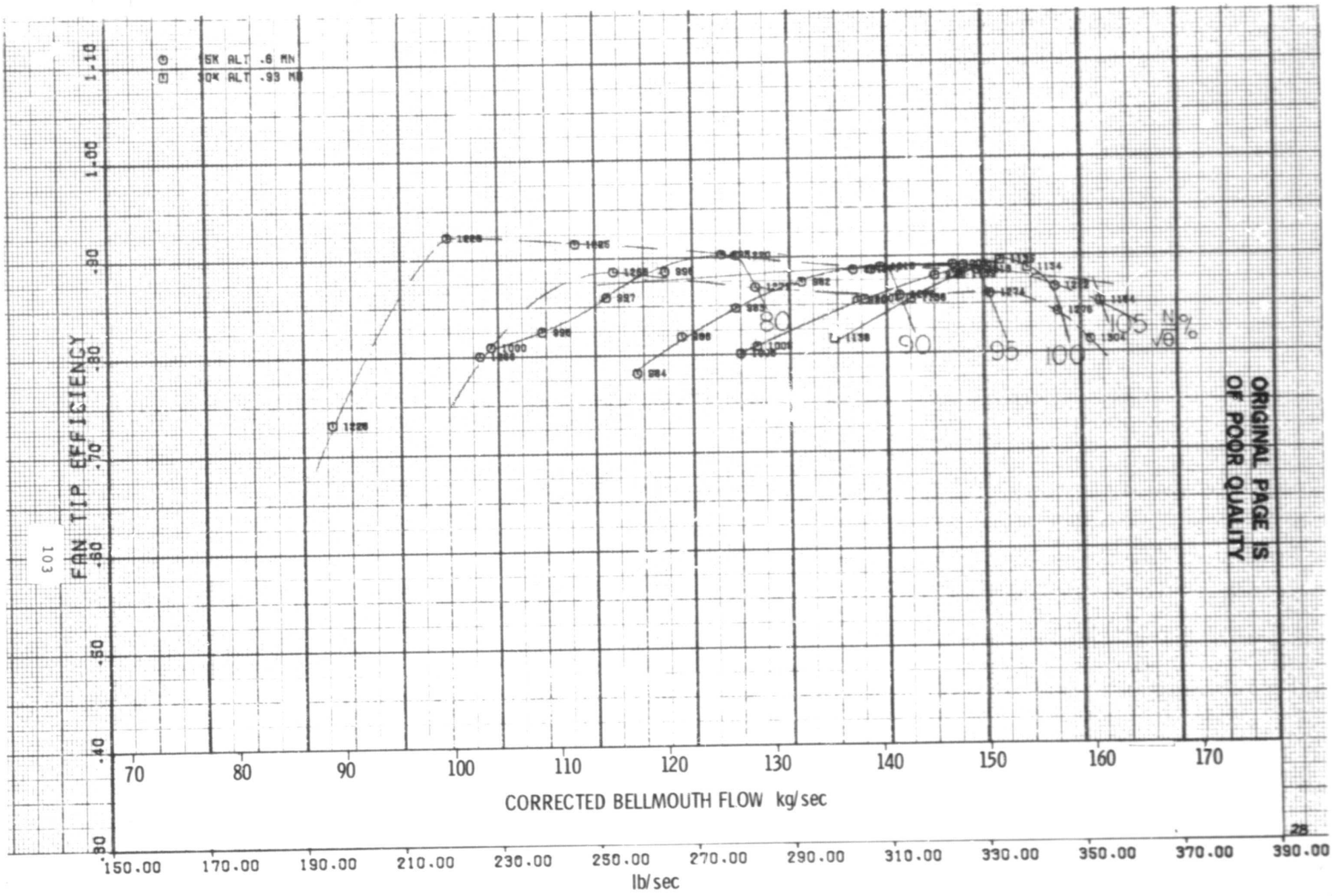

FIGURE II-28 TIP EFFICIENCY AT IGV ANGLE OF 0° (EXTENDED SPLITTER)

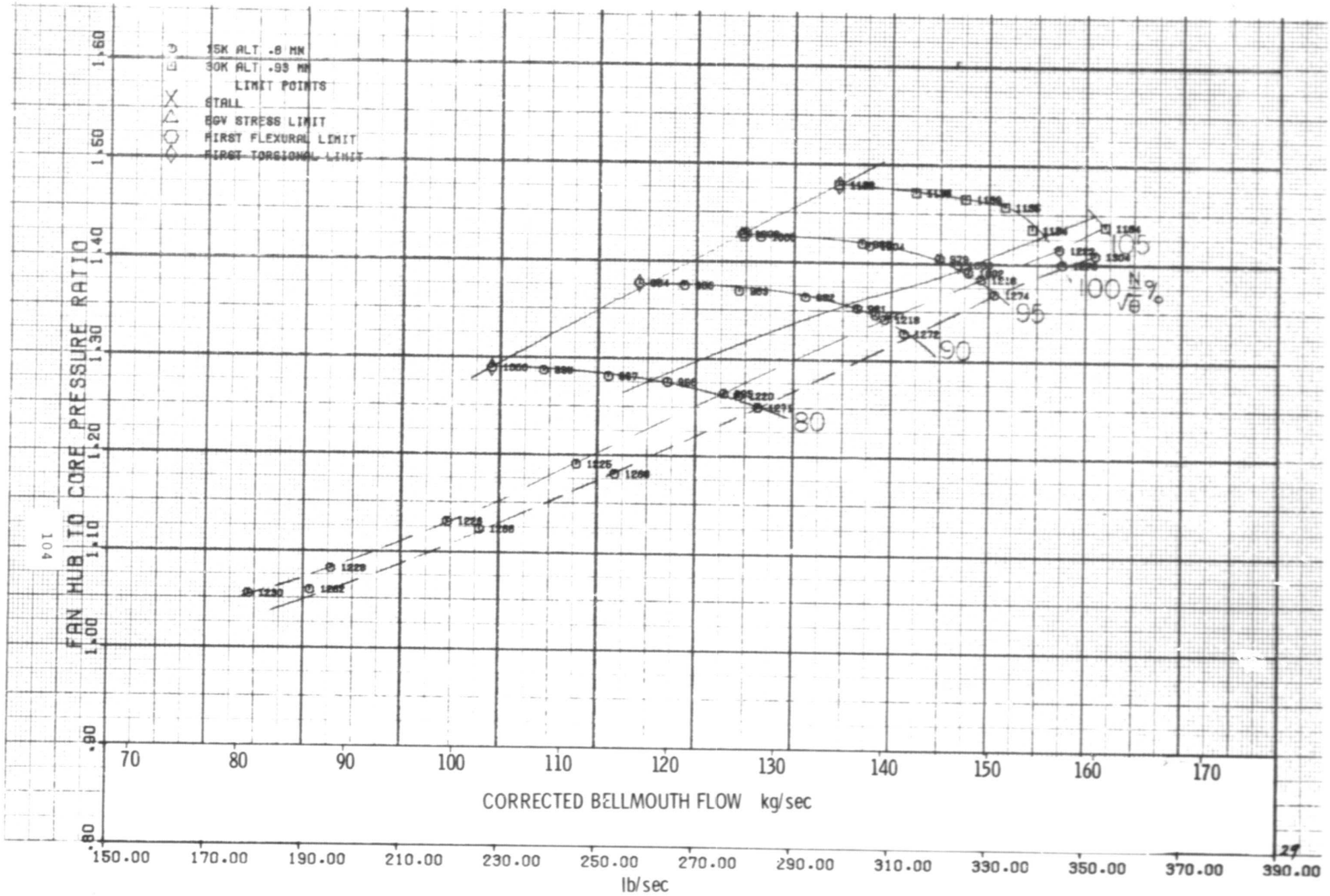

FIGURE II-29 HUB PRESSURE RATIO AT IGV ANGLE OF 0° (EXTENDED SPLITTER)

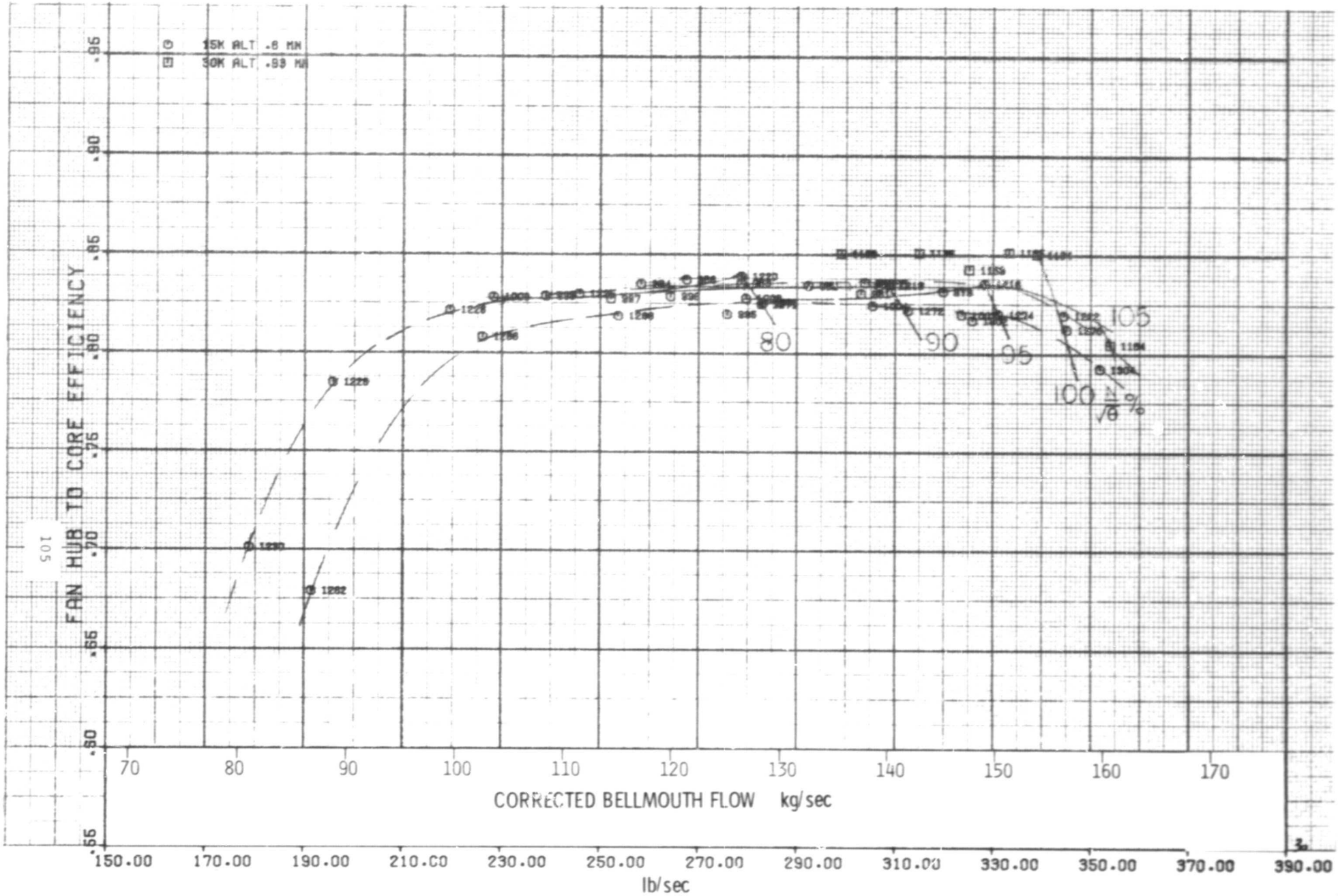

FIGURE II-30 HUB EFFICIENCY AT IGV ANGLE OF 0° (EXTENDED SPLITTER)

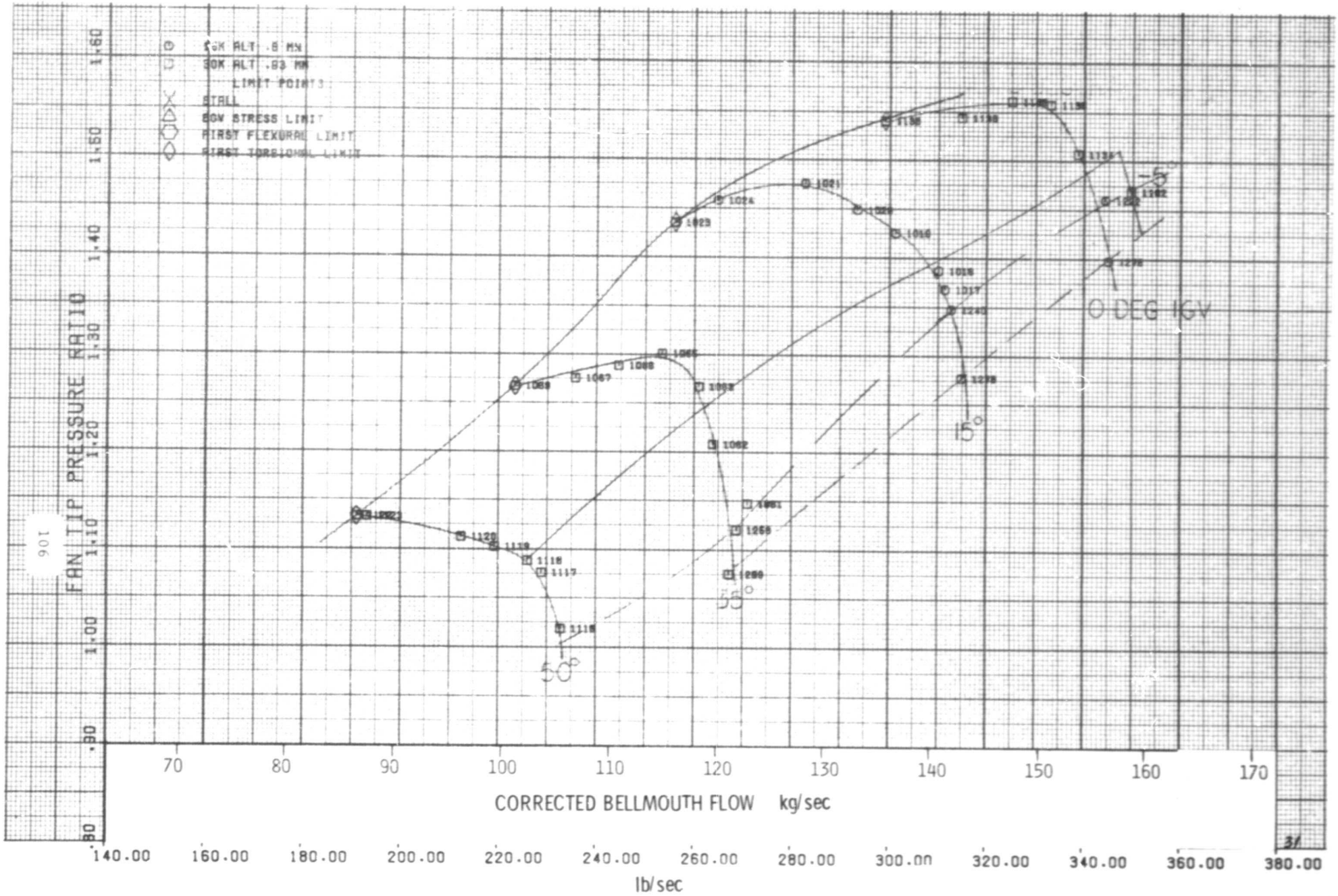

Figure 11-31 Tip Pressure Ratio at 100 Percent Speed (Extended Splitter)

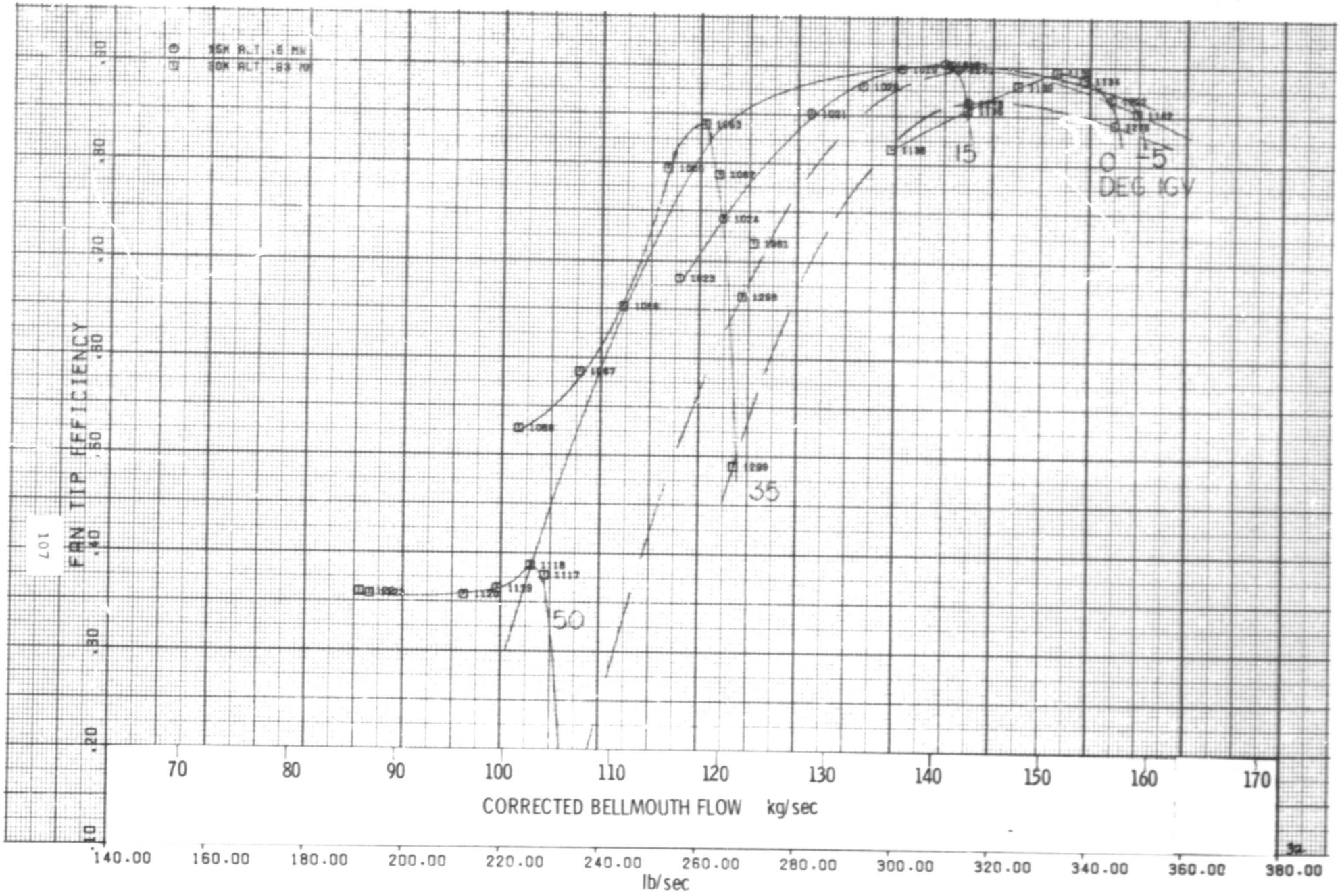

Figure 11-32 Tip Efficiency at 100 Percent Speed (Extended Splitter)

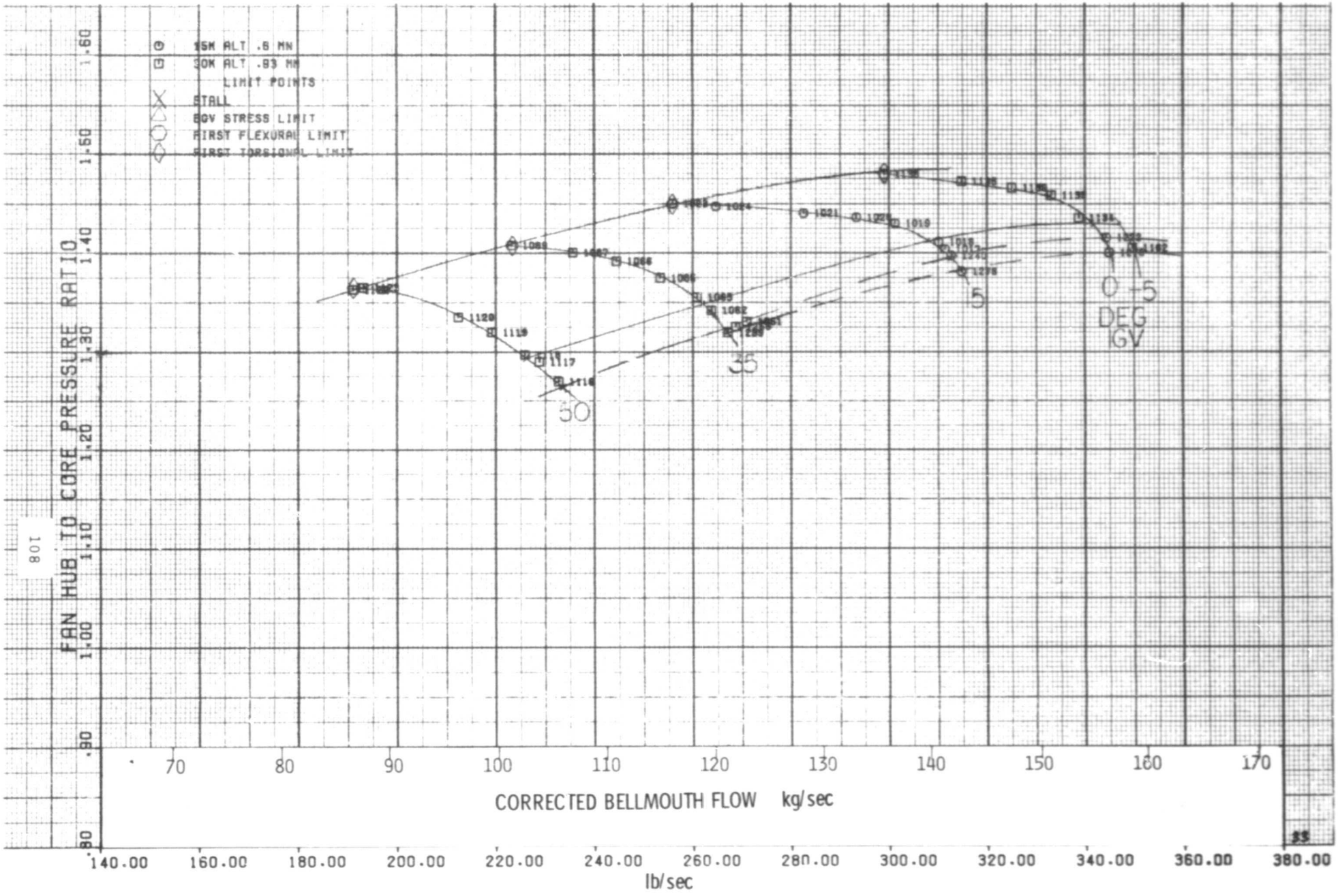

Figure 11-33 Hub Pressure Ratio at 100 Percent Speed (Extended Splitter)

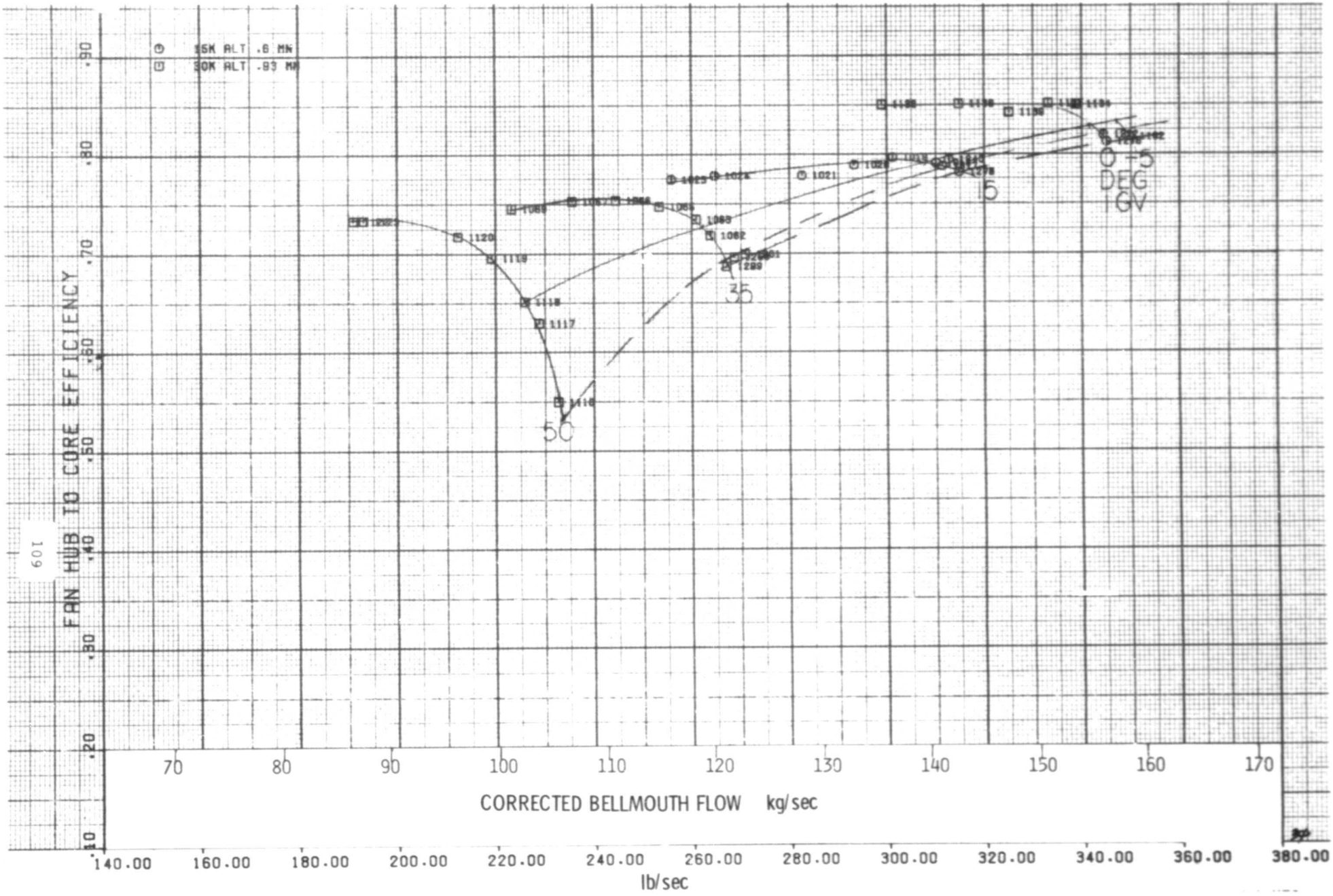

Figure II-34 Hub Efficiency at 100 Percent Speed (Extended Splitter)

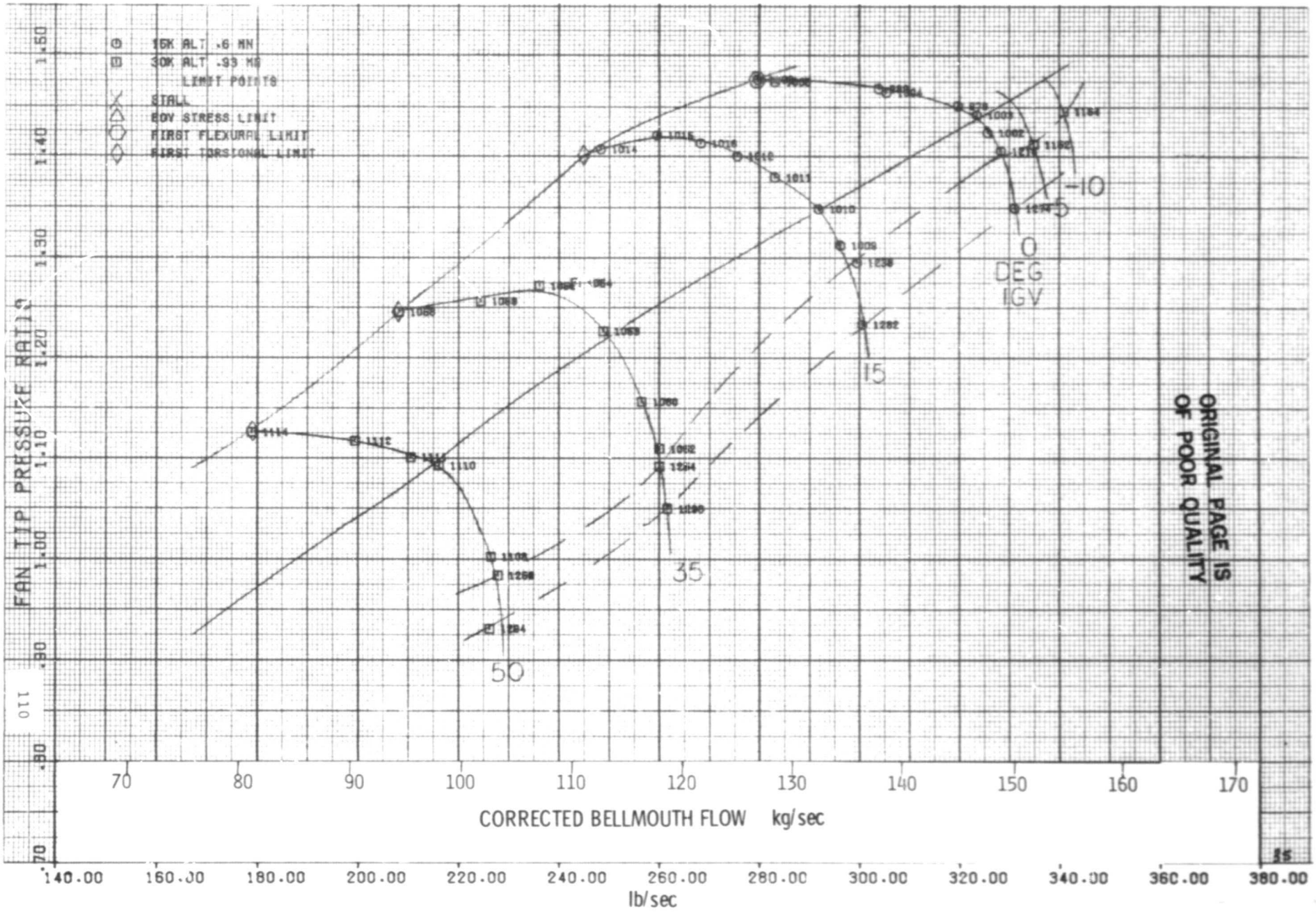

Figure 11-35 Tip Pressure Ratio at 95 Percent Speed (Extended Splitter)

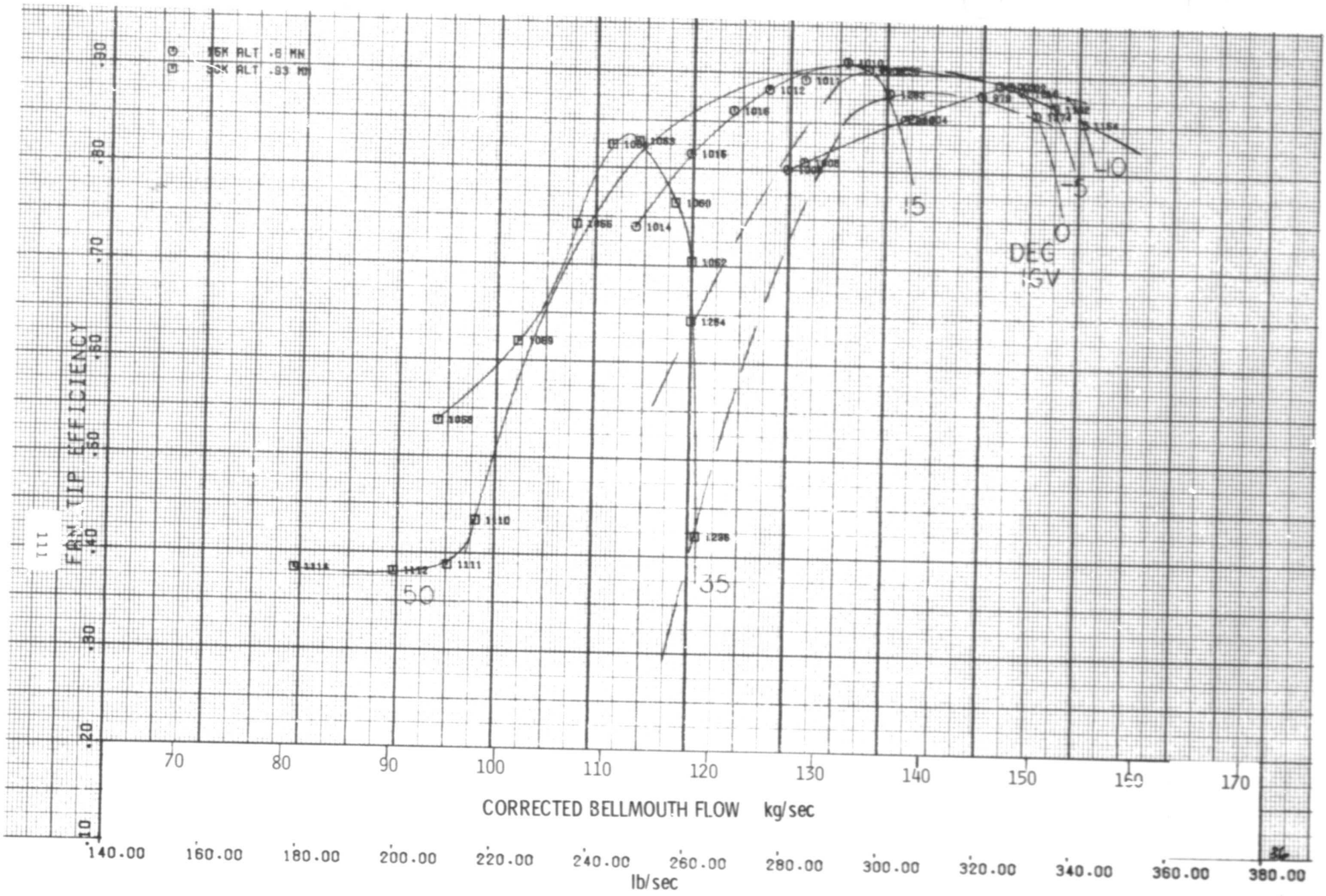

Figure 11-36 Tip Efficiency at 95 Percent Speed (Extended Splitter)

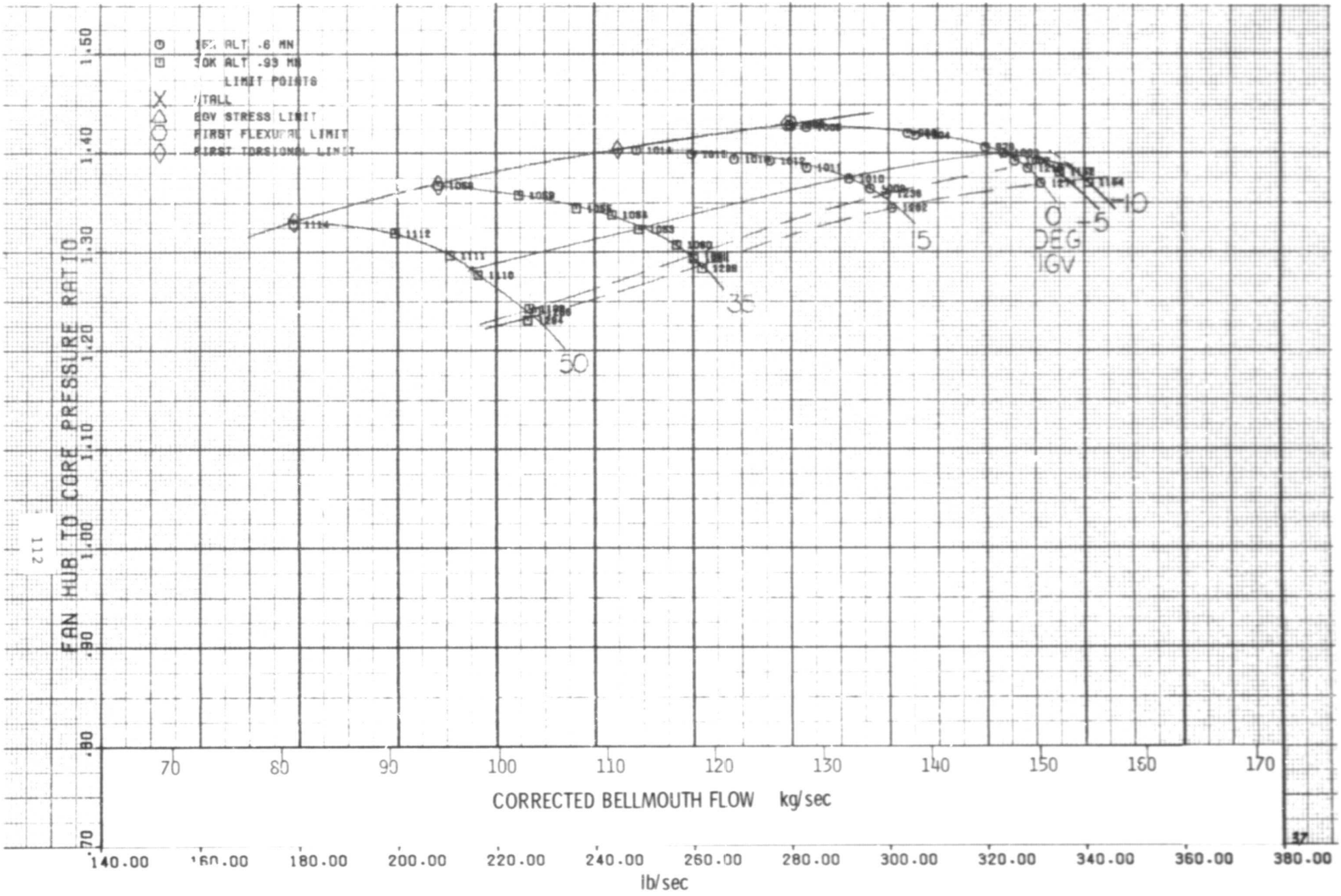

Figure II-37 Hub Pressure Ratio at 95 Percent Speed (Extended Splitter)

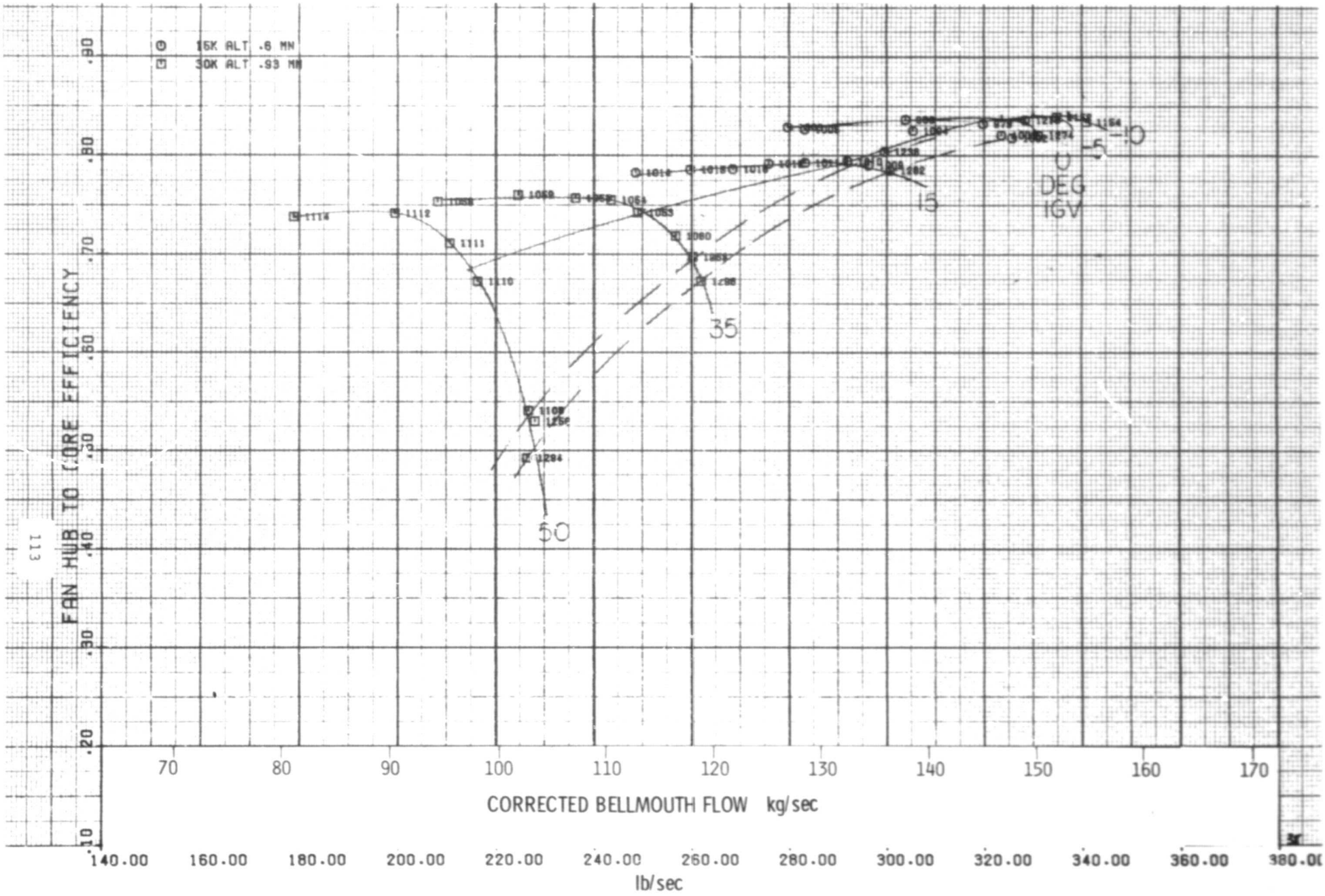

Figure 11-38 Hub Efficiency at 95 Percent Speed (Extended Splitter)

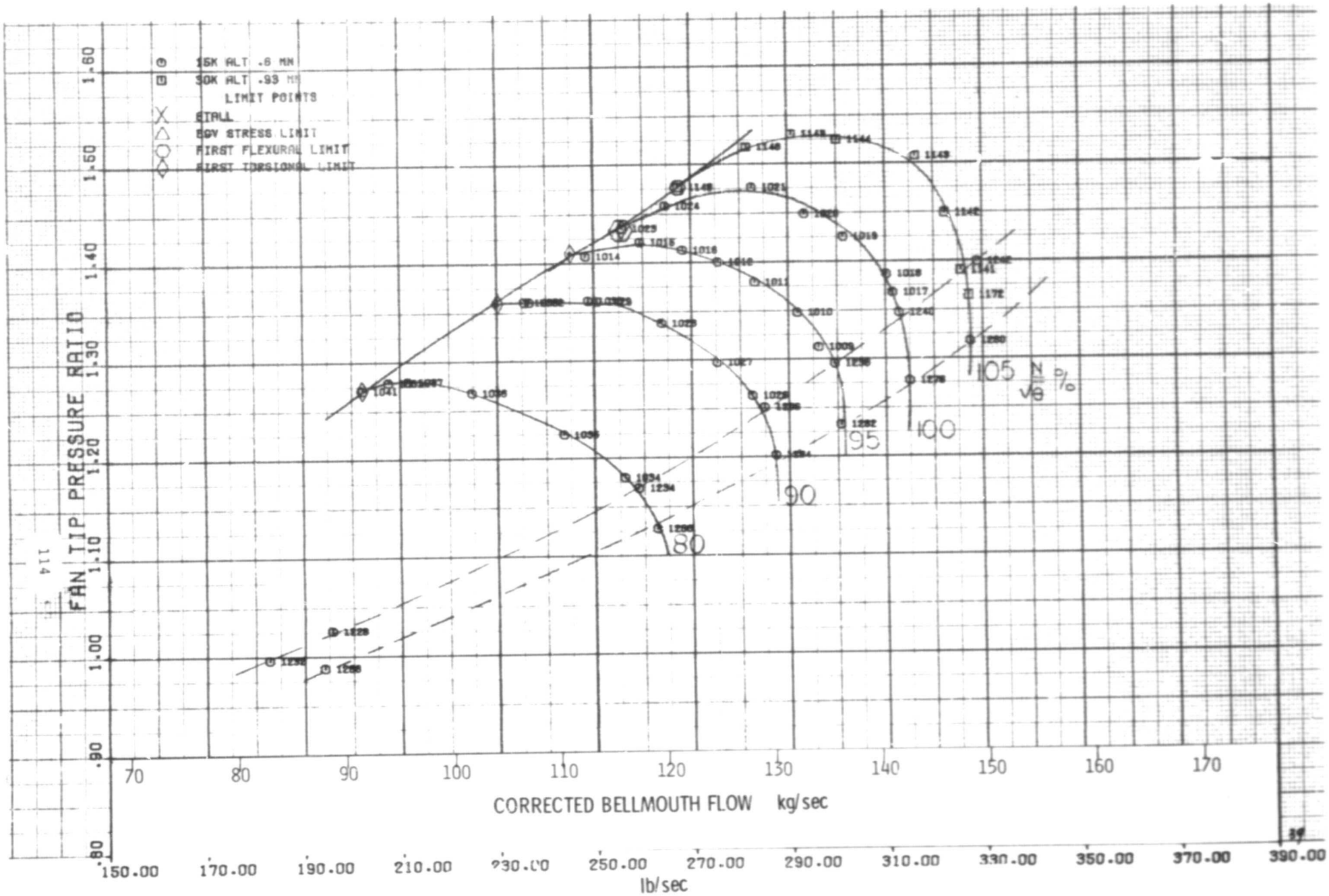

FIGURE II-39 TIP PRESSURE RATIO AT IGV ANGLE OF 15° (EXTENDED SPLITTER)

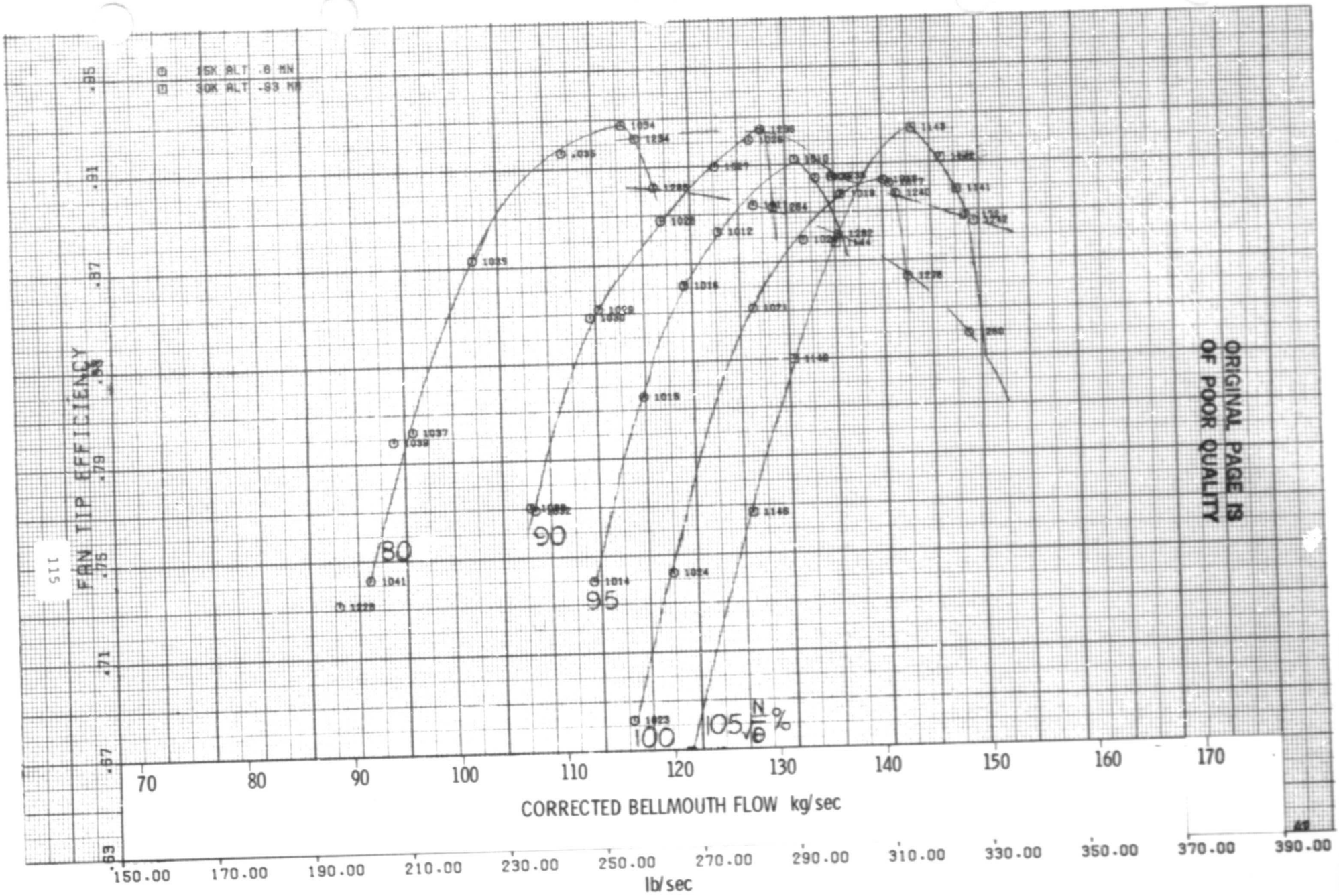

FIGURE II-40 TIP EFFICIENCY AT IGV ANGLE OF 15° (EXTENDED SPLITTER)

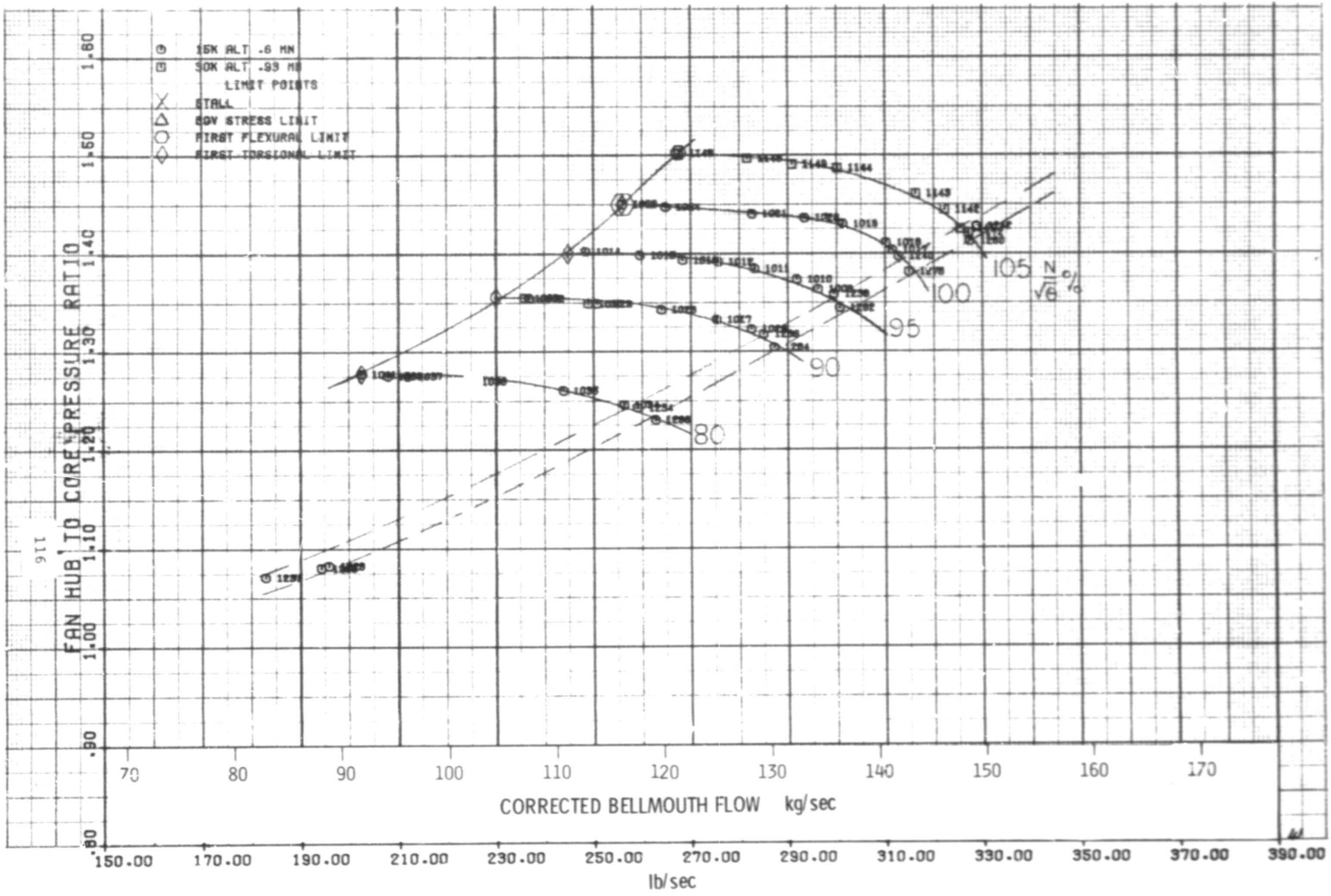

FIGURE II-41 HUB PRESSURE RATIO AT IGV ANGLE OF 15° (EXTENDED SPLITTER)

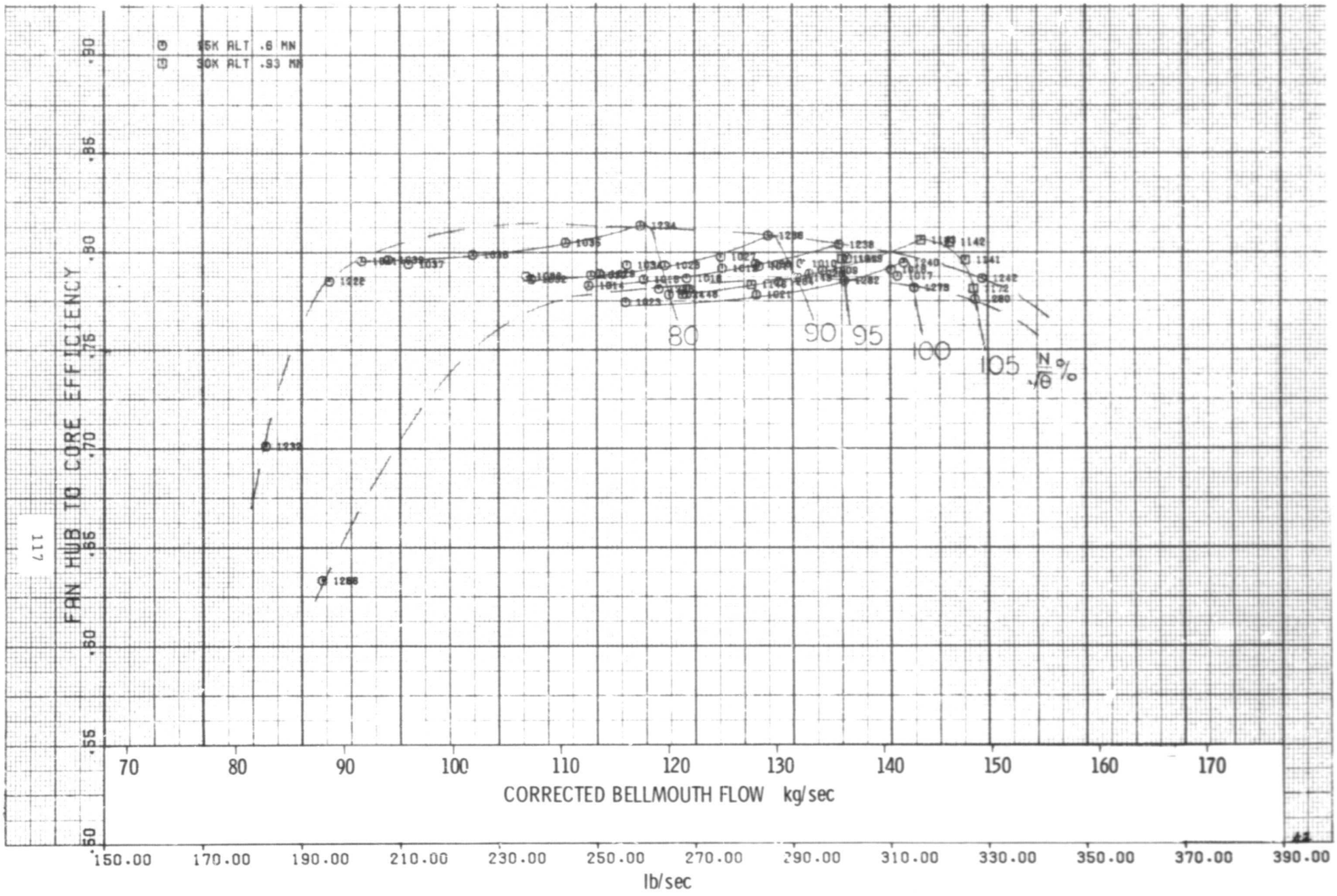

FIGURE II-42 HUB EFFICIENCY AT IGV ANGLE OF 15° (EXTENDED SPLITTER)

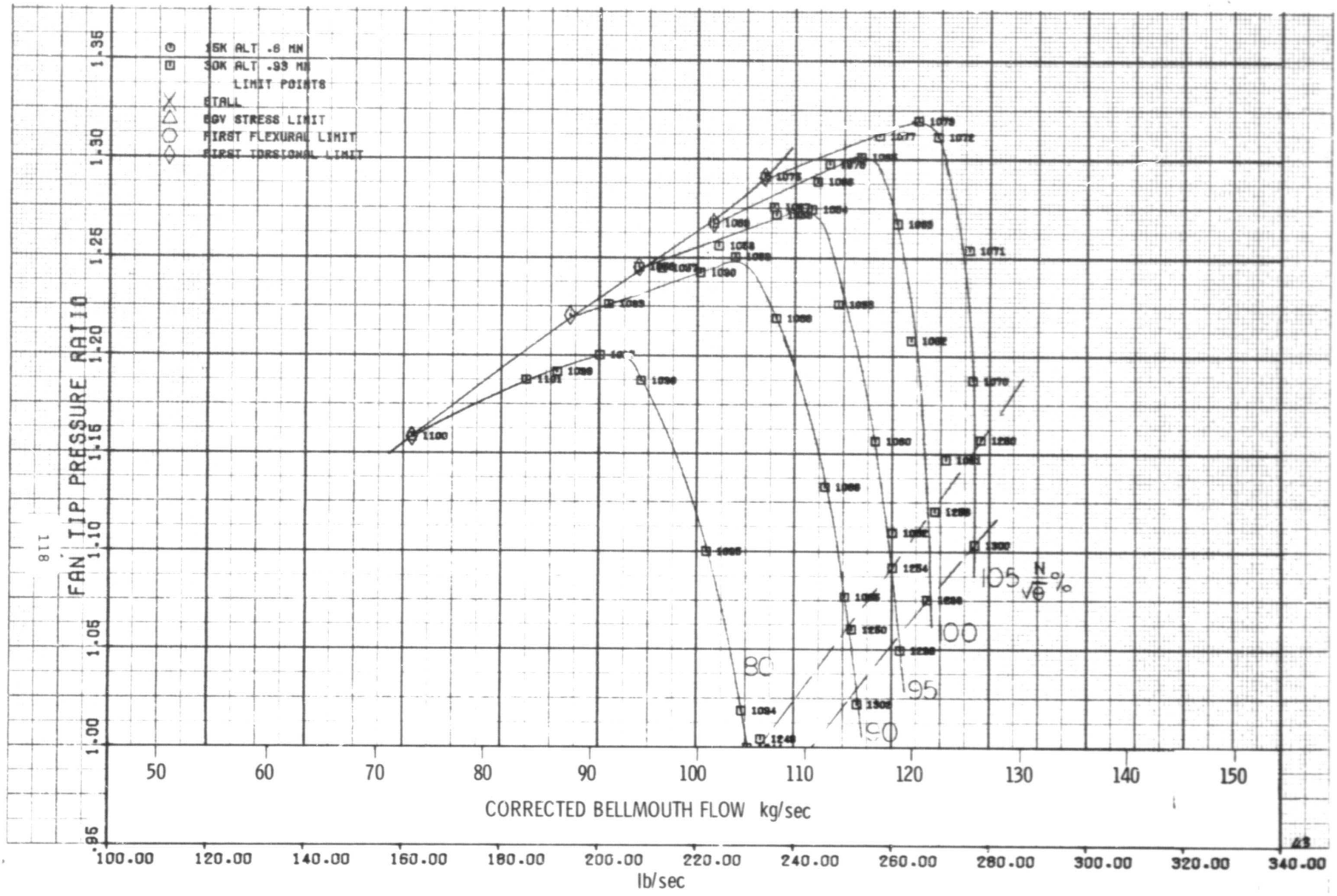

FIGURE II-43 TIP PRESSURE RATIO AT IGV ANGLE OF 35° (EXTENDED SPLITTER)

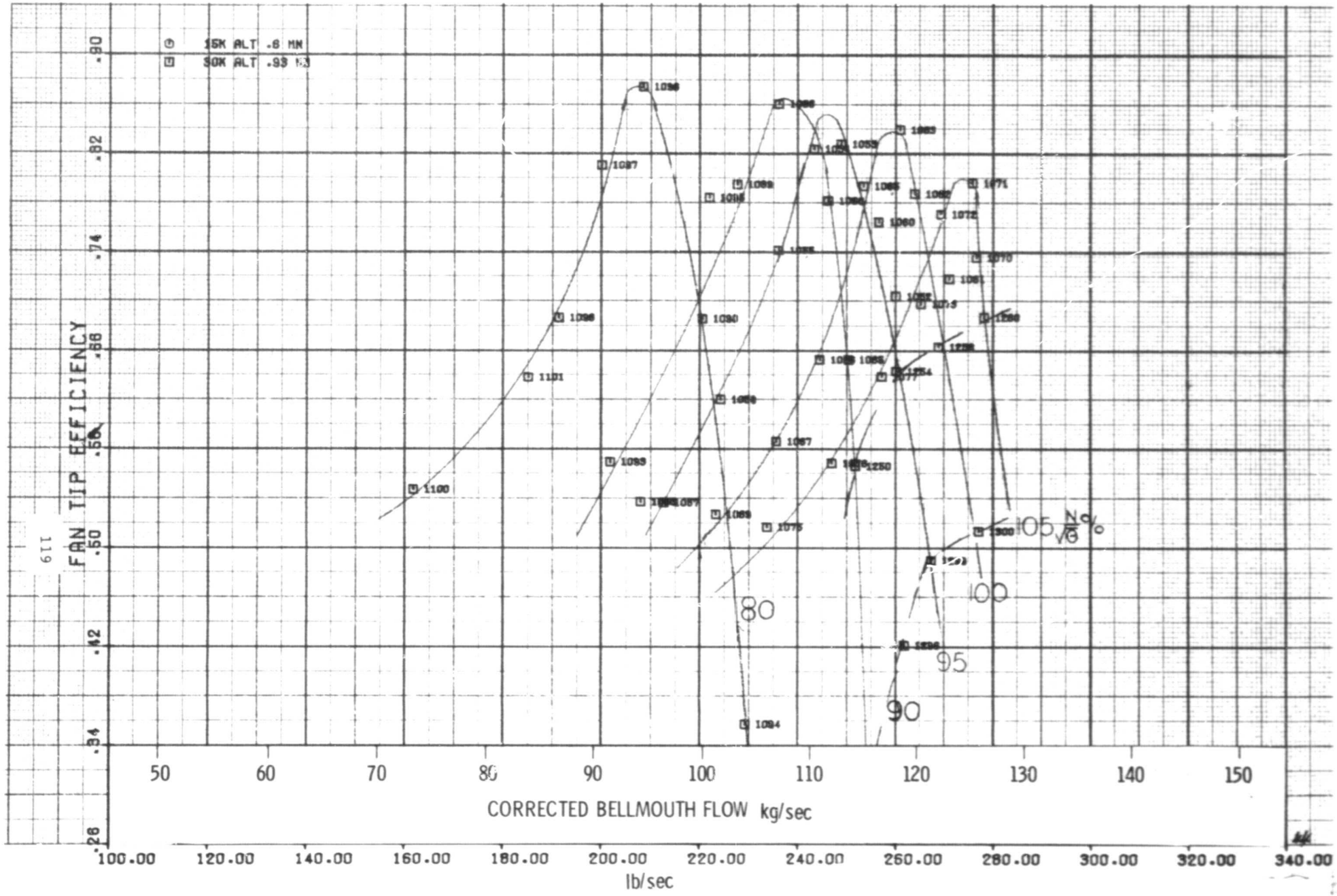

FIGURE II-44 TIP EFFICIENCY AT IGV ANGLE OF 35° (EXTENDED SPLITTER)

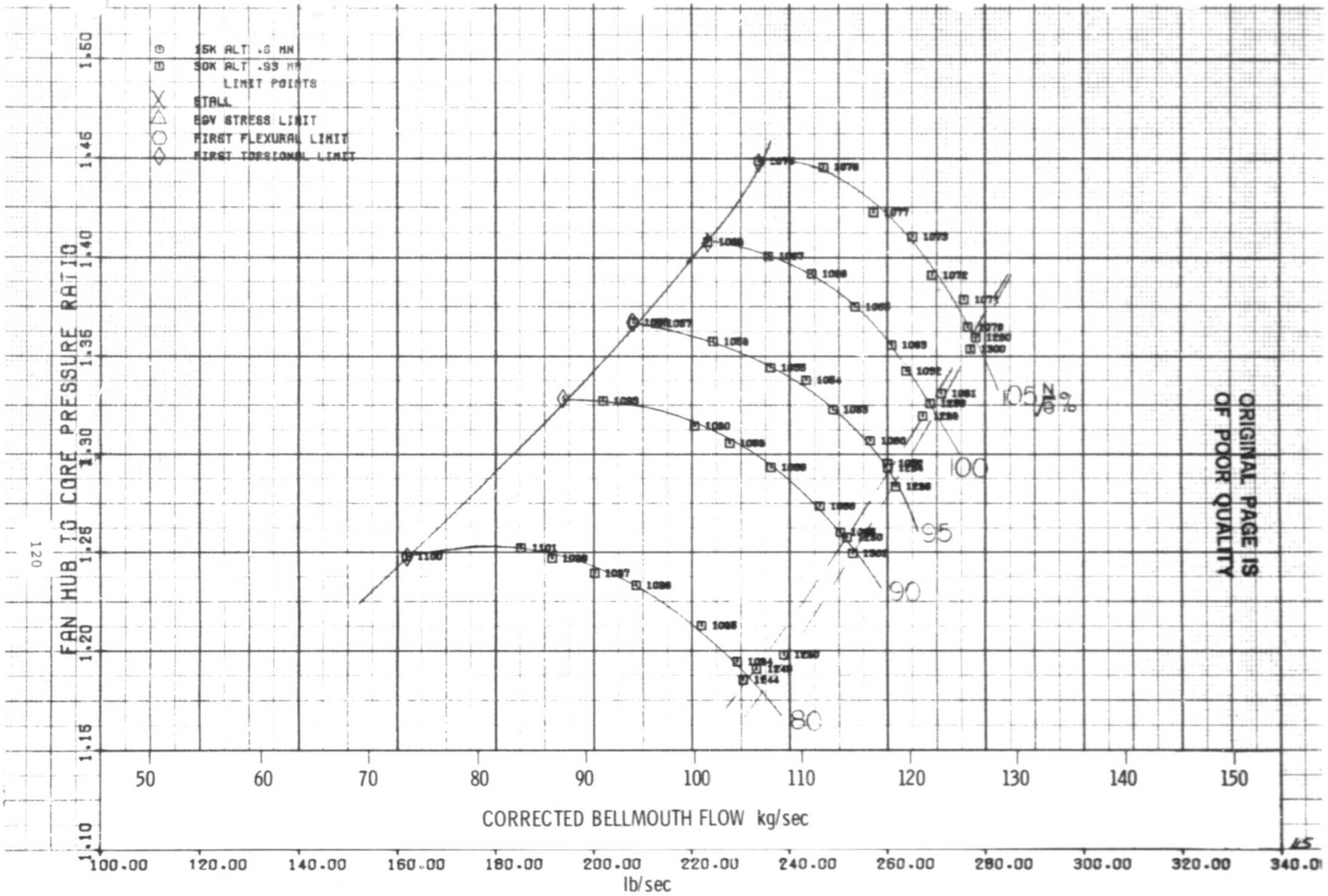

FIGURE II-45 HUB PRESSURE RATIO AT IGV ANGLE OF 35° (EXTENDED SPLITTER)

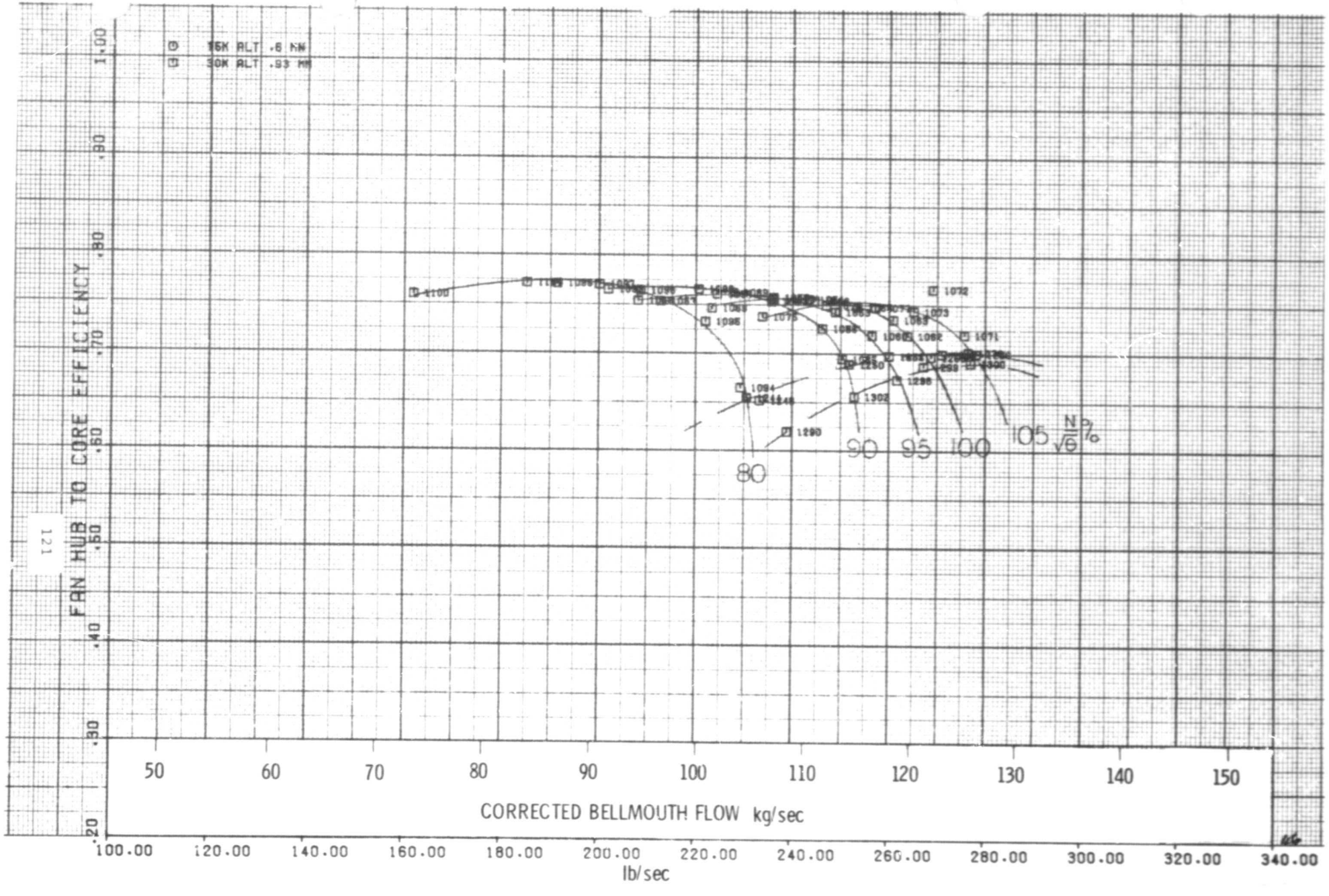

FIGURE II-46 HUB EFFICIENCY AT IGV ANGLE OF 35° (EXTENDED SPLITTER)

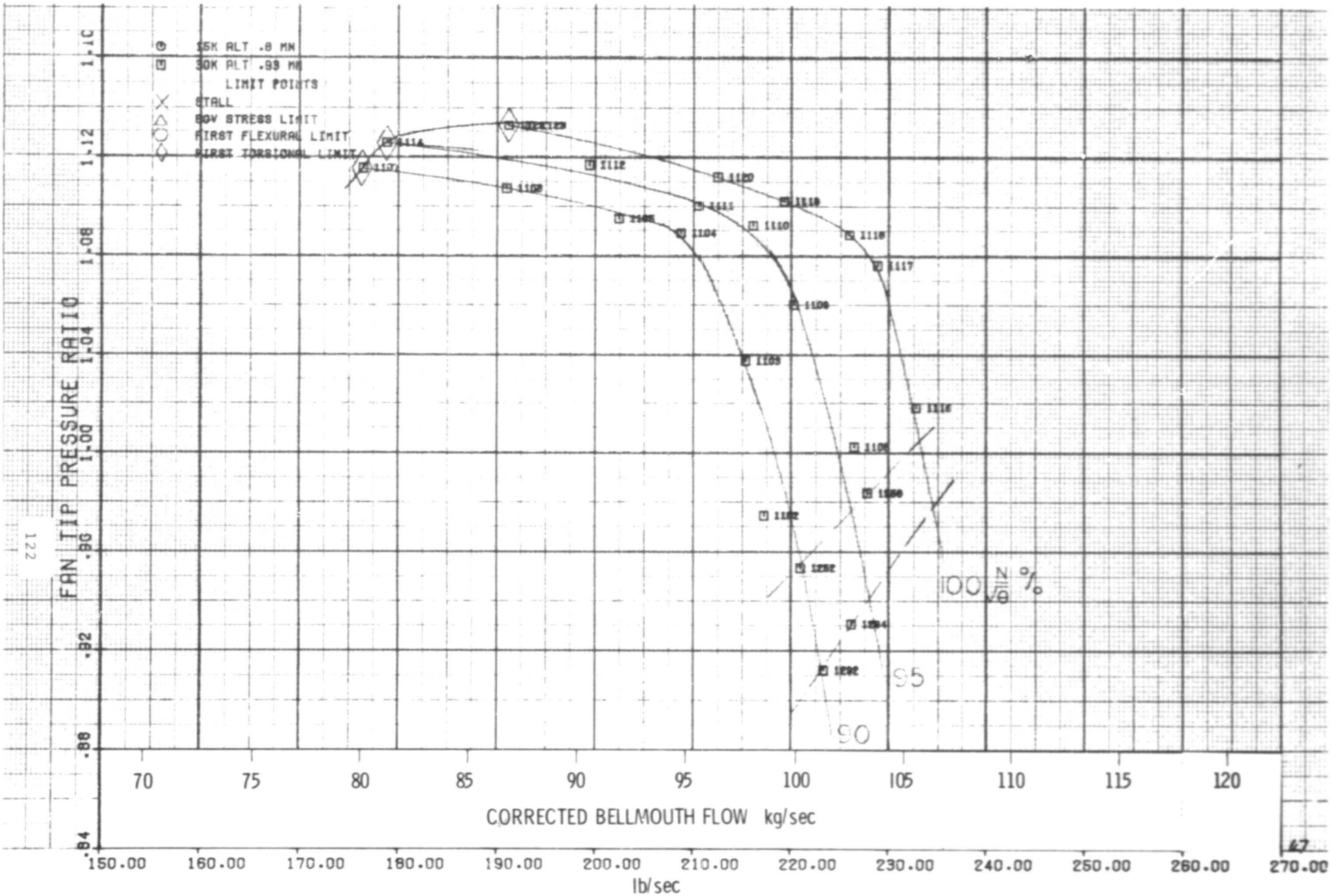

FIGURE II-47 TIP PRESSURE RATIO AT IGV ANGLE OF 50° (EXTENDED SPLITTER)

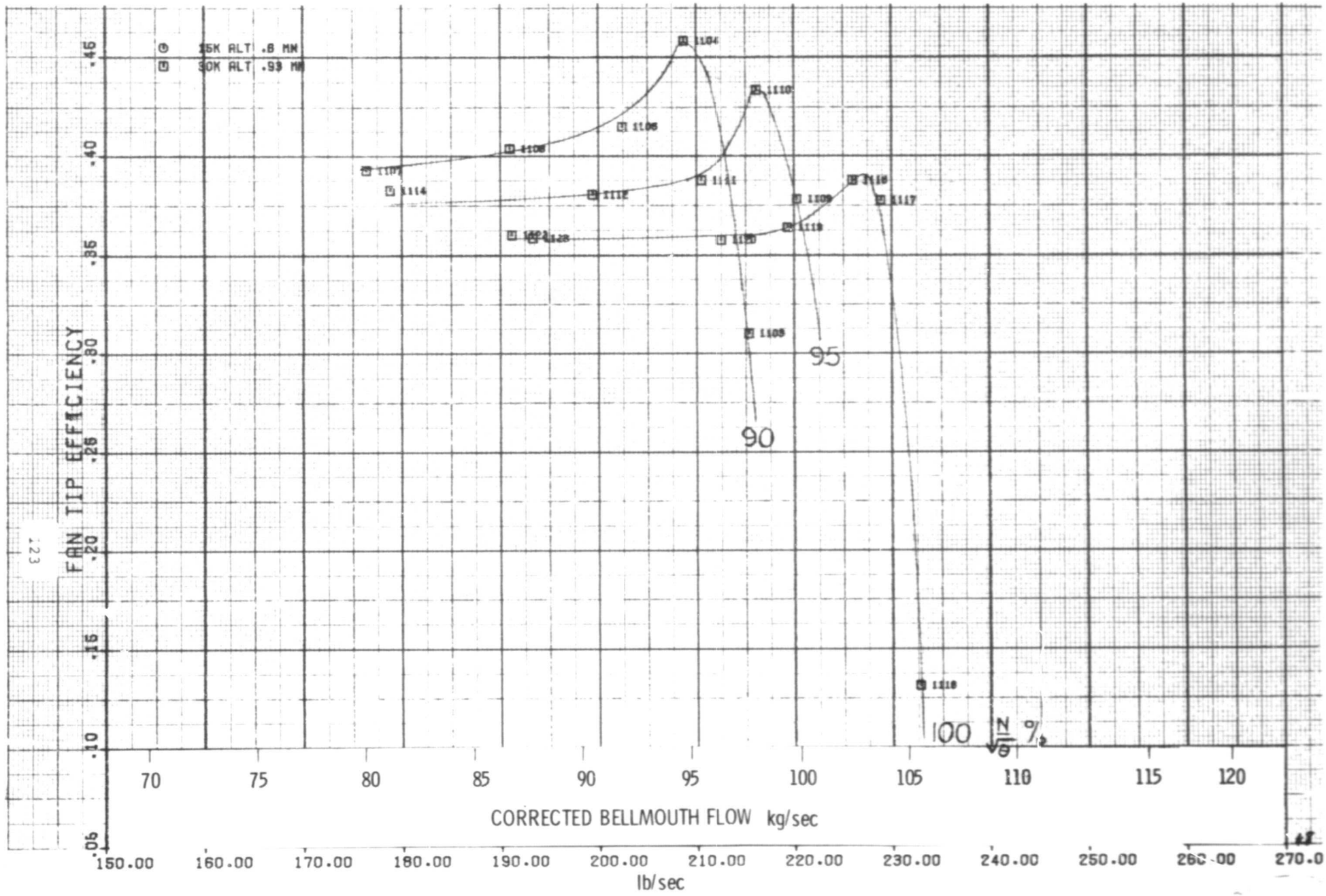

FIGURE II-48 TIP EFFICIENCY AT IGV ANGLE OF 50° (EXTENDED SPLITTER)

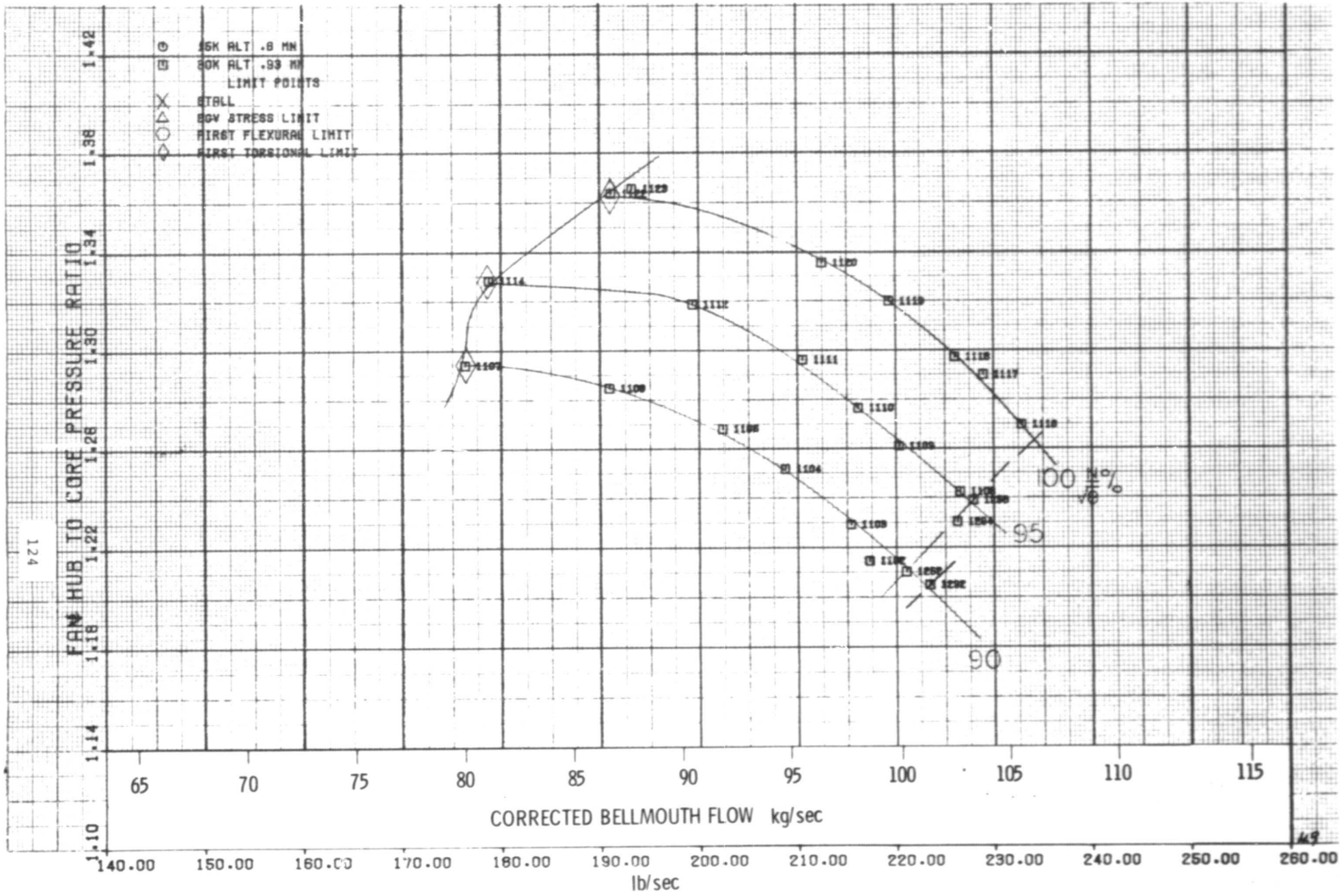

FIGURE II-49 HUB PRESSURE RATIO AT IGV ANGLE OF 50° (EXTENDED SPLITTER)

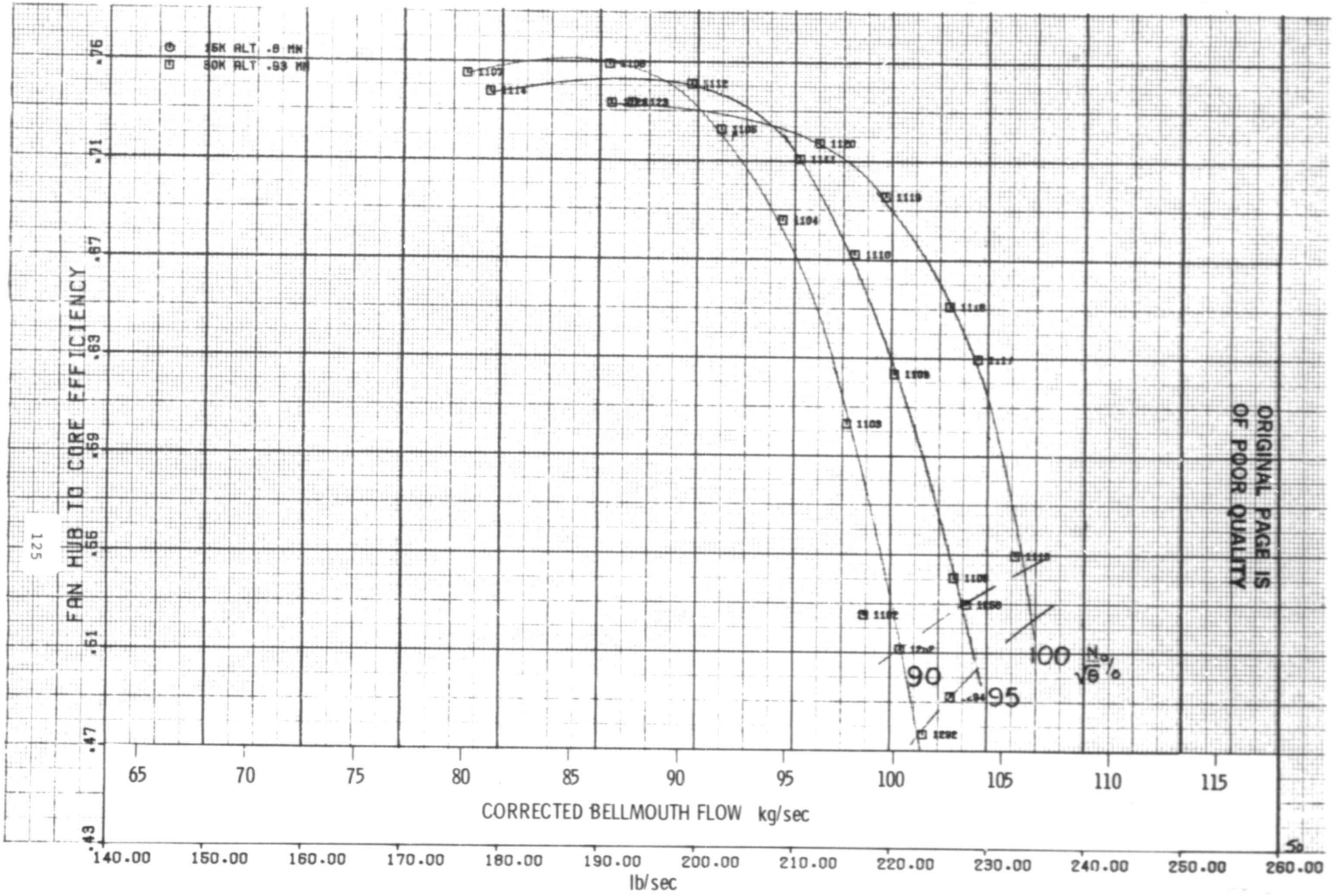

FIGURE II-50 HUB EFFICIENCY AT IGV ANGLE OF 50° (EXTENDED SPLITTER)